Novel Polyfluorene Based Copolymers for Optoelectronic Applications

Dissertation

zur Erlangung des akademischen Grades

Doktor der Naturwissenschaften
(Doktor rerum naturalium)

Bergische Universität Wuppertal
Fachbereich C – Mathematik und Naturwissenschaften

von

Frank Galbrecht

aus Wuppertal

Wuppertal, 2008

„Alles Große in unserer Welt geschieht nur,
weil jemand mehr tut, als er muß.“

Hermann Gmeiner (1919-1986), österreichischer Sozialpädagoge,
Gründer der SOS-Kinderdörfer

„… von den sicheren Dingen
Das Sicherste ist der Zweifel.“

Bertolt Brecht (1898-1956), deutscher Dramatiker und Lyriker,
Begründer des epischen Theaters

Die Dissertation kann wie folgt zitiert werden:

urn:nbn:de:hbz:468-20080323
[http://nbn-resolving.de/urn/resolver.pl?urn=urn%3Anbn%3Ade%3Ahbz%3A468-20080323]

Die praktischen Arbeiten wurden in der Zeit von Juni 2004 bis August 2006 am Lehrstuhl für Makromolekulare Chemie des Fachbereiches C – Mathematik und Naturwissenschaften der Bergischen Universität Wuppertal unter Anleitung von Prof. Dr. Ullrich Scherf durchgeführt.

Herrn Prof. Dr. Ullrich Scherf gilt mein besonderer Dank für die Überlassung des interessanten Themas, seine stete Diskussionsbereitschaft, sowie seine vielfältige persönliche Unterstützung. Die wissenschaftliche Freiheit die mir eingeräumt wurde habe ich als überaus motivierend empfunden. Prof. Dr. Dieter Neher danke ich für gute Zusammenarbeit und die Übernahme des Koreferats.

1. Gutachter: Prof. Dr. U. Scherf (Bergische Universität Wuppertal)
2. Gutachter: Prof. Dr. Dieter Neher (Universität Potsdam)
Eingereicht am: 14.02.2008

Für meine Familie,

Nicole und Ben

Abstract

Organic light emitting diodes (OLEDs) have gained increasing attention because of there remarkable properties and application potential. Therefore chemists are aiming for suitable organic materials for optoelectronic applications. Prominent materials are semiconducting polymers e.g. polyfluorenes. A major problem hereby is the colour purity of the blue-emitting polyfluorene-type materials caused by degradation processes during device operation. Besides the well-characterized keto defects in degraded polyfluorenes which emit at a peak maximum of approximately 530-550 nm, we investigated an additional emission feature localized at 485/515 nm. This particular green emission feature was attributed to alkylidenefluorene defect structures. This proposal is supported with the synthesis of model copolymers and their optical characterization as described in chapter 2.

One focus of material chemists is to design materials with increase of performance in optoelectronic devices. There has been much interest in the application of cyclometalated complexes as emitting components in such devices. The metal complexes may allow for the efficient utilization of both singlet and triplet excitons generated upon electronic operation. Consequently, internal quantum efficiencies approaching 100% may be achieved. Tuning of the emission colour by manipulating the ligand sphere of the metal atom is also a very attractive goal. Up to the present, there are still relatively few examples of electrophosphorescent (co)polymers as single–component OLED materials. These examples include semiconducting polyfluorenes with side-chain or main-chain iridium complexes, ladder poly(*para*-phenylene)s with electrophosphorescent palladium centers, self-assembled Schiff base polymers and platinum-based side chain copolymers. Transition metal (Co, Ni, Zn) Schiff base polymers have been prepared by oxidative polymerisation, transesterification and condensation of salen-type monomers but they have not been applied in OLEDs.

An often observed disadvantage of blend-based devices is a phase separation of polymer and phosphorescent dye. One strategy to inhibit this phase separation is to incorporate the electrophosphorescent dye into the polymer backbone. The approach presented in chapter 3 describes the covalent incorporation of phosphors into the backbone of a solution-processable semiconducting copolymer. The synthesis of platinum(II) salen complexes and the corresponding polyfluorene-based copolymers is reported in this chapter.

OLEDs were subsequently fabricated and showed promising efficiencies and also demonstrated the potential of this stratagem. Further optimization of the copolymer

structure includes modification of the ligand sphere as well as a variation of the backbone e.g. incorporation of suitable comonomers such as benzophenone which should allow for a more efficient and directed energy transfer between the backbone polymer and the chromophore.

Another remaining task is to improve the lifetime and the efficiency of these materials during their application in OLEDs. The synthesis and characterization of new matrix polymers for triplet emitters is presented in chapter 3.3. The incorporation of benzophenone units into the main chain of polyfluorenes resulted in an improved lifetime for operating OLEDs. Further investigations include the variation of the benzophenone content and the incorporation of phosphorescent metal complexes into the main chain of such copolymers.

Table of Contents

1. Introduction

1.1. Polyfluorenes – An Important Class of Semiconducting Polymers

Electroluminescence (EL) of organic compounds was first described by Bernanose in 1953.[1] The work of Tang and Van Slyke[2] at Kodak in 1987 led to a breakthrough for organic light emitting diodes (OLEDs) and their application in commercial products. They built an OLED device utilizing aluminium tris(8-hydroxyquinoline) **1** as the luminescent material.

The discovery of conducting polymers (i.e. polyacetylene) in 1977 led to intensive research activities in the field of conducting and semiconducting polymers.[3] The importance of this novel class of polymers was recognized by awarding the Nobel Prize in Chemistry to H. Shirakawa, A. G. MacDiarmid and A. J. Heeger in 2000.[3] This research area is highly interdisciplinary and strongly affected by collaboration between chemists, physics and engineers.

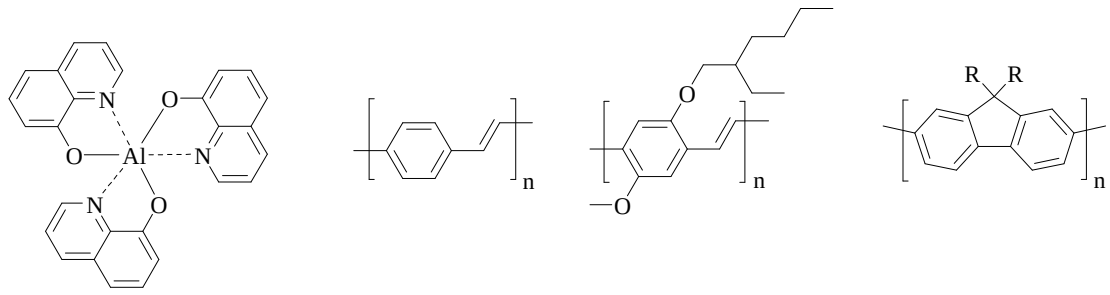

1 **2** **3** **4**

Figure 1. Commonly used electroluminescent materials.

Burroughes *et al*. published the first example of a polymer-based light emitting diode (PLED) in 1990.[4] The polymer which they used as the light emitting layer was poly(*para*-phenylene-vinylene) (PPV) **2**. This discovery led to the development of a series of conjugated polymers used in light emitting diodes (LEDs) like poly[(2-(2-ethylhexyloxy)-5-methoxy-*p*-phenylen)vinylen] (MEH-PPV) **3**, and polyfluorene (PF) **4**.

However, the use of π-conjugated materials is not limited to their application in OLEDs.[5-8] Due to their interesting optical and electronic properties resulting from the extensive π-electron delocalization along the polymeric backbone, these polymers can be applied as the active material in several applications, e.g. organic field effect transistors (OFETs)[9-12], photodiodes[13], sensors[14], polymer lasers[15-19], and organic solar cells.[20-22] The commercialization process of organic electronics is coupled to the availability of appropriate production processes. OLEDs can be for example manufactured based on the technology used for the production of liquid crystal displays (LCDs). Whereas organic transistors have not found a reasonable market until now, they have great promise for highly customized, small-volume products using digital patterning techniques.[23] Polyfluorenes (PF)s are a particularly attractive and promising class of blue light-emitting polymers which exhibit high luminescence quantum yields in solution as well as in the solid state.[24;25] High brightness at acceptable thermal stability is one of their most outstanding features.[26;27] The physical properties of PFs, e.g. thermal stability, colour stability, liquid crystallinity, etc. can be optimized either by modifying the chemical structure or by copolymerization with appropriate comonomers.[28;29] Grell *et al.* first described in 1997 the thermotropic liquid crystallinity of PF.[30] This feature led to the development of an OLED, using an aligned PF layer, which emits linearly polarized light with a polarization ratio of 15 at a reasonable brightness.[31]

The first report on the synthesis of polyfluorenes was published by Yoshino and co-workers in 1989. The polymers were prepared by oxidative coupling of fluorene monomers using $FeCl_3$ as the coupling agent.[32] This non-specific oxidation process produces branched polymers which contain defect structures. In 1991 also blue electroluminescence of polyfluorenes was first described by the Yoshino group.[32;36;37] Investigations on polythiophenes showed that more defined polymers which are free of defects leads to materials with an increased performance of the electroactive and photoactive conjugated polymers.[33-35] Organic chemistry provides a wide range of suitable reactions to produce structurally more defined polyfluorenes. Therefore, the utilization of coupling procedures like Stille-, Heck-, Suzuki- and Yamamoto-type reactions to synthesize fluorene-type polymers and copolymers led to significant improvements. Suzuki- and Yamamoto-type reactions deserve closer attention in particular as they have been very successfully used to

synthesize poly[2,7-(9,9-dialkylfluorene)]s (**4**) and their derivatives with high molecular weight in a well-defined fashion (Figure 2).[26]

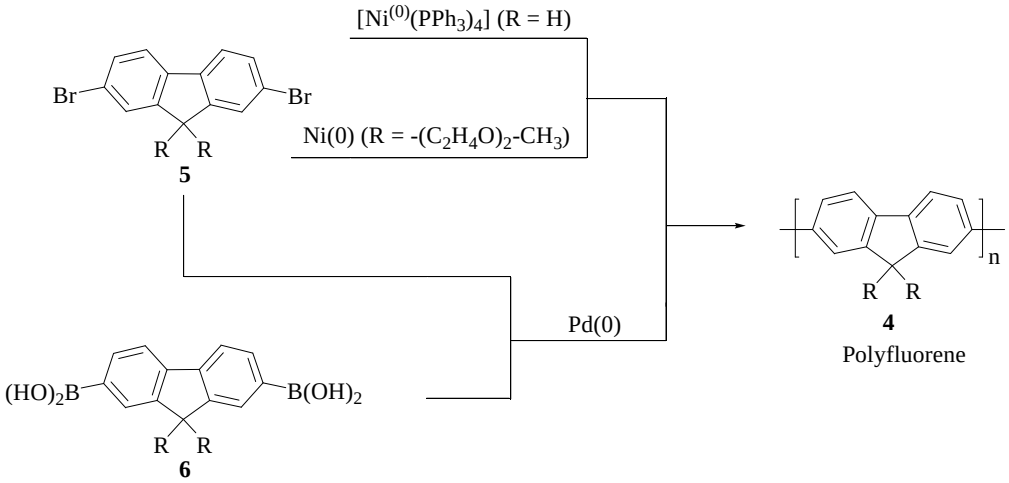

Figure 2. Synthetic pathways to polyfluorenes.

The reductive coupling according to Yamamoto is usually performed using 2,7-dibromofluorene monomers (**5**), but chloro- and iodo-monomers are also viable under these conditions. Percec and co-workers have prepared related polyphenylenes by nickel(0)-mediated coupling of bistriflates and bismesylates.[38;39] Good results were achieved by using bis(cyclooctadiene)nickel(0) ($Ni(COD)_2$) and 2,2´-bipyridyl as the catalyst system. Due to the mild reaction conditions, this procedure has been developed as a valuable alternative to the copper-catalyzed Ullmann-coupling, which requires drastic conditions.[40] A disadvantage of this coupling procedure is the stoichiometrical use of the expensive nickel(0) catalyst. Procedures utilizing inexpensive nickel(II) compounds and a reducing agent such as zinc do not give as good results as those utilizing expensive nickel(0) catalysts.[41] Nevertheless, the use of catalytic systems, for example with manganese or aluminium as the reducing agent, yielded polymers with high molecular weights and similar purities.[42] Suzuki-type cross-coupling polymerizations between 2,7-dihalofluorene and 2,7-diboronylfluorene derivatives (**6**) have also been developed to give polymers with reasonable high number average molecular weight M_n of up to ~ 50,000 $g \cdot mol^{-1}$ using phase transfer agents and boronic ester monomers in a two-phase solvent system.[43;44] Also such Suzuki-type reactions can be carried out in a controllable fashion yielding narrowly distributed polyfluorenes.[45;46]

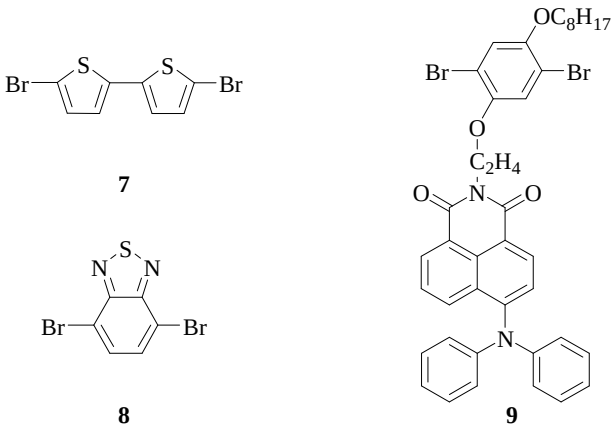

Figure 3. Monomers used to alter the band-gap of PF-type copolymers.

Polyfluorenes exhibit a blue photoluminescence at approximately 420 nm. Modified polyfluorene-type copolymers have been synthesized that emit light in the whole range of the visible spectrum. This could be achieved by a modification of the band-gap energy, e.g. by incorporating monomers with a lower HOMO/LUMO-gap such as 5,5´-dibromo-2,2´-bithiophene **7** or 2,1,3-benzothiadiazole **8** resulting in yellow and yellow-green emission, respectively. Efficient green and white light emission from appropriate polyfluorene-based copolymers with **9** as comonomer was achieved by Tu *et al*. (Figure 3).[47;48]

Investigations of the emission behaviour of polyfluorene derivatives are still underway. Different phenomena as the occurrence of red shifted emission components have been intensively studied and have been related to the formation of excimers or aggregates.[49-52] However, as derived from spectroscopic investigations, the appearance of this undesired spectral features is mainly caused by oxidative degradation under formation of fluorenone sites at the polymer backbone.[24;53-63]

1.2. Organic Light Emitting Devices

This chapter will provide a short introduction into OLED devices including the physical processes of light generation The basic device structure of an organic light emitting diode (OLED) consists of an electroluminescent material which is sandwiched between two electrodes. The material which is used for the cathode should have a low work function and is typically calcium or aluminium/lithium fluoride. The cathode can be vacuum deposited onto the emissive layer. Indium tin oxide (ITO) is mostly used as the anode. It is transparent and can be deposited onto a glass or polymer substrate.

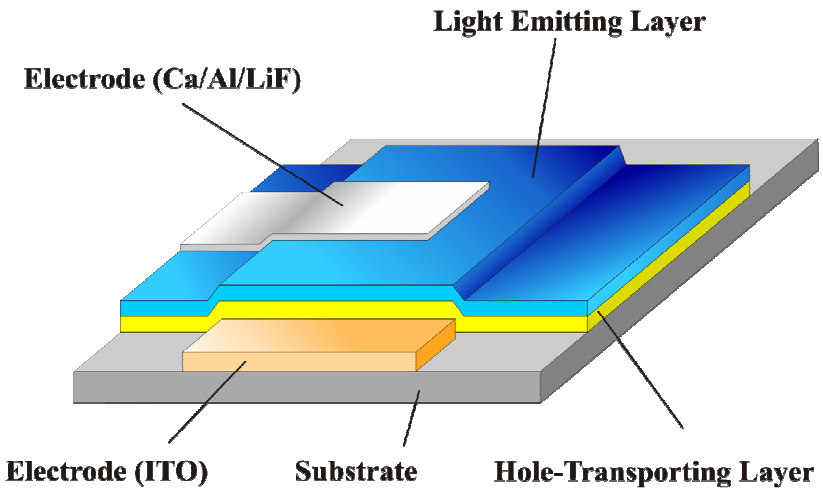

Figure 4. Typical structure of a two-layer electroluminescent organic diode.

This so-called sandwich structure can be modified in different ways (e.g. by optimizing the outcoupling of the light, the use of optimized electrodes, etc.).[64;65] One strategy to increase the efficiency of OLEDs is to use more than one organic layer in order to optimize the charge injection, the charge transport and the charge recombination (Figure 4).

The external quantum efficiency depends dramatically on a balanced injection of charges and the recombination rate of the injected charges in the emission layer. The external quantum efficiency is the product of the radiative quantum efficiency η_R of the emitter and the probability Φ_{ex} that photons, which are generated in the emission layer, leave the device. Greenham *et al*. predicted a range between 15 and 25% for Φ_{ex} depending on the refractive index of the active layer.[66] Due to the separate injection of electrons and holes,

their spin is uncorrelated and therefore, no spin selectivity is taking place in recombination processes. Simple spin statistics give a threefold higher probability for the formation of triplet states than singlet states (see also chapter 1.4.).

Radiative transitions from triplet to singlet states are spin-forbidden so that overall only 25% of the excited states formed could be utilized for light emission. However, some experiments indicate that this limit can be higher, in the order of 45%.[67-69] To reach 100% internal efficiency, it is essential to use also the triplet states for radiative emission. The fundamental steps in OLEDs yielding in emission of light are shown in Figure 5: (a) and (a´) electrons and holes injected into the LUMO and the HOMO, respectively; (b) charge transport and recombination resulting in an excited state; (c) radiative relaxation of the singlet excited states; (d) non-radiative decay of the triplet excited states.

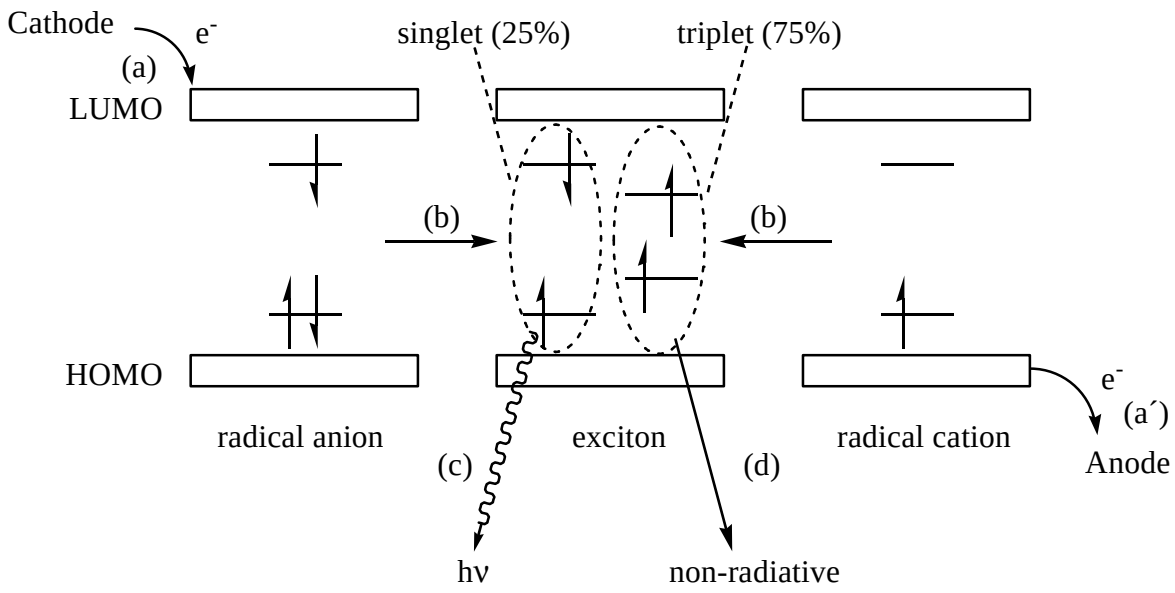

Figure 5. Electron and hole injection forming excitons and their deactivation channels. (a) and (a´) injection of electrons and holes (b) transport through one or more organic layers resulting in an exciton (c) relaxation of the excited singlet state through radiative decay and (d) non-radiative decay of the triplet excited state.

These steps influence the different material requirements for OLED applications. The ionization potential and electron affinity are ,hereby, an important issue of the organic materials. Materials having a low ionization potential (or electron affinity) may function as hole-transporting materials. At the same time materials with a high electron affinity (or ionization potential) can act as electron-transporting materials. This clarifies that electron-

donating or electron-accepting properties affect the hole-transporting or electron-transporting properties of the materials, respectively. Therefore, a sufficient emitting layer in single-layer devices needs to fulfil both requirements. The emitting layer acts as the recombination layer for holes and electrons as well as the transport medium for the charge carriers.

1.3. Properties of Polyfluorenes

The thermal stability of polyfluorene homo- and copolymers are very good as their decomposition temperature exceeds 400°C. Polyfluorene, or to be more precise, dialkylated PFs in solution typically emit blue light at a wavelength region of 415-420 nm (2.99-2.95 eV) in combination with two additional vibronic side bands at 439-445 nm and 470-475 nm assigned to 0-0, 0-1 and 0-2 intrachain singlet transition. In the case of poly[2,7-(9,9-bis(2-ethylhexyl)fluorene)] (PF2/6) the emission properties in the solid state and in solution are more or less identical whereas the solid state properties of poly[2,7-(9,9-dioctyl)fluorene] (PFO) strongly depend on the film preparation and the posttreatment conditions of the film (see chapter 1.3.1 and 2.4). Optical spectra of PF2/6 are shown in Figure 6. The relative low intensity of the 0-0 transition in the solid state is most probably due to self absorption effects. In diluted solution PF polymers exhibit an unstructured π-π^* absorption with a maximum at ca. 383 nm (3.24 eV).

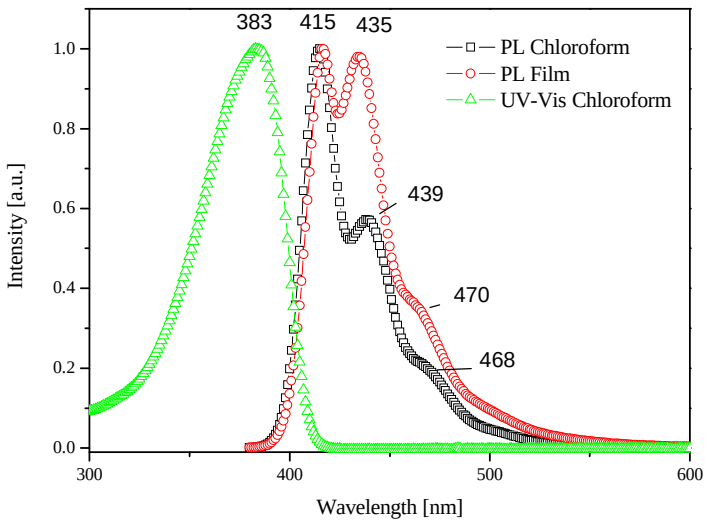

Figure 6. Absorption and emission spectra of polyfluorene.

The photoluminescence quantum yield in solution is ca. 80%[26] and very high photoluminescence quantum yields in the solid state of >50% have been reported.[70;71] PF homopolymers are characterized by high ionization energies. Different values are reported for the absolute energy of the LUMO varying from 5.5 to 5.8 eV.[36;72] This leads to differences in the reported values for the band-gap energy between 3.5 and 3.2 eV.[73] The difference between the optical gap E_g = 2.95 eV (as defined by the absorption onset) and the reported band-gap energies of 3.2-3.5 eV as determined by cyclovoltammetry represents the so-called exciton binding energy of approx. 0.3-0.5 eV.[74]

The sensible interplay between the optoelectronic properties, the solid state structure and defects in polyfluorenes has been the subject of extensive investigations in the last years.[24;75;76] Hereby, the chain conformation defines an very important parameter. Comparing for example PFO and PF2/6 (Figure 7), a minor change in the side chain structure results in distinct differences of the physical properties of these two polymers.
PF2/6 adopts a helical conformation of individual chains. They form crystalline (hexagonal), nematic and isotropic phases with increasing temperature. Absorption and photoluminescence properties of thin films of PF2/6 are not much dependent on the phase and processing history.

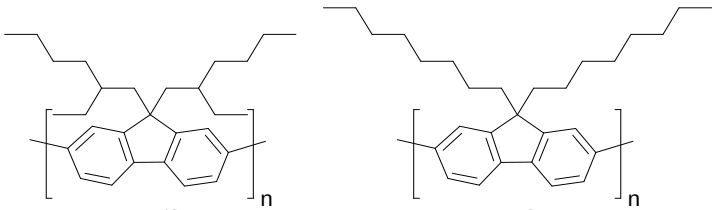

PF2/6 **4a** PFO **4b**

Figure 7. Chemical structures of PF2/6 and PFO.

The photophysical properties of PFO vary strongly with the morphology of the sample.[24;77;78] Different solid-state phases have been observed for PFO, such as a disordered glassy phase and crystalline α- and β-phases.[79] The solid-state structure of PFO as hairy-rod polymer is heavily dependent on the processing history.[71;80-83]

1.3.1. Relationship of Structure and Emission Behaviour - The *β*-Phase

Comparing the absorption maximum of PF2/6 (λ_{max}=383 nm) and PFO (λ_{max}=389 nm) in dilute solution the maximum of PF2/6 shows a slight hypsochromic shift of ~ 6 nm. This can be attributed to a somewhat larger distortion angle between two neighboring fluorene units in PF2/6.[84]

In the solid state, PFO shows the formation of a higher ordered phase (*β*-phase) in addition to the common hexagonal *α*-phase.[71] This *β*-phase is characterized by a bathochromic shift of the absorption and emission spectra. This is due to the formation of a sheet-like solid-state structure forced by side-chain crystallization.[85] Several approaches to suppress the formation of the *β*-phase such as the use of bulky side groups or the incorporation of spiro-bifluorene units into the main chain have been described.[50;86]

One other approach, which was investigated in our group is the incorporation of non-planar 1,1´-binaphthyl structural units into the main chain of polyfluorenes to suppress *β*-phase formation. In fact, it was found that the random incorporation of binaphthyl units into the PFO backbone sufficiently suppresses the *β*-phase formation in the solid state (Figure 8).[87] PFO homopolymers (0%) exhibited PL features originating from the *β*-phase with the main band peaking at 442 nm. With increasing concentration of binaphthyl units (4.2, 9.4 and 12.1%) the contribution originating from the *β*-phase at 442 nm becomes weaker and is even absent for a copolymer with 12% of binaphthyl units.

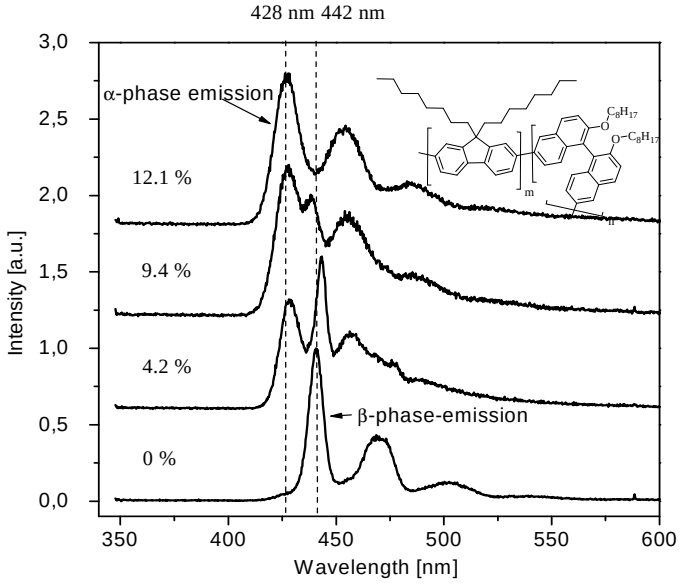

Figure 8. Emission of PFO homopolymer (0%) and binaphthyl-9,9-dioctylfluorene-copolymers at low temperature (T=30K). Films were spin cast from toluene solutions**.**

1.3.2. Origin of the Green Emission

Polyfluorenes have been the subject of intense research as they are promising materials for blue light emitting diodes. One major problem of polyfluorenes is their colour instability especially in electroluminescence (EL) leading to a broad low-energy EL band with its maximum located at 525-540 nm. The pure blue emission changes as a result of this degradation to a blue-green emission. The origin of the green emission is still the subject of intense research. More and more accepted by the majority of research groups, this emission is caused by defects, which may result from an oxidative degradation of only monoalkylated fluorene units which are present as a small impurity. The defects have been assigned to keto defects (fluorenone defects). Other researchers have postulated the formation of crosslinked fluorene units as the origin of the defects (Figure 9).[24;54;56;63;88;89]

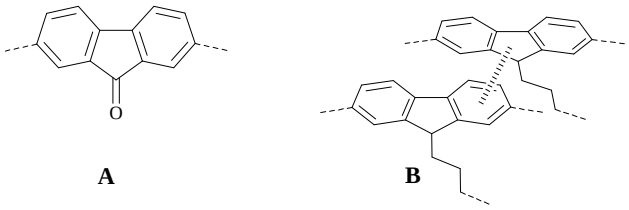

Figure 9. Possible degradation products of fluorene-based polymers (A: keto defect, B: crosslinked units).

The origin of residual monoalkylated building blocks should be caused by monoalkylated fluorene monomers that remain after the workup of the monomer **5**. The amount of monoalkylated fluorene monomer is difficult to determine. These monoalkylated building blocks are expected to form fluorenone defects in an oxidative degradation process. Standard analytical detection methods of organic chemistry failed since low impurity levels within the monomers can not be detected. HPLC and GCMS do not show any traces of impurities in the monomers purified by column chromatography. The process of fluorenone defects generation can be explained as following: The monoalkylated fluorene units are deprotonated into fluorenyl anions. Subsequently, the formed fluorenyl anions are oxidized by oxygen to hydroperoxide anions.

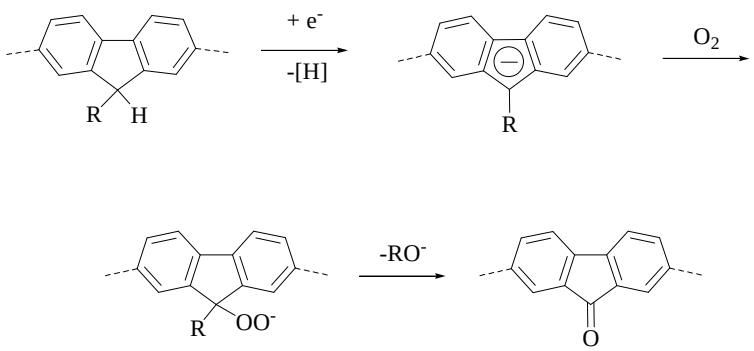

Figure 10. Possible pathway for the generation of fluorenone defects**.**

Finally, the fluorenone defects are formed in a rearrangement step. This oxidation pathway is shown in Figure 10. In polyfluorenes these fluorenone defect sites can act as traps for excitons or electrons. Excitons can be accumulated in these traps and this results in the emission of the lower energy light (keto-defect emission).[56;89]

The typical featureless emission band of such keto-defects is peaking at ca. 535 nm. Meijer *et al*. prepared polyfluorenes starting from specially purified monomers.[88] They observed the absence of the green emission band for polyfluorenes synthesized from such monomers of highest purity.

As outlined, the origin of the green emission is addressed to oxidatively formed defects within the polymer backbone as origin of emission instability[24;53;56-59;61] beyond simple quenching.[90] A dispute about the role of chain conformation and in particular interchain or intersegmental interactions is still actively taking place,[51;53] especially due to the formation of intermolecular excimers* between two polyfluorene chains with or without the participation of fluorenone defect units.[54] Bliznyuk *et al.* first assigned the formation of a green emission band at 520 nm to an excimer emission. However, they also carried out *in-situ* FTIR studies during device degradation and observed the formation of fluorenone defects which quench the blue luminescence component of the polymer.[54] Scherf *et al.* extensively studied the degradation of polyfluorenes and the green emission band at 535 nm. They concluded that the emission is not caused by an excimer formation and can be addressed to a monomolecular process.[53;91] In contrast, Sims *et al*. related the green emission to excimers of two fluorenone defects located at adjacent chains or chain

* An excimer (short for excited dimer) is a dimeric molecule or complex formed from two species where at least one of them is in its electronic excited state.

segments.[51] Montilla and Mallavia described an additional green band located at 485/515 nm which preferably occurs in degraded light-emitting devices which were fabricated and operated under inert conditions.[89;92-94] For this electrochemical degradation they proposed the occurrence of crosslinked polyfluorene chains as supported by IR and FTIR spectroscopy.

1.4. Electrophosphorescence

The following section gives a short introduction into the application of electrophosphorescent materials in OLEDs. As mentioned before, it is favourable to also utilize triplet excited states in operating OLEDs to achieve, at least in principle, a four times higher electroluminescence efficiency compared to singlet emitters. Electrically driven phosphorescence in OLEDs without phosphorescent dopants have only been observed at low temperatures.[95] Impurities of heavy metals into organic molecules can lead to an electrically driven phosphorescence (electrophosphorescence).[96;97] Remarkably, whether it is due to design or serendipidity, only a trace amount of the heavy metal atoms is necessary for efficient triplet emission. However, no efficient OLED has yet been reported based on such approaches. Baldo *et al*. showed in 1998 that the use of phosphorescent dyes as dopants improves the efficiency of OLEDs.[98] The phosphorescent dye octaethyl-porphyrine platinum (PtOEP) (**10**) (Figure 11) was doped into a small molecule organic host at low concentration. In 1999 Friend and Tessler *et al*. applied PtOEP as a dopant in a semiconducting polymer host.[99]

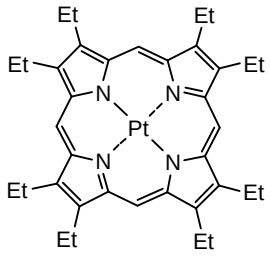

PtOEP

10

Figure 11. Structure of PtOEP.

Research on the application of such phosphorescent small molecule dopants has revealed efficiencies of 11.6%,[100] 19.2%[101;102] and 10.3%[103] for blue, green and red emission, respectively.

Recombination of charges in the organic material doped with a triplet emitter occurs in different steps. The first step is trapping of a charge carrier at the emitter molecule (electron or hole).[104] This trapped charge carrier can induce an electronic force to its neighbourhood. If the opposite charge carrier migrates along the matrix towards the electrode (due to the applied external voltage) and is not close to the trapped charge, it will not be influenced by the Coulomb attraction of the trapped charge. Thus, it migrates independently towards the electrode.

If the charge (e.g. a hole) comes under the trapped electron's influence, it will result in a bound hole-electron pair. The two spins of electron and hole are coupled to four new combined states, a singlet state and a triplet state, with the triplet state having three sub-states. The Coulomb attraction forces the hole to move towards the trapped electron. When the hole reaches the hole-trapping triplet emitter an excited state is formed. The system will then show the typical behaviour of an optically excited molecule with its emission properties.[105] Herein, the heavy metal of the triplet emitter repeals the spin forbidden transition resulting in phosphorescence. Very frequently used phosphorescent emitters are often based on iridium complexes (Figure 12, Table 1).

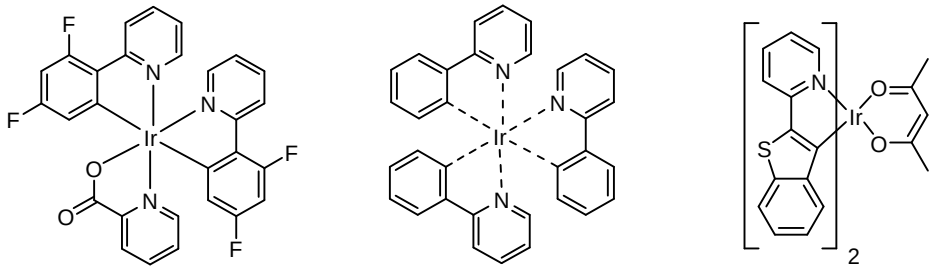

FIrpic **11** | $Ir(ppy)_3$ **12** | $Btp_2Ir(acac)$ **13**

Figure 12. Electrophosphorescent iridium complexes: bis(2-(4,6-difluorophenyl)pyridyl-N,$C^{2'}$)iridiumpicolinate (**11**) (FIrpic), fac-tris(2-phenylpyridine)iridium (**12**) ($Irppy_3$) and bis(2-($^{2'}$benzothienyl)-pyridianto-N,$C^{3'}$)iridium(acetylacetonate) (**13**) ($Btp_2Ir(acac)$).

There has been much progress in the application of cyclometalated complexes as emitting components in electroluminescent (EL) devices.[106-112] Consequently, internal quantum efficiencies approaching 100% by utilizing of both singlet and triplet excitons (which are

generated upon charge injection from the electrodes) may be achieved. Although many examples of electrophosphorescent metal complexes have been described, there are still relatively few examples of electrophosphorescent (co)polymers as single–component OLED materials.

Table 1. Properties of common Ir-emitters and their colour coordinates in the International Commission on Illumination (CIE)-diagram (right).

Name	$Btp_2Ir(acac)$	$Ir(ppy)_3$	FIrpic
Colour	**red**	**green**	**blue**
CIE	**0.66/0.33**	**0.31/0.60**	**0.17/0.30**
Efficiency [cd/A]	**10**	**75**	**19**

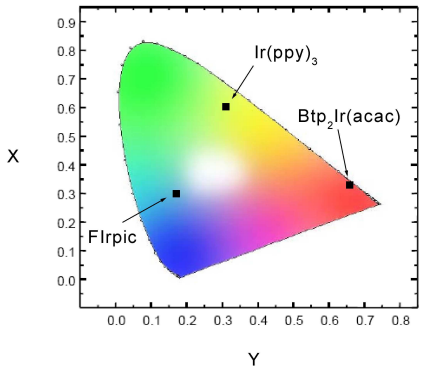

Examples include semiconducting polyfluorenes with side-chain or main-chain iridium complexes,[113;114] ladder poly(*para*-phenylene)s with electrophosphorescent palladium centres,[97] self-assembled Schiff base polymers[115] and platinum-based side chain copolymers.[116] Transition metal (Co, Ni, Zn) Schiff base polymers have been prepared by oxidative polymerisation, transesterification and condensation of salen-type monomers, but they have not been applied to OLEDs.[117]

1.4.1. (Matrix)polymers for Electrophosphorescence

To guarantee an efficient energy transfer from the matrix polymer to the triplet emitter, the matrix has to be designed in a well-defined fashion. Most phosphorescent dyes used in OLEDs have their absorption maximum in the UV-wavelength region. To insure efficient energy transfer, wide bandgap materials are suitable hosts. Two commonly used hosts are shown in Figure 13. The function of the guest has also to be taken into account. The dye can act as a charge trap and a recombination site if there is a significant offset between the HOMO (or LUMO) positions of the host and the guest.[118] This has also a great impact on the operating voltage of OLEDs. For example, an effective injection and transport of charge carriers lowers the operating voltage.[119] However, the charge-trapping by the dopants increases the driving voltage of OLEDs.[92;120;121] If the dopant material acts as a hole trap, the HOMO level could be above that of the host material. For efficient triplet

exciton harvesting it is necessary that the triplet energy of the emitter is lower than that of the host. Using high-energy triplet emitters (e.g. in the green or blue) the “back”-transfer of triplet excitons from the triplet emitter to the host material has to be avoided.

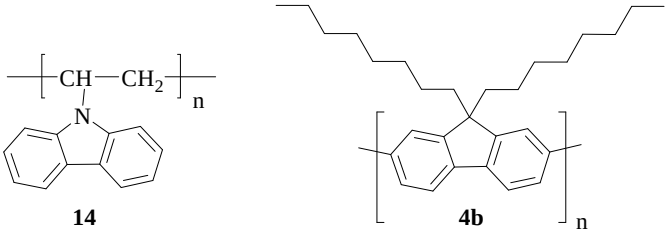

Figure 13. Typical Host Polymers**.**

Contrary to small molecule based OLEDs, usually no additional charge injection layers are used. Therefore, the HOMO and LUMO levels of the host polymer should be close to the Fermi-levels of the anode and cathode, respectively. One approach to highly efficient polymeric OLEDs was presented by Neher and co-workers based on the poly(vinylcarbazole) (**14**) (PVK) host doped with the electron-transporting molecule 2-(4-biphenyl)-5-(4-tert-butylphenyl)-1,3,4-oxadiazole (**15**) (PBD) and a soluble Ir-dye as guest.[122] A promising but more expensive approach is the fabrication of multi-layers devices where a hole blocking/electron transporting layer is finally evaporated onto a solution-processed emissive layer.[123;124] The multi-layer fabrication of solution-processed OLEDs can also be achieved by the conversion of soluble precursors to an insoluble polymer film via crosslinking of reactive side groups as extensively demonstrated for hole-transport layers.[125-127]

A schematic representation of the electronic levels of phosphorescent dyes, charge-transporting materials and some host materials is given in Figure 14. For example, in the case of green-emitting dyes, PVK (**14**) is an ideal host because its triplet energy is only slightly higher than that of $Ir(ppy)_3$. The HOMO of PVK is rather low so the charge injection at the ITO electrode is hindered due to a large hole-injection barrier. The electron mobility of PVK is very low causing the need of additional electron-transporting dopants such as PBD[128;129] or other electron-transporting molecules (Figure 15).[130] The lifetime of PVK-based OLEDs is rather short. Therefore, the application potential in commercial products is limited.

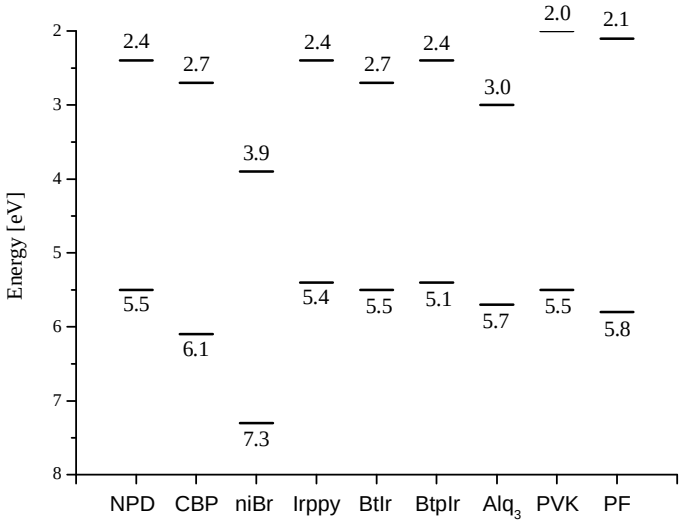

Figure 14. Positions of the HOMO and LUMO levels for various phosphorescent dyes, charge-transport- and host materials commonly used in OLEDs. [Alq_3: Aluminium(III)-tris(8-hydroxyquinoline), BtIr: bis(2-phenyl-benzothiozolato-n,$C^{2'}$)iridium(acetyl-acetonate), Btp(Ir): $btp_2Ir(acac)$, NPD: 4,4´-bis(N-(1-naphthyl)-N-phenylamino)-biphenyl, CBP: 4,4´-N,N´-dicabazolebiphenyl, Irppy: $Ir(ppy)_3$, niBr: N-2,6-dibromophenyl-1,8-naphthalimide, PF: polyfluorene, PVK: poly(vinylcarbazole)]

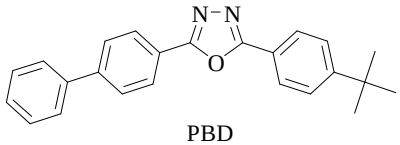

PBD

15

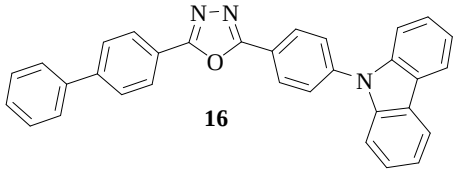

16

Figure 15. Electron transporting moieties based on 1,3,4-oxadiazoles**.**

As alternative to PVK, only few host polymers have been successfully applied to red and green phosphorescent dyes. One example is poly(2-(6-cyano-6-methyl)-heptyloxy-1,4-phenylene) (CNPPP).[131] Polyfluorenes are suitable hosts for red but not for green emitting iridium dyes because of its small triplet energy (2.1-2.3 eV).[132;133] Brunner *et al.* studied carbazole-based homo- and copolymers as hosts for green emitting phosphorescent dyes.[134] They found that the triplet energy of the host is determined by the maximum length of conjugated oligo(*para*-phenyl) segments in the macromolecule. This finding led to a valuable design rule towards host polymers for a certain triplet emitter.

1.5. Aim and Scope

The interplay between the chemical structure of π – conjugated polymers or oligomers and their macroscopic optical or electro-optical properties is complex in nature and not fully understood at the moment. It is crucial to design novel materials at the molecular level to tune the electronic properties and to improve the performance of devices made of these materials. Moreover, the nature of impurities and defects has also attracted great attention because of their remarkable influence on device performance.

Therefore, the first part of this thesis (chapter 2) deals with the origin of unwanted lower energy emissions in polyfluorenes. There is solid evidence that the formation of green PL/EL bands is not only caused by the formation of keto defects. To get a better insight into the degradation-based lower energy emission bands of polyfluorenes, novel polymeric model systems containing a certain amount of alkylidene “defects” incorporated into the main chain have been synthesized. Optical characterization is presented which implies that the green emission component observed preferably in electroluminescence can be addressed to additional defect structures besides the keto defect.

The second part of this work deals with the synthesis and characterization of electrophosphorescent copolymers. The syntheses of triplet emitters which are suitable as monomers for the preparation of electrophosphorescent polymers are described. Hereby, triplet emitters based on Pt(II)-salen complexes were synthesized and tested in OLEDs. In this first case the emitting layer (as blend) was solution-processed by mixing the dye as dopant into a polymeric host. The main target was to incorporate the triplet emitter into the main chain of a conjugated polymer (polyfluorene). This strategy should avoid morphological problems like phase separation. These (co)polymers were then tested as light emitting materials in phosphorescent OLEDs.

Chapter 3. also describes the synthesis of novel host materials with the aim of realizing improved device lifetimes. Consequently these results are adopted onto the synthesis of main-chain electrophosphorescent copolymers.

2. Polyfluorenes

2.1. Motivation

Polyfluorenes emerged as important candidates for blue light emission in OLEDs with its emission maximum located at approx. 420 nm. Some of the remarkable properties of polyfluorenes have been described in chapter 1.3, e.g. their thermal stability, high photoluminescence quantum yields etc. However, the lifetime of OLEDs with PF as the emitting layer especially concerning the colour stability of electroluminescence is limited. Therefore, this issue is very important and still the subject of intense research. There are several reports in the literature which deal with different explanations for the origin of additional green emission components in polyfluorenes. Moreover, different types of such green emissions at different spectral positions have been observed. The green emission located at 535 nm has been mainly addressed to keto defects. An alternate assumption involving interchain crosslinks as defects formed during the degradation was made by Zhao *et al*.[135] Another green emission band has been observed in the region of approx. 480-515 nm, especially in electroluminescence. In light emitting devices which were build under inert conditions this particular green band also appears. Possible pathways for an oxidation of PF segments in the absence of oxygen have been discussed.[89;92]

The oxidation of monoalkylated fluorene under formation of keto defects has already been discussed in the introduction. The prerequisite for an oxidation of fluorene to fluorenone units is the presence of oxygen either during work up of the polymer or during device operation. Polyfluorene-type copolymers containing non-planar binaphthyl-spacers have been used to investigate if a spacial separation of the defects is possible in order to avoid exciton migration to the defect sites.

2.2. Polyfluorenes containing Alkylidene Building Blocks

As the nature of different green emission bands in polyfluorenes is still not fully understood at the moment we started to deal with another potential class of defects which probably maybe also involved in the degradation processes. The formation of alkylidene-type defect structures (alkylidenefluorene units) is proposed in Figure 16. This kind of defect formation has not been investigated until now to the best of our knowledge. In the generation of such alkylidenefluorene defects as during keto defect formation, the acidic hydrogen of the methylene bridge of only monoalkylated fluorene units (**I)** can easily be deprotonated to the corresponding aromatic fluorenyl anion (**II)**. Radicals (**III**) can be formed by abstraction of an electron (e.g. at the cathode). A second deprotonation step finally results in the formation of alkylidene species (**IV**). This pathway for the formation of alkylidene species (Figure 16) should probably include the formation of hydrogen produced in the reduction of protons at the cathode. Investigations to prove this assumption are ongoing, e.g. the possible detection of hydrogen in an operating OLED device.

As mentioned, the green emission band localized at 485/515 nm has been reported several times but not identified.[92;136-138] Scherf and List *et al.* observed this emission component and attributed it to interface defects but without any assignment of a concrete defect structure.[89] In 2006 Galambosi and Scherf *et al*. proposed the occurrence of alkylidene defect structures.[139]

As done in the modeling of keto (or fluorenone) defects where different amounts of fluorenone units were randomly incorporated into polyfluorenes, we decided to synthesize a new model copolymer with randomly incorporated alkylidene units.[53;140] The random incorporation of alkylidene-defects into the PF main chain should allow for an detailed insight into the origin of the green emission components. Copolymers with different amounts of an alkylidenefluorene comonomer have been, therefore, synthesized and investigated for a correlation between the concentration of the alkylidene units and the emission behaviour.

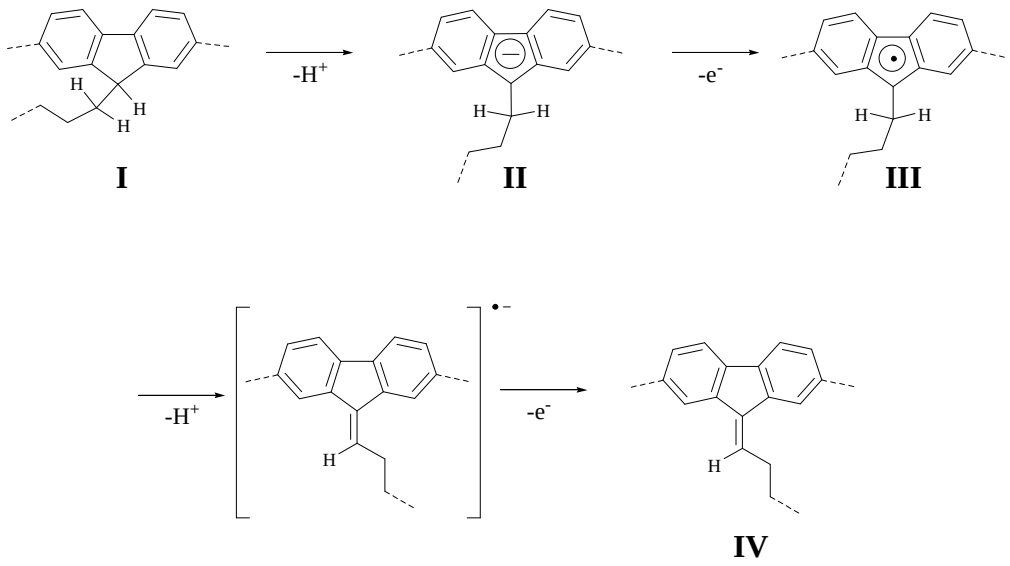

Figure 16. Possible pathway to alkylidene defects**.**

2.2.1. Results and Discussion

2.2.1.1. Monomer Synthesis

Alkylidene-substituted fluorenes containing methyl and ethyl side chains have previously been prepared by Leclerc *et al*. by the reaction of fluorenones with the corresponding alkyl Grignard reagent.[141] They synthesized copolymers containing such an alkylidene moiety to prepare base-doped, anionic polyfluorenes which showed an electrical conductivity of up to 10^{-2} S/cm. These materials are expected to be useful as polymeric electrolytes in solid-state electrochemical devices as well as n-type electrically conducting polymers. McCulloch *et al*. prepared alkylidene-substituted fluorenes with longer side chains in two steps starting from dibromofluorene.[142] The first step involves the formation of a ketene dithioacetal by condensation of a preformed fluorenyl anion with carbon disulfide, followed by an in situ alkylation of the resulting ketene dithiolate anion with methyl iodide to give dimethylated thioacetal. Treatment of the ketene dithioacetal with alkyl Grignard reagents resulted in the dialkylated products with yields varying from 20-60% (Figure 17). The OFET properties of poly(alkylidenefluorene)s were investigated with regard to the ability to form a closely packed, π-stacked morphology. However, none of the above

described alkylidene-substituted fluorene (co)polymers were examined concerning their luminescent properties.

Different synthetic strategies can lead to 2,7-dibromo-9-alkylidene fluorene monomers (**18**) (Figure 17) which are suitable for a copolymerization with 2,7-dibromo-9,9-dioctylfluorene. The synthesis according to Bachman and Polansky via a condensation of fluorene with the corresponding aldehyde under basic conditions gave product mixtures which were difficult to purify (Figure 17).[143] Better results were obtained utilizing fluorenone in a Wittig-type reaction with the corresponding ylide. The pure product **18** was obtained after column chromatography with hexane as the eluent and recrystallization from ethanol in a yield of only 15% following procedure C (Figure 17) (reaction conditions not optimized).

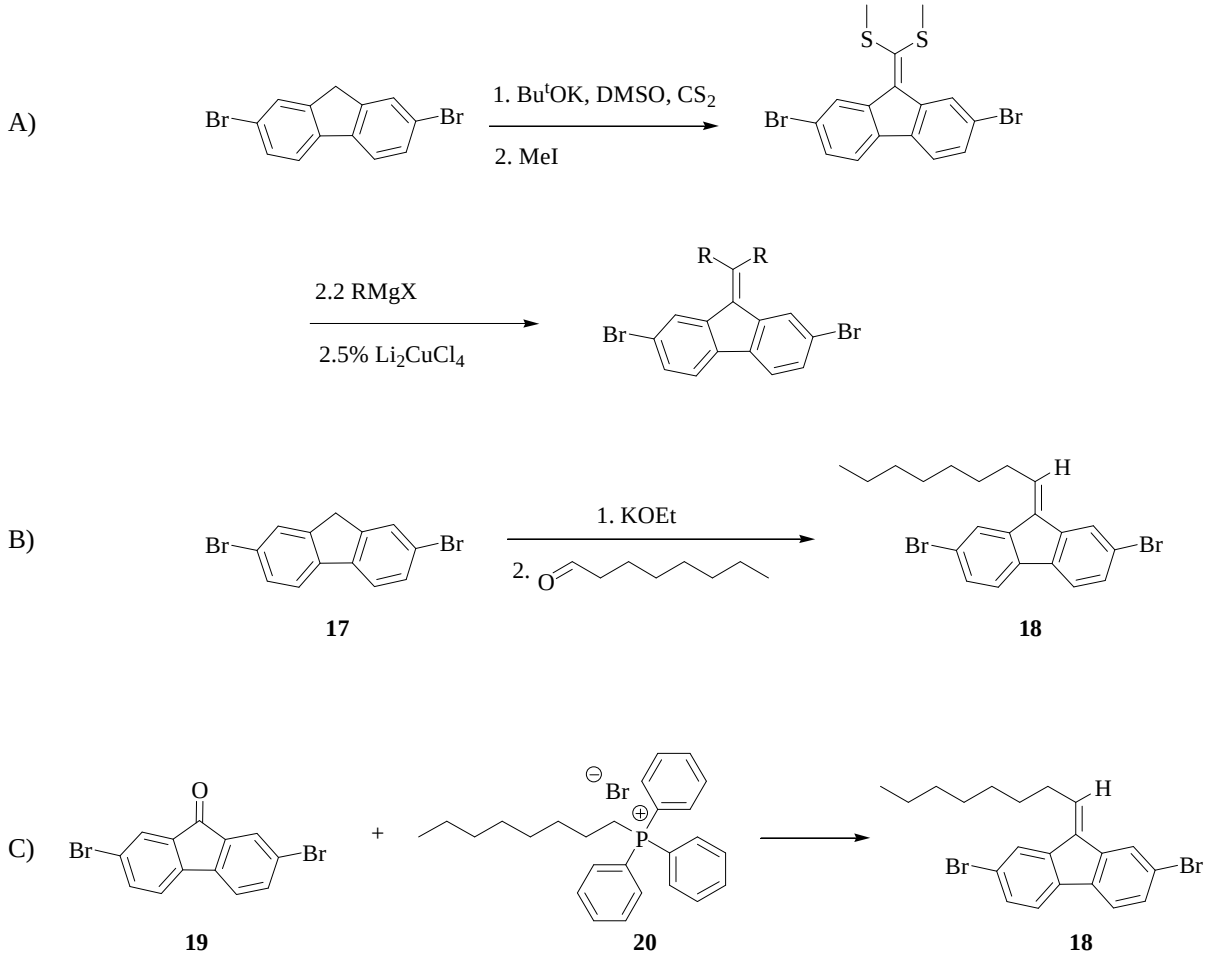

Figure 17. Synthetic pathways towards alkylidene substituted fluorene monomers.

^{1}H NMR analysis of **18** shows the formation of the alkylidenfluorene. The alkylidene proton shows a triplet at 6.76 ppm with a coupling constant of J = 7.4 Hz (Figure 18).

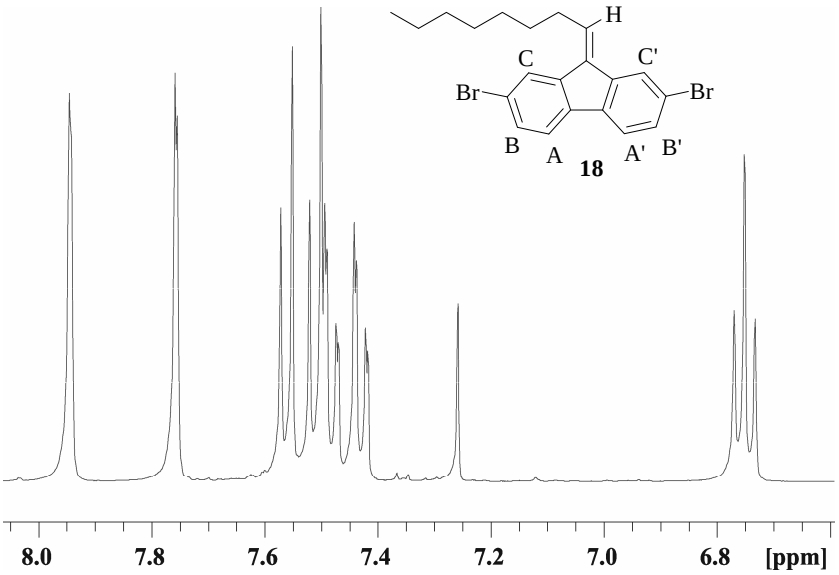

Figure 18. ^{1}H NMR of the aromatic region of **18** in $CDCl_3$ with residual $CHCl_3$ at 7.27 ppm.

Compared to 2,7-dibromo-9,9-dioctylfluorene (**5b**) where the mirror symmetry of the molecule leads to a simplified NMR spectrum, the mirror symmetry is not given for **18** due to the presence of the alkylidene substituent. The two doublets at 7.87 and 7.69 ppm can be assigned to C and C´. Two AB systems are peaking between 7.6 and 7.4 ppm with 4 pseudodoublets as an ABA´B´ spinsystem. The pseudodoublets of B and B´ at 7.43 and 7.37 ppm are coupled to two doublets of doublets.

9,9-Dioctyl-2,7-dibromofluorene (**5b**) was obtained by the alkylation of 2,7-dibromofluorene (**17**) under basic conditions (Figure 19).[144]

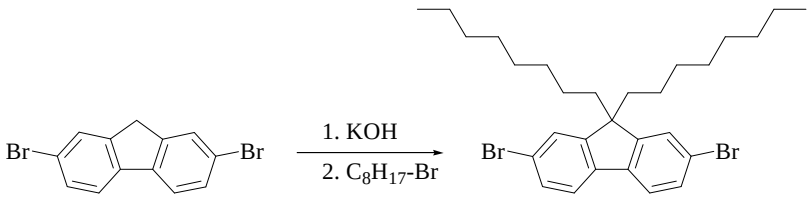

Figure 19. Synthesis of 9,9-dioctyl-2,7-dibromofluorene **5b**.

To avoid residues of mono- or non-alkylated monomer **5b,** the purification of **5b** has to be done very carefully. The crude product was purified by column chromatography. Hexane was used as the eluent under generous fractionation to avoid the presence of

monoalkylated monomer. Recrystallization from ethanol gave the pure product which was not contaminated with byproducts in the sensitivity limit of standard analytical methods (HPLC, NMR and MS). Our experience has shown that melting of the monomers under high vacuum is suitable to eliminate traces of alcohol, which remain from the recrystallization, necessary to obtain high molecular weight polymers.[145]

2.2.1.2. Polymer Synthesis

Subsequently, the copolymers were synthesized using the standard nickel(0)-mediated coupling method according to Yamamoto (Figure 20). The synthesis was slightly modified using THF instead of DMF/toluene mixtures as the solvent to stabilize the reactive nickel(0) species.[146;147] It has been shown that this synthetic protocol resulted in increased molecular weights and in a more convenient reaction procedure.[146]

Two series of "defect" containing polymers were synthesized. One was made with a "standard" monomer **5b** (**P4**-**P7**) and the other with a monomer **5c** which was additionally purified according to Meijer *et al.*[88] (**P1**-**P3**). To exclude the formation of fluorenone defects originating from an oxidation of residual monoalkylated fluorene units the monomer **5b** was treated three times according to this procedure with the use of Schlenk techniques and with extensively dried basic aluminium oxide to give the monomer **5c**. The additional purification was performed by treating the monomer with potassium *tert*-butoxide in dry THF to deprotonate monoalkylated species followed by filtration through aluminium oxide to remove the deprotonated, anionic species.

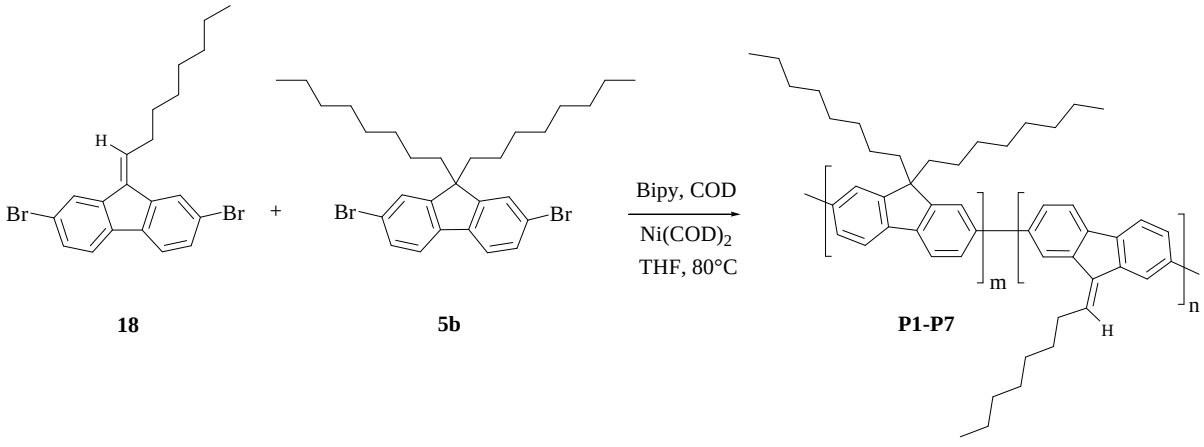

18 **5b** **P1-P7**

Figure 20. Synthesis of the alyklidene-containing polyfluorenes **P1**-**P7**.

In the case of the monomer **5c** copolymers with three different defect concentrations of 1, 2 and 5% (**P1**, **P2** and **P3**) were synthesized. Four different concentrations were used for the synthesis of the copolymers based on the "standard" monomer **5b** (0.5, 1, 2 and 5%). The monomers **5b** and **5c** should be incorporated into the copolymers in a random fashion.

After 5 days of reaction bromobenzene as monofunctional endcapper was added and the mixtures were stirred for further 24 hours to remove unreacted bromine end-groups. Thereafter, the reaction mixtures were treated with dioxane/HCl and stirred for 15 minutes to stop the reaction. This reaction protocol is known to yield in polymers containing only a very small amount of bromine end-groups.[144] The crude polymers were precipitated from a concentrated chloroform solution into methanol.

The polymers **P1**-**P3** (made of monomer **5c**) were Soxhlet extracted with ethyl acetate for one day to remove low molecular weight fractions. A summary of the molecular weights and the thermal properties of the copolymers are given in Table 2.

Table 2. Molecular weight and thermal properties of polymers **P1**-**P7**.

Polymer	Defect [%]	M_n [g/mol]	M_w [g/mol]	PD [M_w/M_n]	T_g [°C]	$T_{C\rightarrow LC}$ [°C]
P1	1[a)]	63,700	125,200	2.0	97	160
P2	2[a)]	59,800	115,200	1.9	n.o.	158
P3	5[a)]	58,200	108,900	1.9	78	151
P4	0.5[b)]	44,000	103,000	2.3	n.m	n.m
P5	1[b)]	28,700	60,300	2.1	n.m.	n.m.
P6	2[b)]	58,700	223,000	3.8	n.m.	n.m.
P7	5[b)]	91,300	281,500	3.1	n.m.	n.m.

a) monomer **5c** purified according to Meijer *et al.*[88] b) "standard" monomer **5b**;
n.m.: not measured; n.o.: not observed

The incorporation of the alkylidene monomer should be quantitative due to the structural similarity of the monomers. The glass transition temperature (T_g) and the phase transition temperature C→LC (T_{LC}) show no significant difference to polyfluorenes.

2.2.1.3. Optical Spectroscopy

The optical properties of the polymers have been investigated both in chloroform solution as well as in thin films. The absorption of **P1-P7** are coincident with the typical absorption spectra of polyfluorenes with a maximum at *ca*. 380 nm (Figure 21). An additional low energy shoulder can be observed at ca. 435 nm. This shoulder could either be assigned to the 0-0 absorption band of the *β*-phase or the absorption of the alkylidene-fluorene defect.[71]

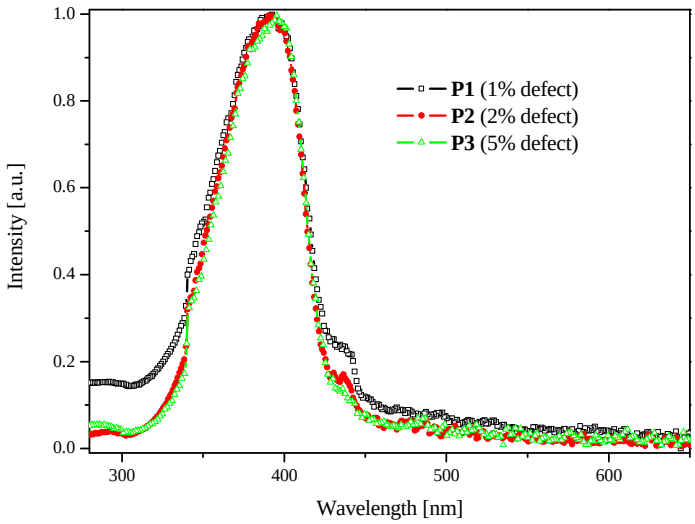

Figure 21. UV-Vis spectra of thin films of the copolymers **P1**-**P3**.

The intensity of the absorption shoulder in thin films of **P1**-**P3** at approx. 435 nm depends on the amount of alkylidene units, increasing amounts of the defect units suppress the low energy absorption band. Therefore, the absorption has to be assigned to a *β*-phase formation. Figure 21 therefore indicates that the occurrence of this shoulder is not caused by the alkylidene defects.

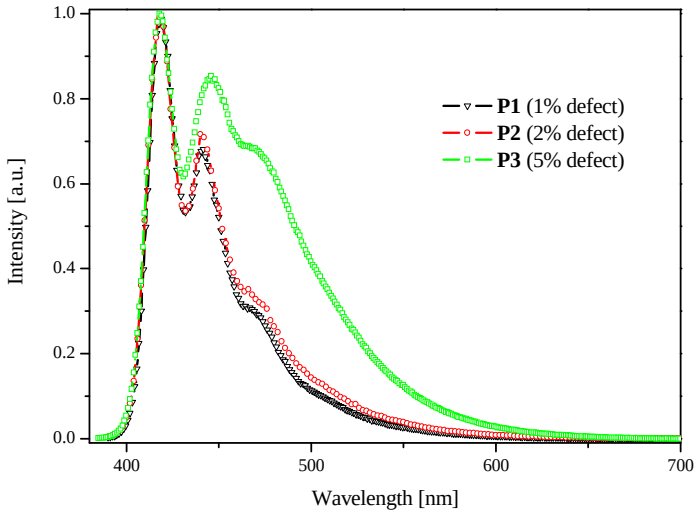

Figure 22. Photoluminescence of alkylidene-containing polyfluorenes **P1**-**P3** in dilute solution (λ_{ex}=390nm).

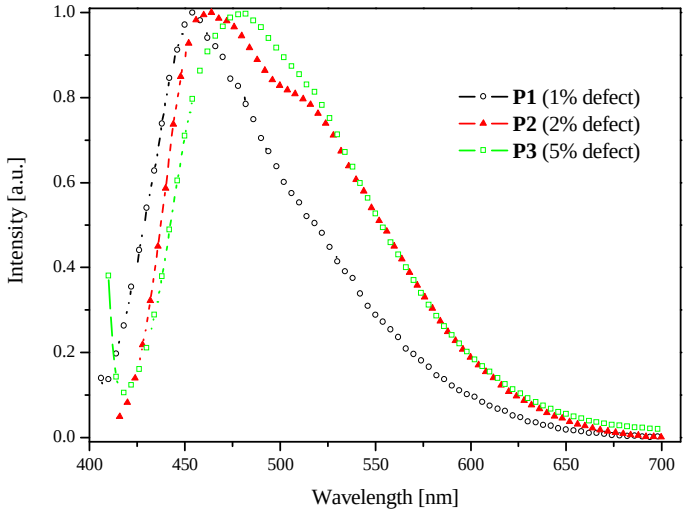

Figure 23. Photoluminescence of thin films of alkylidene-containing polyfluorenes **P1**-**P3** (λ_{ex}=390nm)**.**

The emission maximum in the solid state shifts from 455 nm for **P1** to 462 nm for **P2**, and to 481 nm for **P3** (Figure 23) whereas the emission in dilute solution of **P1** and **P2** remains nearly the same. Only a minor shift of the 0-1 and 0-2 transition of **P3** of ca. 5 nm can be observed. Both transitions shows increased intensity compared to the corresponding emission bands of **P1** and **P2** (Figure 22). The optical properties of **P1**-**P3** are summarized in Table 3. The optical properties of the alkylidene containing polyfluorenes **P4**-**P7** in dilute solution are presented in Figure 24.

Table 3. Optical properties of alkylidene-containing polyfluorenes.

Polymer	$\lambda_{max.}$ ($CHCl_3$-solution) [nm]		$\lambda_{max.}$ (thin film) [nm]	
	absorption	emission	absorption	emission
P1 (1% defect)	391	418, 441, 470	393	455
P2 (2% defect)	391	418, 442, 470	391	462, 513
P3 (5% defect)	391	418, 446, 472	396	481

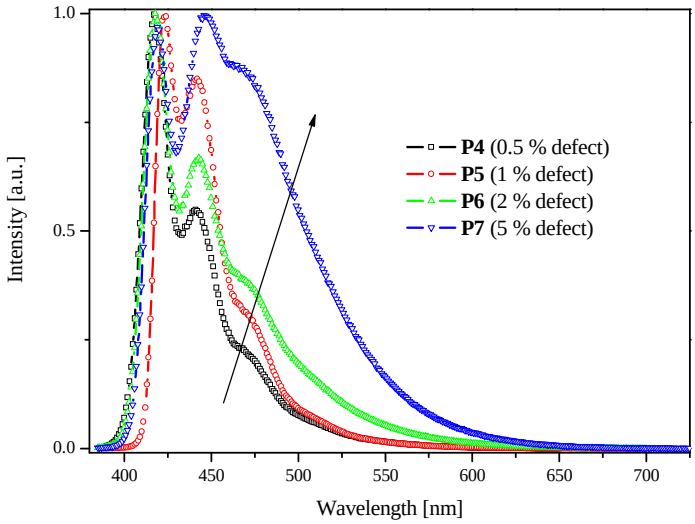

Figure 24. Photoluminescence of alkylidene-containing polyfluorenes **P4**-**P7** in dilute solution (λ_{ex}=390nm).

Figure 25 shows the photoluminescence of a thin film (spin cast from toluene) and of a dilute chloroform solution of the polyfluorene **P7** containing 5% Alkylidene units. The solid state fluorescence is strongly influenced by a green emission component. This spectral feature is in good accordance to the reported defect emission of degraded polyfluorene-based emissive layers in OLEDs as described by Gamerith *et al.* (Figure 26). They studied defect-related emissions of PF-based OLEDs which are observed at 479/506 nm. This emission feature was attributed to interface defects at the polymer/cathode interface. The similarity of the reported green emission maximum at 479 nm (Figure 26(a), open squares) and the observed emission maximum of **P7** in the solid state located at 481 nm suggest that the emission is probably caused by the proposed alkylidene defects. Gamerith *et al.* also observed an emission component at 530 nm in

devices which were heated in air or prepared taking less care to exclude oxygen during device preparation which was addressed to well-described keto defects.

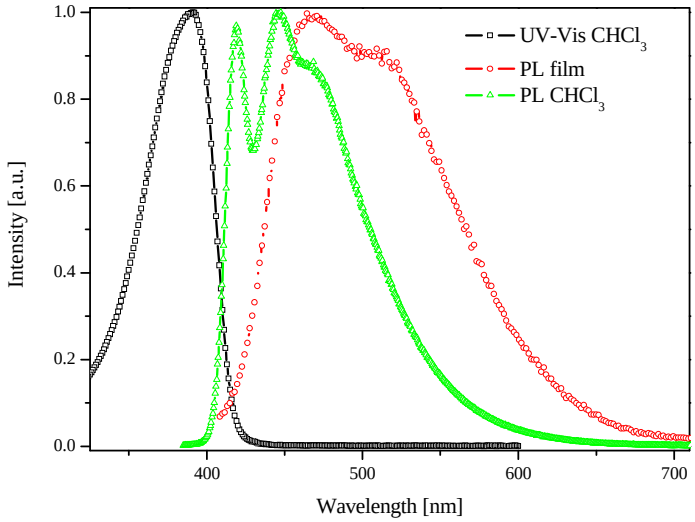

Figure 25. Photoluminescence and absorption of polyfluorene **P7** containing 5% alkylidene units (λ_{ex}=390nm).

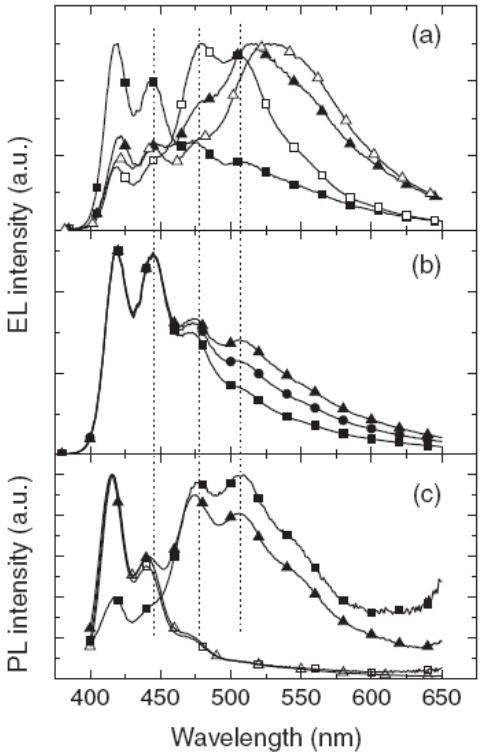

Figure 26. Normalized PL and EL spectra of PF Films and PLEDs. (a) Degradation of the electroluminescence of PF-based OLEDs. Filled squares: pristine device emission; open squares: after operation in argon atmosphere; filled triangles: after operation in argon atmosphere and storage in air (45 min. at 150°C); open triangles: device prepared without proper exclusion of oxygen. (b) Voltage dependence of the electroluminescence: triangles: 5.3 V; circles: 6V pulsed (100 kHz 50% duty cycle); squares: 50 V pulsed (100 kHz 5% duty cycle). (c) PL measurements of very thin (triangles: approx. 20 nm; squares: approx. 4 nm) films before (open symbols) and after (filled symbols) deposition of Ca/Al electrode.

One interesting finding of Gamerith *et al.* was that the spectral feature at 479/506 nm could reversibly be reduced as the driving voltage under pulsed operation was increased (Figure 26(b)). The spectral change of the EL with driving voltage can be understood as a shift of the recombination zone into a device region with different optical properties (e.g. with less emissive defects). Figure 26(c) shows PL measurements of thin films (20 and 4 nm, respectively) before and after deposition of a Ca/Al electrode. The contribution of the blue PF emission is more intense in the 20 nm-film after deposition of the electrode. The emission of the 4 nm-film displays a 2-fold increase of the relative contribution from the emission feature at 479 and 506 nm compared to the 20 nm-film. This indicates that this emission feature is caused by defects located near the polymer/metal interface. A direct analysis of the chemical nature of these defects is a difficult task as the detection of only very small amounts of impurities is necessary.

2.3. Polyfluorenes containing Fluorenone Building Blocks

As mentioned before, fluorenone defects are known to be the source for the occurrence of green PL bands in the presence of oxygen. Investigations on fluorenone defects (keto defects) have been based on fluorenone-containing copolymers and cooligomers as model compounds.[53;148-150] The incorporation of fluorenone building blocks into PF can lead to materials that emit white light.[157] The additional incorporation of non-planar binaphthyl units is expected to decouple the fluorenone-containing segments and may allow for a fine-tuning of the relative contributions of the emissive segments.

Novel fluorene/fluorenone/binaphthyl copolymers have been, therefore, synthesized with different molar ratios of the building blocks (**P8**-**P10**). Figure 27 shows the chemical structure of the copolymers. For comparison a fluorenone containing PF (**P11**) without binaphthyl units was also synthesized. The polymerization was done in a random fashion utilizing the Yamamoto protocol.

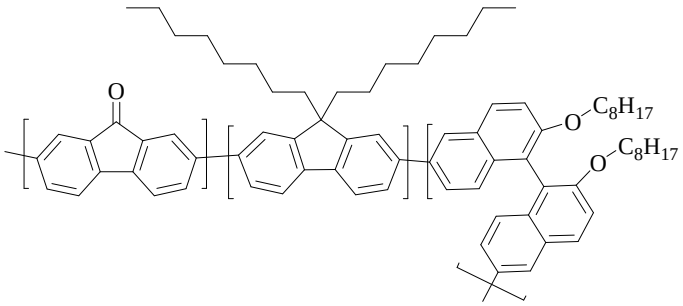

Figure 27. Chemical structure of binaphthyl-fluorenone-fluorene copolymers **P8**-**P10**.

2.3.1. Results and Discussion

2.3.1.1. Synthesis

6,6´-dibromo-2,2´-dihydroxy-1,1´-binaphthyl (**21**) is commercially available or can be made by bromination of the 2,2´-dihydroxy-1,1´-binaphthyl.[151;152] The corresponding ether is accessible by treatment of **21** with *n*-octylbromide under basic conditions to give **22** in good yields (Figure 28).[153-155] 2,7-Dibromofluorenone (**19**) was prepared from 2,7-dibromofluorene (**17**) via oxidation with sodium dichromate in acetic acid.

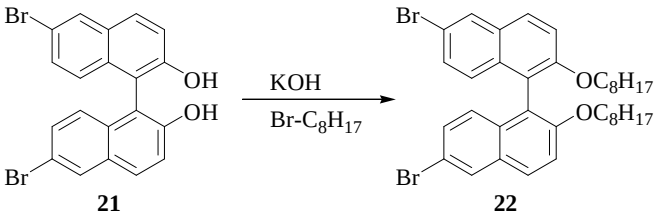

21 **22**

Figure 28. Synthesis of monomer **22**.

The copolymers were synthesized via a standard Yamamoto-type polymerization. Synthesis of the copolymers is outlined in Figure 29.

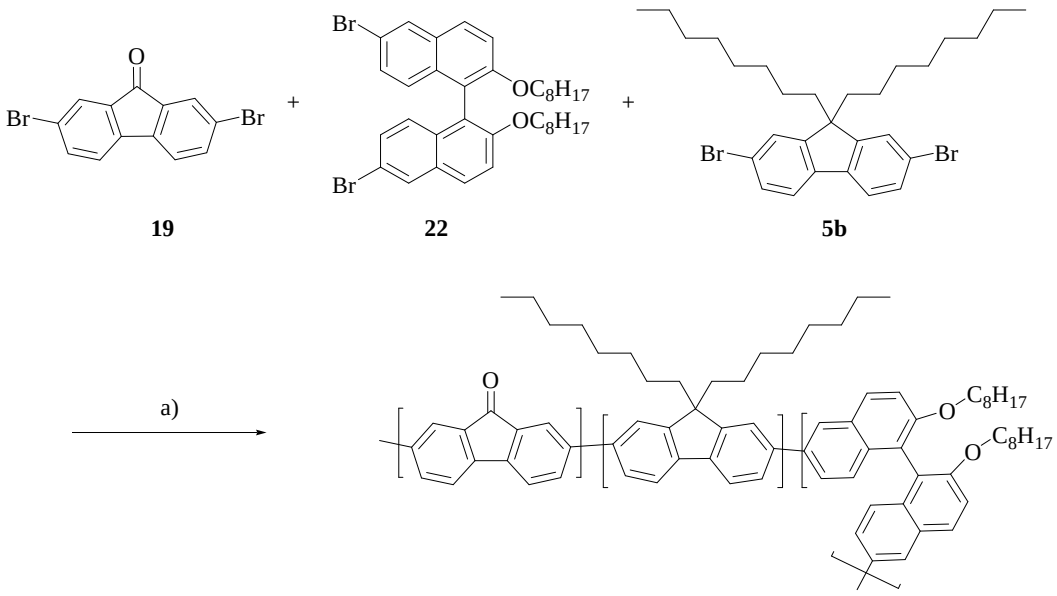

Figure 29. Synthesis of copolymers **P8**, **P9** and **P10** containing various amounts of fluorenone; reaction conditions: a) $Ni(COD)_2$, bipyridyl, COD, THF, 80°C, 3d.

The polymers were precipitated after aqueous workup from a chloroform solution into methanol. To remove low molecular weight fractions and oligomeric byproducts the polymers were Soxhlet-extracted with ethyl acetate for one day. The molecular weights of **P8**-**P10** are summarized in Table 4.

Table 4. Molecular weights of copolymers **P8**, **P9** and **P10**.

Polymer	Feed Ratios [%] [binaphthyl (**22**) : fluorenone (**19**) : fluorene (**5b**)]	M_n [g/mol]	M_w [g/mol]	PD [M_w/M_n]
P8	15 : 0.06 : 84.94	164,000	357,000	2.2
P9	15 : 0.1 : 84.90	172,000	368,000	2.1
P10	15 : 0.5 : 84.50	169,000	443,000	2.6

2.3.1.2. Optical Properties

The optical properties of the copolymers have been investigated in dilute solution as well as in thin films. Electroluminescence and low temperature spectroscopy measurements were carried out in the group of Prof. E. List (TU Graz). Figure 30 shows the photoluminescence spectrum of copolymers **P8** (0.06% fluorenone), **P9** (0.1% fluorenone) and **P10** (0.5% fluorenone). Copolymer **P10** (0.5% fluorenone) shows a dominant green emission with a maximum at 539 nm which is characteristic for the fluorenone building block and resembles the emission of fluorenone defects in degraded polyfluorenes.

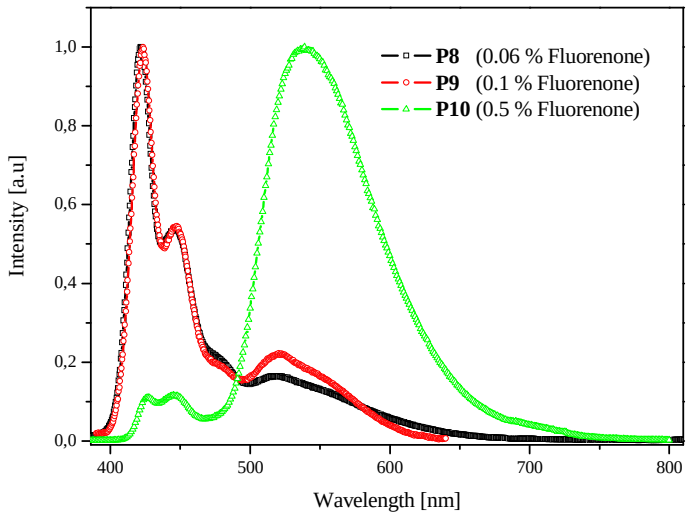

Figure 30. Photoluminescence of copolymers **P8**, **P9** and **P10** in dilute solution (λ_{ex}=380 nm).

Competition occurs after photo-excitation between the blue photoluminescence of oligofluorene segments and energy transfer to the acceptor (fluorenone) via a Förster-type dipole-dipole energy transfer process.[156] At low acceptor concentrations the emission in the PL is dominated by the oligofluorene segments due to the inefficient energy transfer to the acceptor. This is the case for **P8** and **P9** with fluorenone concentrations of 0.06 and 0.1%, respectively. By incorporation of higher concentrations of fluorenone (**P10,** 0.5%) the emission is dominated by the fluorenone acceptor moiety which implies a more efficient Förster energy transfer (Figure 30). This was also shown by Heeger and Moses *et al.*[157] They studied PL and EL of polyfluorene copolymers containing 1% fluorenone.

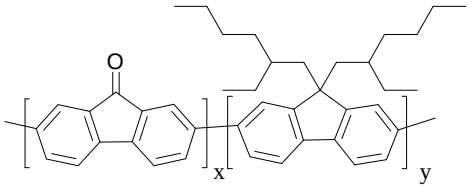

Figure 31. Chemical structure of fluorene-fluorenone copolymer **P11** (1% fluorenone).

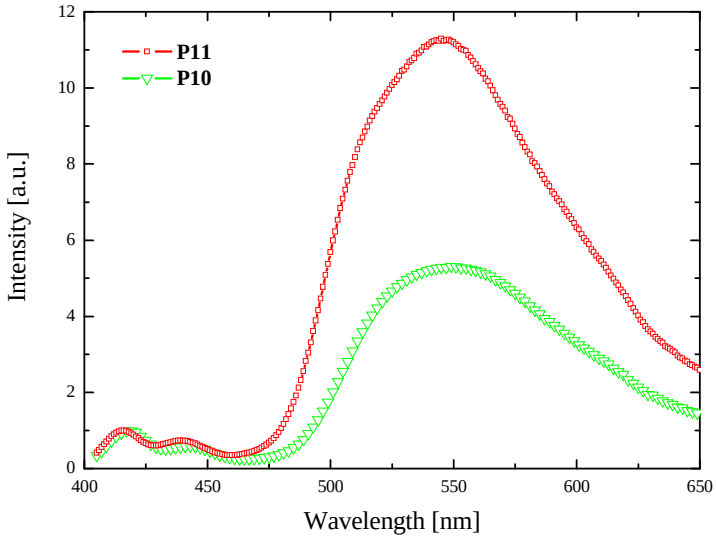

Figure 32. Photoluminescence of thin films of copolymer **P10** and **P11** (λ_{ex}=380 nm).

A comparison of the emission characteristics of copolymer **P10** (15% binaphthyl and 0.5% fluorenone) and copolymer **P11** (1% fluorenone) in Figure 31 shows that the energy transfer from the fluorene segments to the acceptor units is more efficient at room temperature (Figure 32) and hindered at lower temperatures (T = 33 K) (Figure 33). This results in an increased relative intensity of the emission of the oligofluorene segments at lower temperatures. The green emission at lower temperature is more structured and two maxima are observed at 530/565 nm for copolymer **P10** and 521/553 nm for the copolymer **P11**, respectively. The hypsochromic shift of the emission bands of **P11** if compared to **P10** may illustrate the presence of shorter oligofluorene segments in **P11** or the electronic influence of the on chain 2-alkoxynaphth-6-yl units of **P10**.

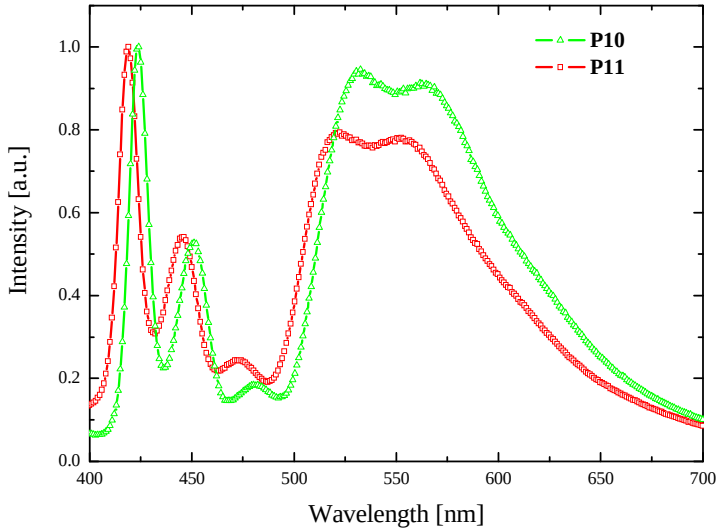

Figure 33. Photoluminescence spectrum of copolymers **P10** and **P11** at a temperature of T = 33 K (λ_{ex}=380 nm).

In electroluminescence the excitons are generated by charge recombination. The fluorenone units hereby act as a charge carrier trap and the recombination will take place at the defect-containing fluorenone sites. The increased intensity of the lower energy (green) emission for **P10** (Figure 34) cannot be simply explained.[148;158] Heeger *et al.* found that the amount of the green EL emission component in fluorenone-containing polyfluorenes results from a combination of efficient energy transfer, charge carrier trapping, and improved charge injection into the fluorenone traps.[157]

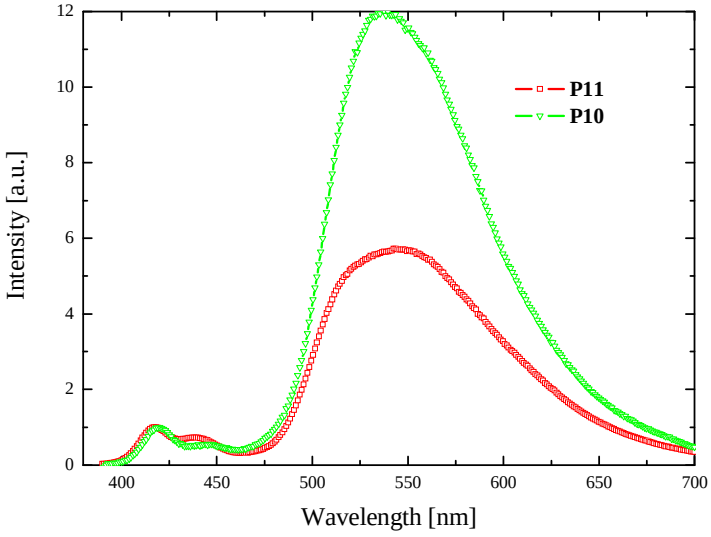

Figure 34. Electroluminescence spectrum of **P10** and **P11**.

Table 5 summarizes the emission properties of the investigated fluorenone-containing copolymers **P8**-**P11**.

Table 5. Optical properties of fluorenone-containing polyfluorenes.

Polymer	Defect concentration [%]	$\lambda_{max.}$ ($CHCl_3$-solution) [nm]	$\lambda_{max.}$ (thin film) [nm]	$\lambda_{max.}$ (EL) [nm]
P8	0.06	421, 446, 520	422, 447, 481, 522	n.m.
P9	0.1	421, 446, 520	423, 447, 520	n.m.
P10	0.5	538, 426, 446	424, 452, 481, 530, 565 [a)]	539
P11	1.0	417, 441	419, 446, 472, 521, 553 [a)]	546

a) measured at a temperature of T = 33K

2.4. Conclusion

The chapter focuses on model experiments towards the characterization of defect-related electroluminescence emissions in polyfluorenes. Especially a green emission band peaking at 479/506 nm which is formed in degraded OLED devices under exclusion of oxygen is investigated. Model copolymers containing dioctylfluorene and alkylidenefluorene units exhibit solid state emission bands peaking in the range of 455 nm (**P1**) to 481 nm (**P3**) with increasing amount of alkylidene units (1%-5%). Regarding this and other results alkylidenefluorene units has to be taken into account as the origin of the green emission feature at 479/506 nm. However, the real occurrence of such defect structures in degraded OLEDs has to be investigated in further experiments. The low concentration of such defects limits the possible analytical methods which can be applied.

The incorporation of non-planar binaphthyl spacers into polyfluorene chains affects the solid state morphology (suppression of β-phase formation) resulting in improved amplified spontaneous emission (ASE) properties.[159]

3. Electrophosphorescent Polyfluorenes

3.1. Introduction and Motivation

Semiconducting materials are gaining much interest as they have found to be important materials for an application in organic light emitting devices (OLEDs). Organic materials have to match basic prerequisites e.g. colour purity and long-term stability (see chapter 1). There has been much progress in the application of triplet emitters as light emitting components in OLEDs to increase their efficiency. Different techniques of utilisation of such triplet emitters have been reported. One prominent method is doping the triplet emitter [e.g. $Ir(ppy)_3$] into a polymer matrix [e.g. polyfluorene or poly(vinylcarbazole)]. Another important strategy is to incorporate the metal complex into the polymer chain. This can be realized by attaching the complex onto the side-chain or into the main-chain of the polymer.

Prominent examples of triplet emitters are based on electrophosphorescent iridium(III) complexes which are mostly incorporated into the side-chain.[113;160] The strategy to incorporate the phosphor into the polymer-chain (side-chain or main-chain) seems to avoid morphology problems like phase separation. Fréchet and Thomson *et al*. utilized platinum(II) which was incorporated into the side-chain, whereas Swager and his coworkers synthesized a copolymer containing a phenylpyridine (ppy) Pt(II)acac complex in the main-chain.[116;161] Our strategy towards main-chain electrophosphorescent copolymers involves the covalent incorporation of Pt(II)-salen phosphors into the backbone of a solution-processable semiconducting copolymer. A recent paper by Che *et al*. described the utilization of vapour-deposited Pt-salen complexes as efficient electrophosphorescent dyes in multilayer OLED devices with a maximum efficiency of 31 cd/A.[162] Schiff base ligands based on N,N´-bis(salicylidene)-1,2-ethylenediamine and related structures have been investigated in a number of research areas for at least the last decade, with enantioselective organic oxidation being the most prominent example.[163] However, application of metal-salen-type derivatives in material science is still relatively

meagre.[115;162;164-166] Sano *et al*. investigated the utilization of zinc(II) Schiff base complexes **23** and **24** in OLEDs as shown in Figure 35.[167]

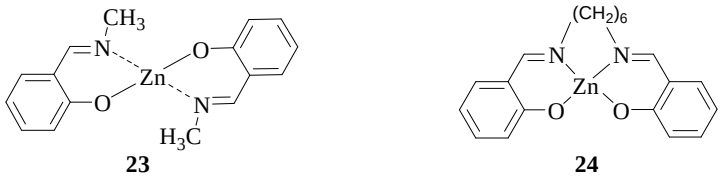

23 **24**

Figure 35. Zinc(II) Schiff base complexes of Sano *et al.*[167]

3.2. Results and Discussion

3.2.1. Metal-containing Complexes

To incorporate a phosphorescent dye into the backbone of a polymer, the ligand-sphere has to be suitably modified resulting in an AA- or AB-type monomer. We started our investigations with the synthesis of suitable Schiff base ligands as precursors for polymerizable Pt(II) complexes. Chloro-aryl monomers can also undergo Yamamoto-type couplings and are also viable under Suzuki conditions.[147] During this work some non-functionalized complexes were also synthesized to investigate the properties of the monomeric molecules by doping them into a polymer matrix. The chemical target for a variation of the ligand-sphere of the Schiff base ligands was the bridging diamine unit as well as the corresponding aromatic aldehyde unit as shown in Figure 36.

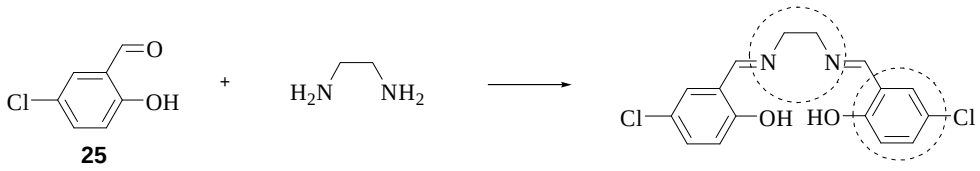

25

Figure 36. Possible variations of the Schiff base ligands.

3.2.1.1. Synthesis of Schiff Base Ligands

A series of different Schiff base ligands which were suitable for copolymerization were synthesized by a condensation reaction of the corresponding aldehydes and the bridging diamines by heating them to reflux in toluene with the use of a Dean Stark apparatus. 2-Chloro-5-hydroxy-benzaldehyde (**25**) was commercially available, whereas the naphthalene derivative **26** was synthesized according to Royer and Buisson.[168] The reaction of 1,1-dichloromethyl-methylether with a Friedel-Crafts catalyst ($AlCl_3$, $TiCl_4$) gave the reactive electrophil which subsequently reacted with the naphthalene to give the corresponding aldehyde **26** after aqueous work up. The reaction mechanism for the formylation of aromatic systems with the use of dichloromethyl-methylether in the presence of $AlCl_3$ as Lewis acid is outlined in Figure 37.

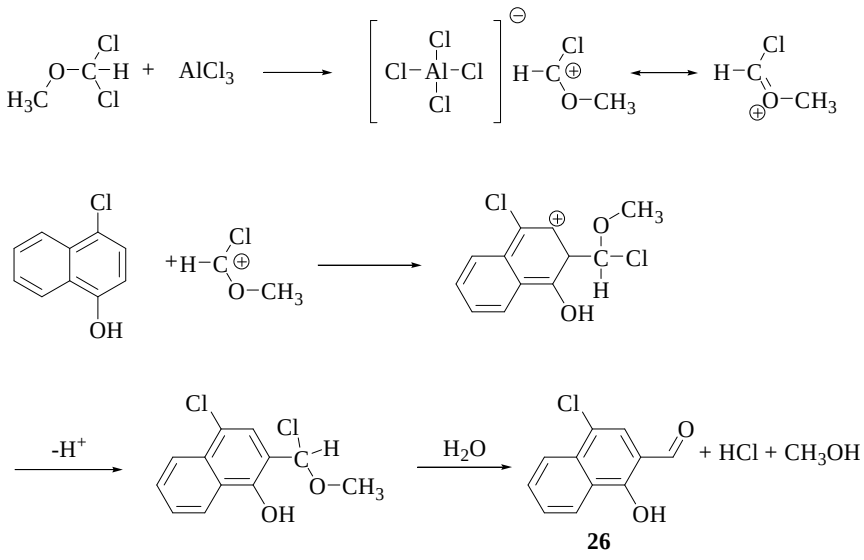

Figure 37. Formylation of 1-chloro-4-hydroxynaphthalene towards **26**.

The use of aluminium trichloride led to reaction mixtures with various amounts of side products and subsequently difficult work up. The use of the softer Lewis acid titanium(IV) chloride gave reaction mixtures which allows an easy work up (Figure 38). The crude product was purified by column chromatography using THF/hexane (10:90) as the eluent. Recrystallization from ethanol gave the product in reasonable high yield of 65 %.

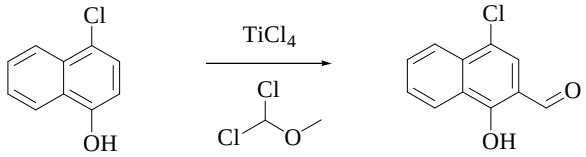

26

Figure 38. Synthesis of 4-chloro-1-hydroxy-naphth-2-aldehyde (**26**).

The ^{1}H NMR of **26** shows a AA´BB´ spin-system with two doublets at 8.4 and 8.1 ppm with a coupling constant of J_{AB} and $J_{A'B'}$ of 8.65 Hz and two triplets at 7.85 and 7.69 ppm with a coupling constant of $J_{BB'}$ of 7.63 Hz (Figure 39). The singlet of the proton in 3 position is observed at 7.82 ppm. Isomers of **26** were not observed in the ^{1}H NMR.

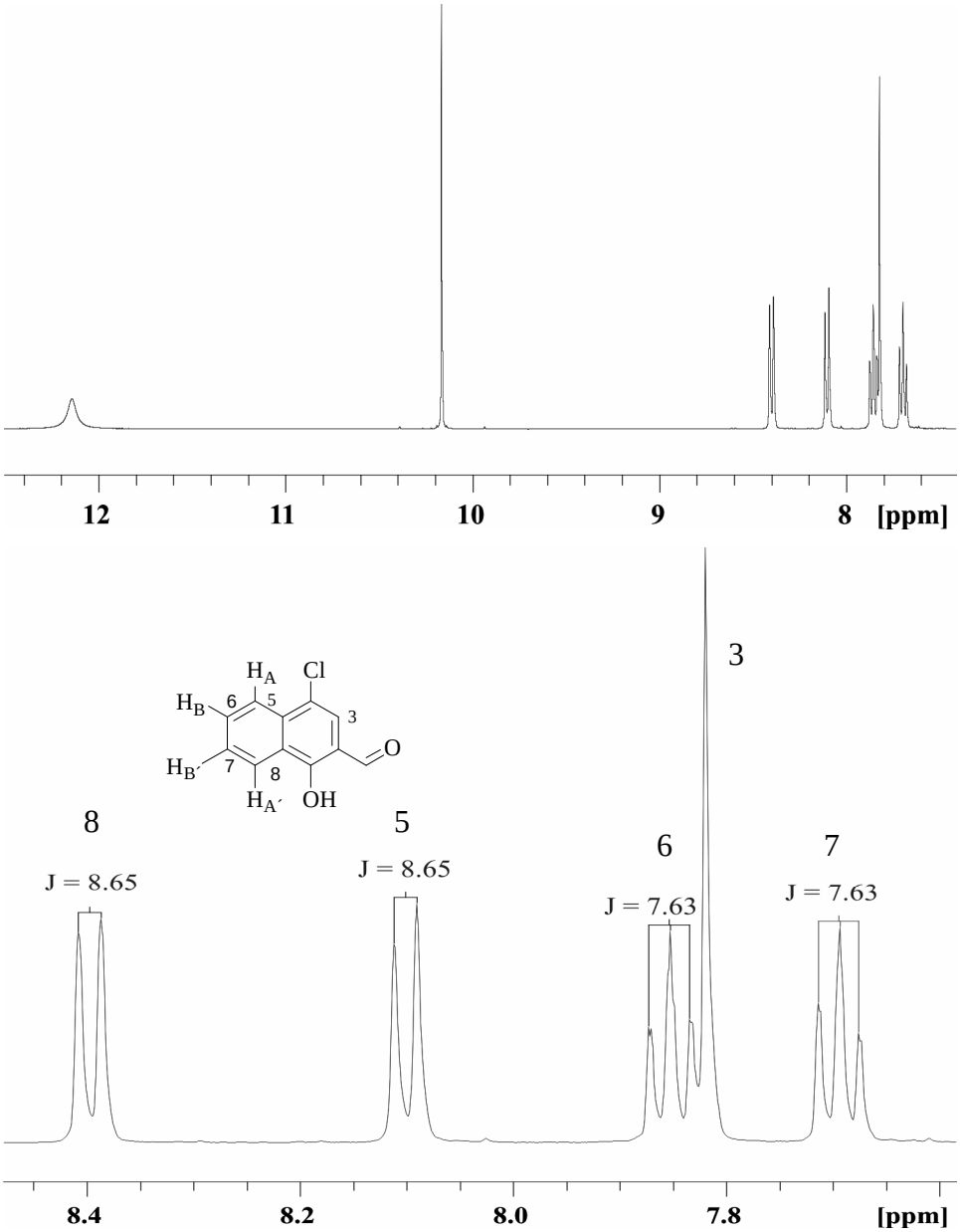

Figure 39. ^{1}H NMR spectrum of **26** in deuterated DMSO.

A subsequent reaction with commercial available diamines with the use of a Dean stark apparatus gave the salen ligands in good to excellent yields (50-90%) after recrystallization from acetonitrile/DMSO or ligroin/DMSO mixture (Figure 40).

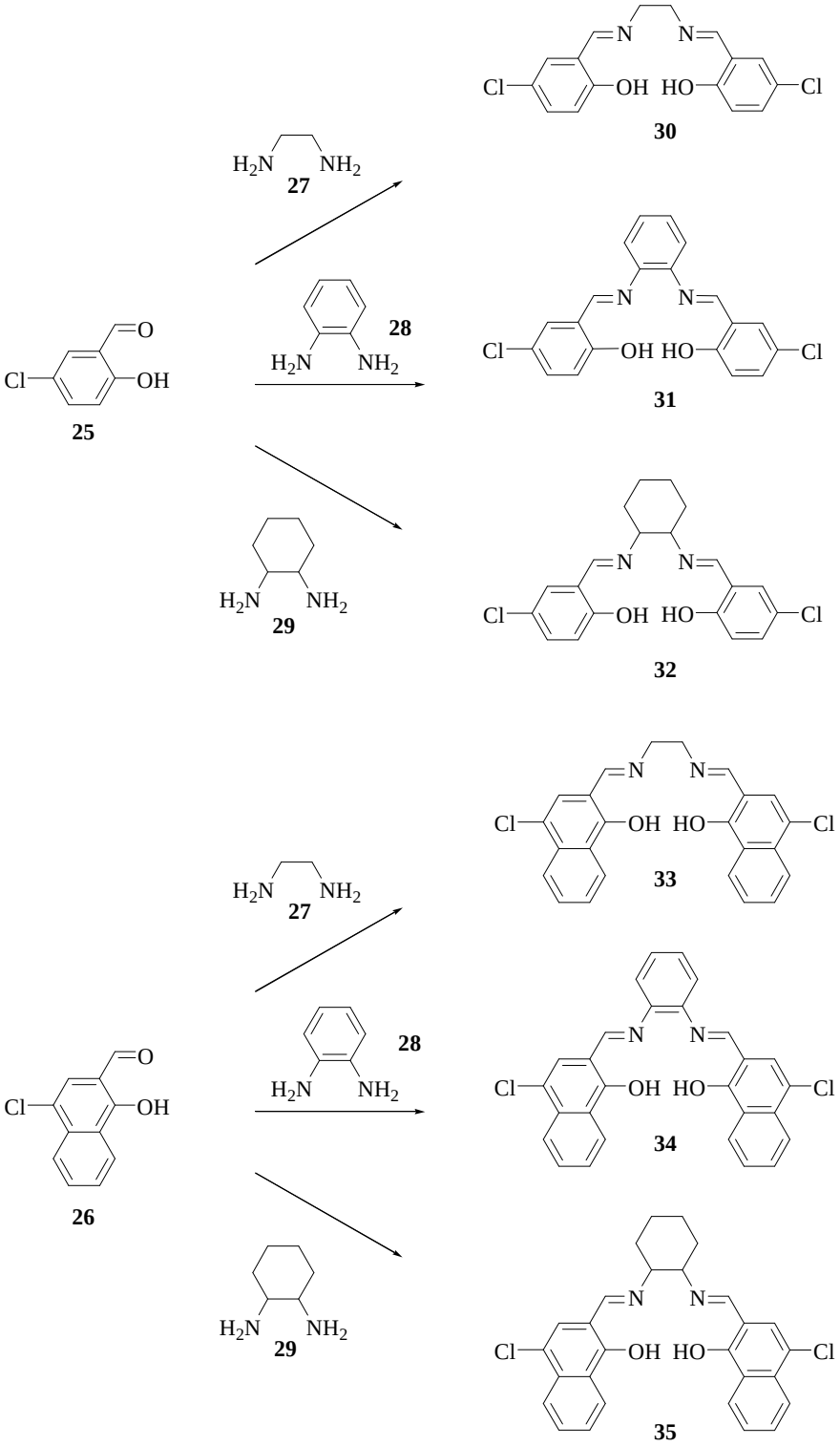

Figure 40. Synthesis of Schiff base ligands.

Three different commercially available diamines 1,2-diaminoethane (**27**), *o*-benzodiamine (**28**) and 1,2-diamino-cyclohexane (as a mixture of cis and trans) (**29**) were used to synthesize the salen ligands shown in Figure 40. The metal complex of the latter one should in principle be useful to fabricate OLEDs which emit circularly polarized light if the chiral *trans*-isomer (R,R or S,S) of **29** is used. The synthesis of corresponding naphthalene-based ligands (Figure 41) gave less soluble salen ligands. The solubility of the corresponding complexes was also lower (see next chapter). Indeed, the synthesis of **38** and **39** failed probably because of the low solubility, whereas **36** and **37** were accessible with a yield of 48 and 63%, respectively.

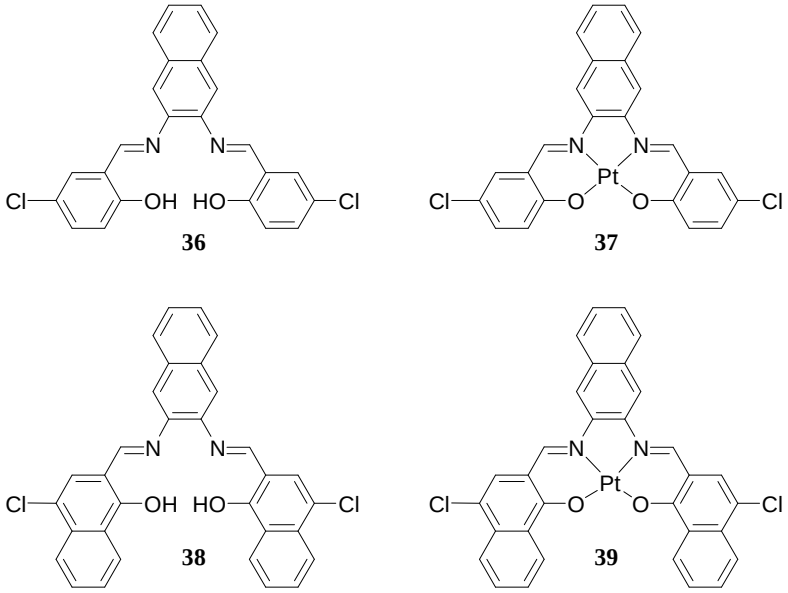

Figure 41. Naphthalene-bridged salen ligands and complexes.

3.2.1.2. Synthesis of the Platinum(II)-Schiff Base Complexes

The Pt(II)-salen complexes were prepared from the reaction of K_2PtCl_4 with the corresponding ligand in the presence of a base. As the base aqueous solutions of NaOAc or KOH were used (Figure 42).

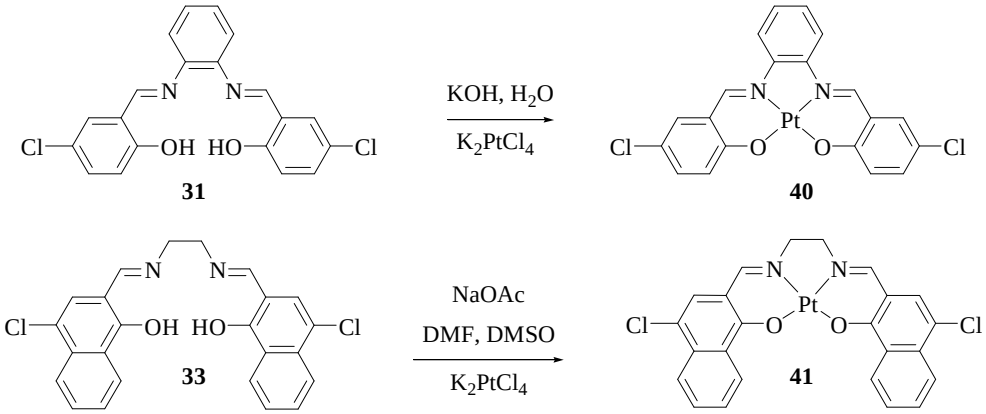

Figure 42. Synthesis of Pt(II) Schiff base complexes.

Figure 44 summarizes the synthesized Pt-complexes. The incorporation of the platinum was proved by mass-spectroscopy and by NMR analysis. In the latter, the absence of the OH-protons and the platinum satellites of the alkylidene protons which shows a coupling constant of approx. 70 Hz proved the incorporation of the platinum(II) into the complex. The ^{1}H NMR of **42** is presented in Figure 43 where the platinum satellites are highlighted. The coupling constant of the ^{195}Pt doublet is J = 70.7 Hz.

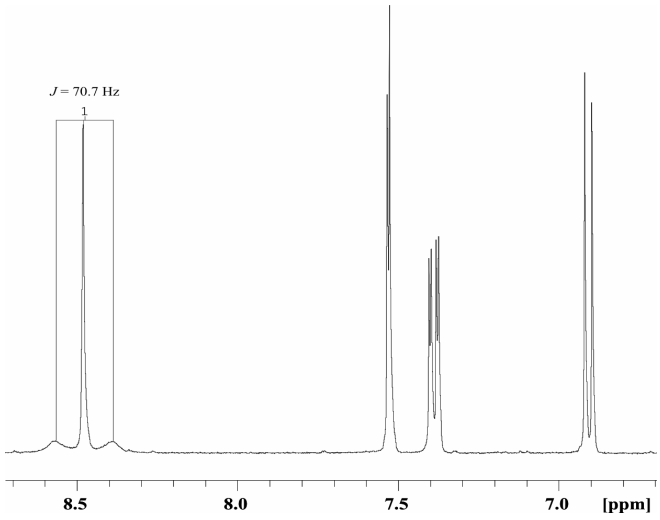

Figure 43. ^{1}H NMR spectrum of Pt(II) Schiff base complex **42.**

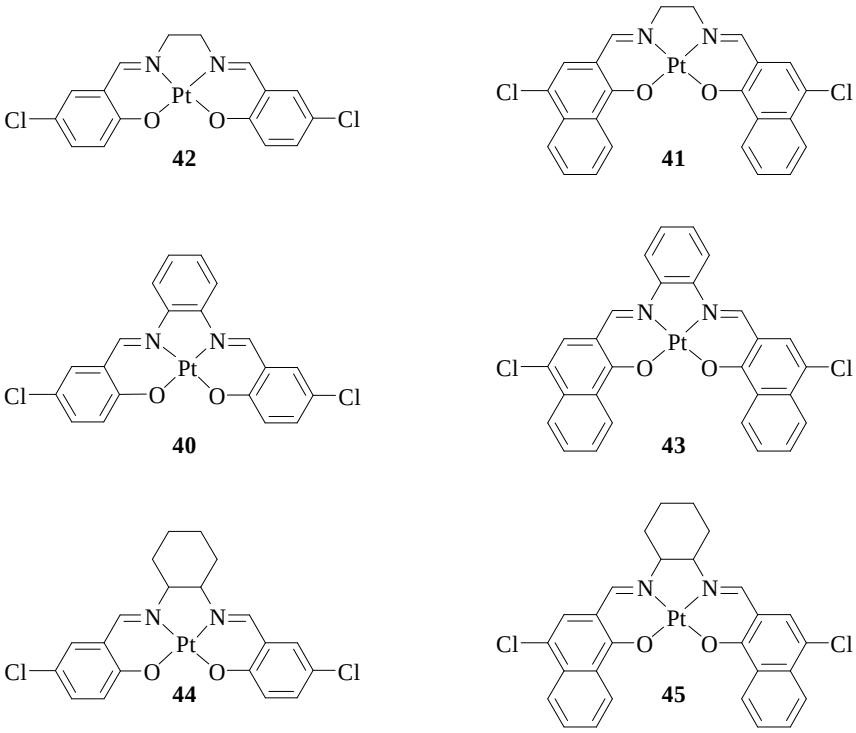

Figure 44. Chemical structures of Pt(II) Schiff base complexes.

For the naphthalene-based Pt(II) complexes the ^{1}H NMR of **43** is exemplarily presented in Figure 45. Again, the platinum satellites of the alkylidene protons are highlighted. The doublet of the platinum satellite shows a coupling constant of $^{3}J_{\text{H-Pt}}$ = 65.0 Hz at 9.40 ppm.

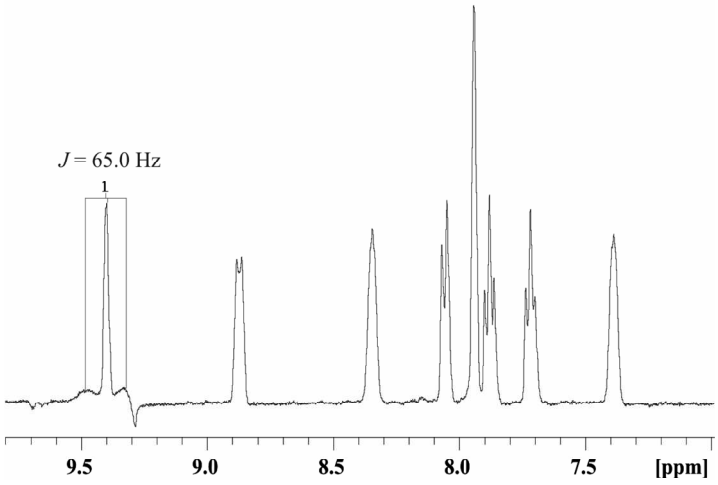

Figure 45. ^{1}H NMR of Pt(II) Schiff base complex **43**.

3.2.2. Optical Properties

3.2.2.1. Optical Spectroscopy

The Pt(II)-salen complexes show long wavelength absorption maxima between 455 and 557 nm and emission maxima varying from 563 to 652 nm. Figure 44 shows the chemical structures of the used Pt(II) complexes. Absorption and emission characteristics are summarized in Table 7. It was not possible to prepare adequate films of the complexes, so only the absorption and emission properties in dilute solution are reported here.

Table 7. Absorption and emission parameters of the used Pt(II) complexes in dilute chloroform solution. The listed maximums are ordered regarding to their descending intensities**.**

Compound	Absorption ($CHCl_3$) λ_{max} [nm]	Emission ($CHCl_3$) λ_{max} [nm]
37	257, 359, 557	652, 716
40	383, 365, 321, 475, 541	642
41	331, 450, 480	592, 655
42	352, 321, 433, 455	563
43	302, 324, 385, 367, 505, 556	647, 708
44	351, 323, 431, 456	554, 600
45	331, 451, 478	589, 640

Figure 46 shows the absorption spectra in dilute chloroform solution of the complexes **41**, **42**, **44** and **45**. The absorption spectra of complexes **40** and **43** are shown in Figure 47.

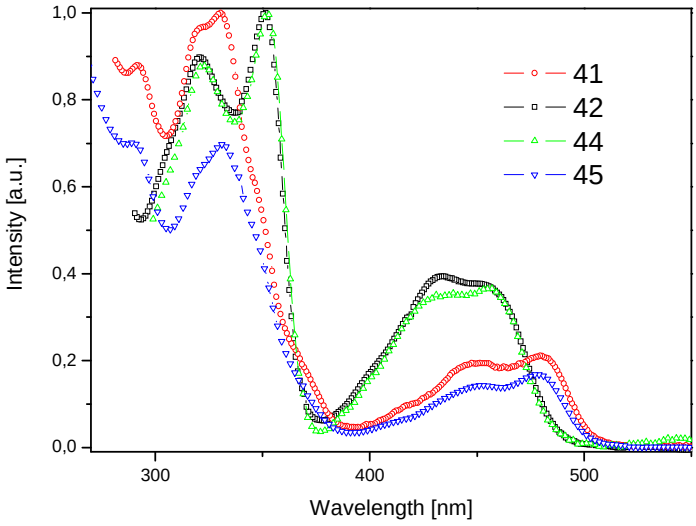

Figure 46. Absorption spectra of complexes **41**, **42**, **44** and **45**.

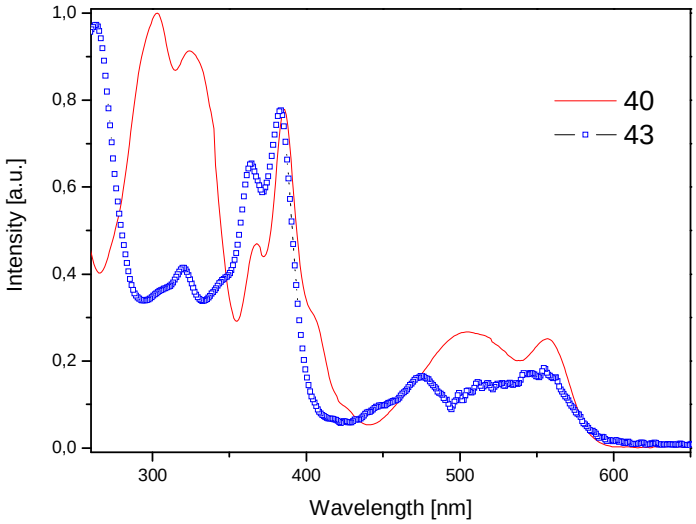

Figure 47. Absorption spectra of complexes **40** and **43** in dilute solution.

In addition to the intense π-π^* absorption bands at ≈ 300-400 nm all complexes display low energy absorption bands in the region of 420 - 570 nm which can be attributed to metal to ligand charge transfer (MLCT) transitions.[104] When excited at their absorption maxima, the complexes exhibit efficient room temperature phosphorescence in chloroform solution. Excitation into the π-π^* or MLCT absorption bands can be used to promote phosphorescence in these complexes.

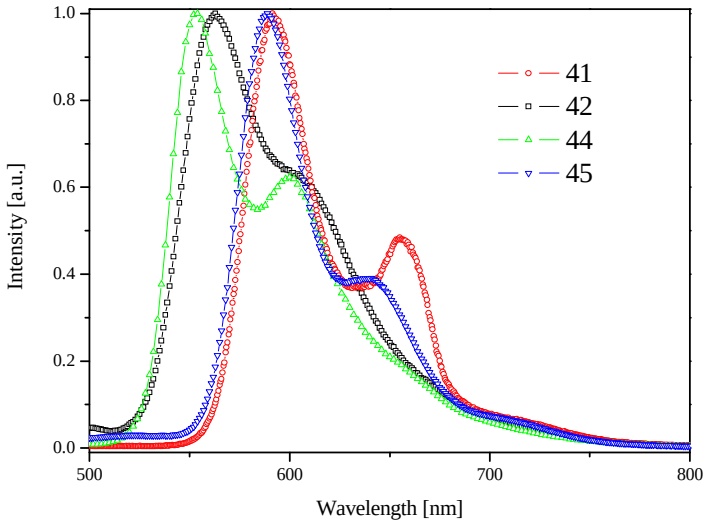

Figure 48. Emission spectra of complexes **41** (λ_{ex} = 480 nm), **42** (λ_{ex} = 455 nm), **44** (λ_{ex} = 455 nm) and **45** (λ_{ex} = 480 nm).

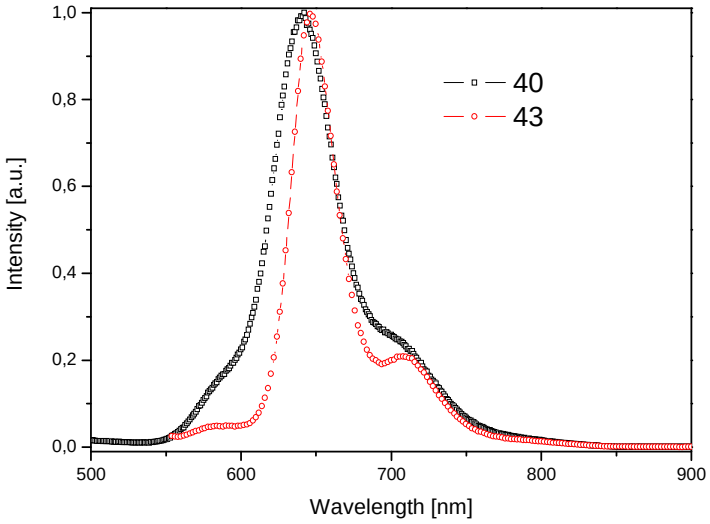

Figure 49. Emission spectra of complexes **40** (λ_{ex} = 475 nm) and **43** (λ_{ex} = 505 nm).

The alkyl-bridged Pt-complexes show phosphorescence with well-resolved vibronic sidebands peaking at 592, 563, 554 and 589 nm for **41**, **42**, **44** and **45**, respectively (Figure 48). The Pt-complexes **40** and **43** show phosphorescence emission peaking at 642 and 647 nm, respectively (Figure 49). The shoulders at approx. 575 nm are probably caused by residue ligand emission.

Some non-functionalized Pt(II)-salen complexes **51**-**53** were also synthesized (Figure 50) and subsequently used for the built up of OLED devices based on the Pt(II) phosphors doped into a polymer matrix [polyfluorene and poly(vinylcarbazole)].

The complexes also show efficient phosphorescence at room temperature in dilute chloroform solution. Absorption and emission properties of complexes **51**, **52** and **53** are shown in Figure 51-53.

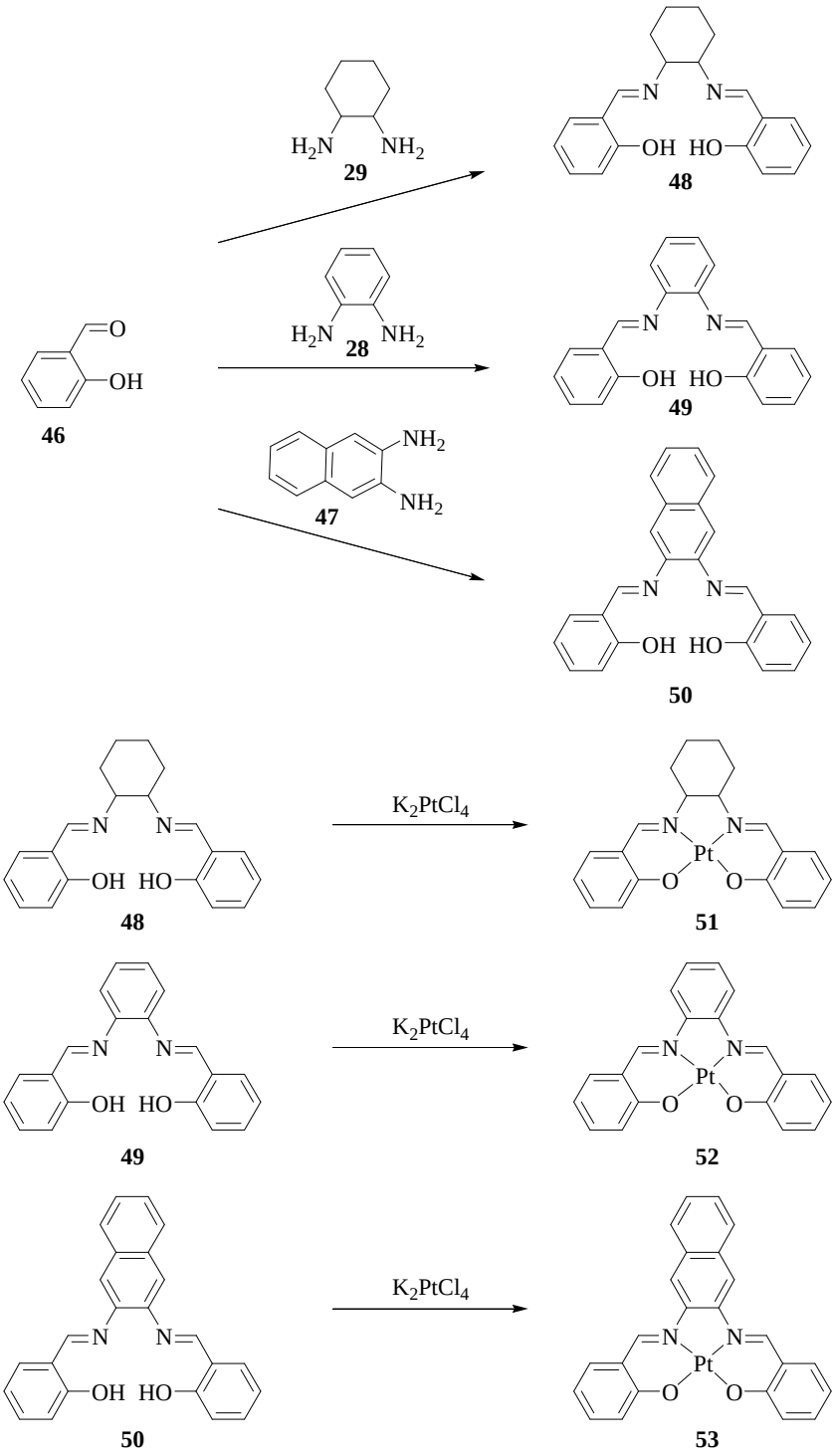

Figure 50. Synthesis and chemical structures of non-functionalized Pt(II)-salen complexes **51**, **52** and **53**.

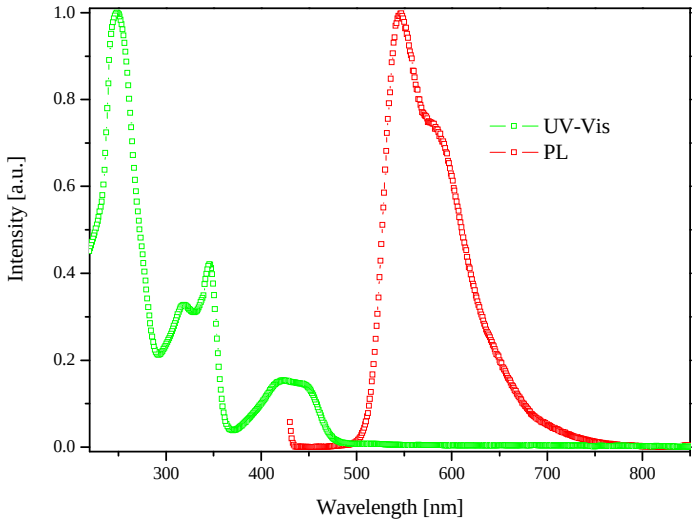

Figure 51. Absorption and emission spectra of **51** (λ_{ex} = 430 nm).

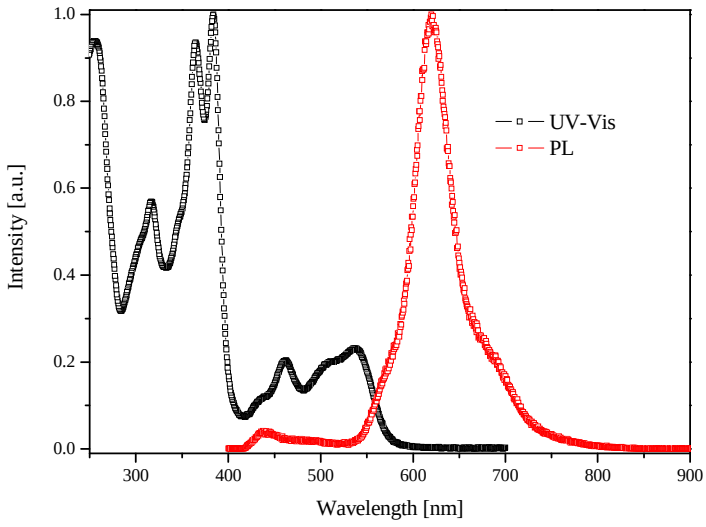

Figure 52. Absorption and emission spectra of **52** (λ_{ex} = 385 nm).

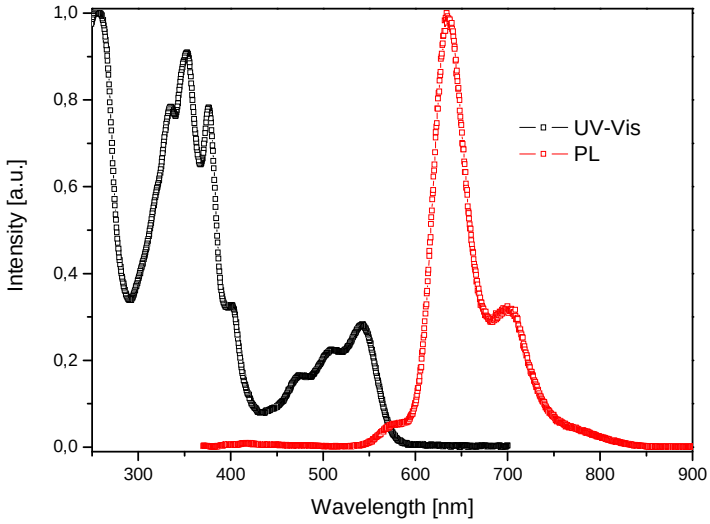

Figure 53. Absorption and emission spectra of **53** (λ_{ex} = 370 nm).

Again the absorption spectra show the MLCT absorption bands at λ ≈ 431-542 nm beside the π-π* absorption bands located at λ ≈ 300-400 nm. Complex **52** emits orange-red light and its emission maximum is located at 621 nm with a shoulder at 687 nm. **53** is a red emitter with an emission maximum at 635 nm and a well-resolved vibronic side band at 700 nm (Figure 53). The shoulder at approx. 570 nm is probably caused by residue ligand emission. **51** emits greenish-yellow light with the maximum located at 547 nm. Table 8 summarizes the optical properties of these three Pt(II)-salen complexes.

Table 8. Optical properties of Pt(II) complexes **51**, **52** and **53**.

Polymer	$\lambda_{max.}$ absorption [nm]	$\lambda_{max.}$ emission [nm]
51	250, 346, 319, 431	547, 585
52	385, 365, 257, 316, 461, 537	619
53	259, 352, 377, 475, 508, 542	569, 635, 700,

3.2.2.2. Electroluminescence Properties

OLEDs based on **51**-**53** were fabricated and tested in the group of Prof. Neher (University of Potsdam). The emitting layers of doped polymer films were produced by spin casting the polymer solutions containing the dissolved phosphors. The devices were prepared as described in the following: Poly(3,4-ethylenedioxythiophene) doped with poly(styrene sulfonate) (PEDOT:PSS) (Baytron P purchased from H.C. Starck) was spin-coated onto pre-cleaned and O_2-plasma treated indium tin oxide (ITO), yielding layers of ca. 60 nm. The PEDOT:PSS layers were heated to 80°C for half an hour to remove residual water. Solutions of polymers (PF or PVK) and Pt-phosphors were spin-coated on top of the PEDOT:PSS films. The thickness of the emissive layer was ca. 80-100 nm as measured by Dektak profilometry. The devices were completed by thermal deposition of 5 nm layers of Ca and 100 nm layers of Al. The brightness of the devices was recorded with a Minolta CS100A camera. EL spectra of the devices were measured using a charge coupled device fiber spectrometer (Ocean Optics). With the exception of the deposition of the PEDOT:PSS layer, all processes were carried out in a dry nitrogen atmosphere.

OLEDs were prepared based on complex **52** as the phosphorescent guest with poly(vinylcarbazole) (PVK) and polyfluorene as the hosts. The OLED prepared with PF as the host material showed dominant emission from the Pt(II)-salen complex **52** at 639 nm and only a small contribution from the host (Figure 54).

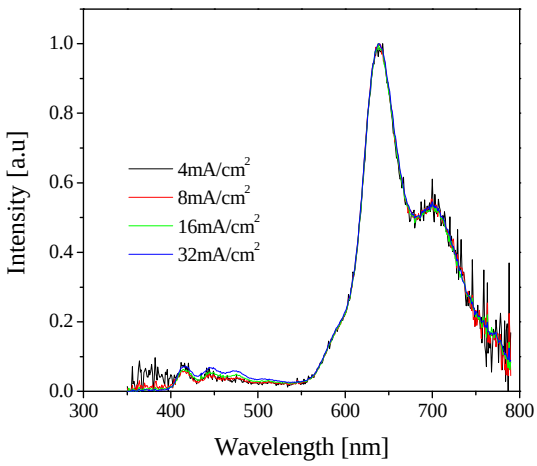

Figure 54. EL spectra of devices with the structure of ITO/PEDOT/PF: **52**(4%)/Ca/Al.

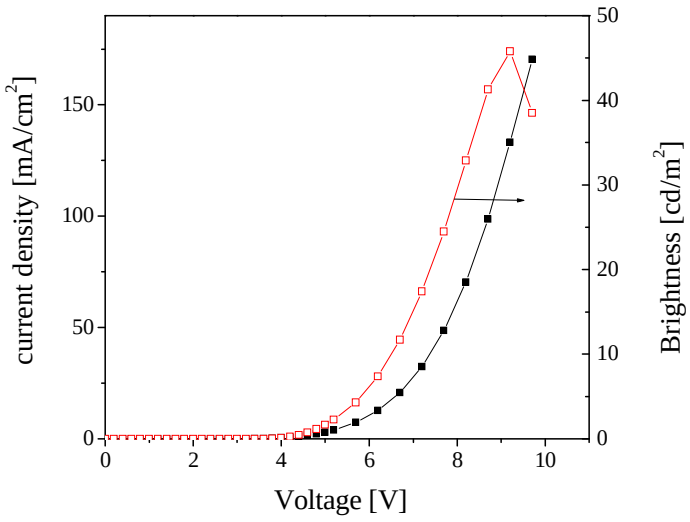

Figure 55. I-B-V characteristics of PF + **52** (4%).

I-B-V characteristics of OLEDs based on **52** (4%)/PF are shown in Figure 55. EL efficiencies of the OLEDs based on **52** with PF as host are quite low (ca. 0.04 cd/A). This might be due to the low amount of the Pt-salen phosphor in the matrix. Even though the dye concentration was used as high as possible, the very low solubility of **52** of ca. 0.4 mg/mL in chlorobenzene limits the content of **52**. In order to improve electron transport in the emitting layer, an electron transporting compound was mixed into the hosts to facilitate electron transport.[169] Solution-processed polymer electrophosphorescent devices based on a PVK host with additional 2-(4-biphenyl)-5-(4-tert-butylphenyl)-1,3,4-oxadiazole (PBD) as electron-transporting dopant were described by Lamanski *et al.*[104;170] Figure 56 shows the EL spectra of **52** with PBD as electron transporting dopant in a PVK or PF matrix. The light emitting layers in these OLEDs were composed of (a) PVK (57.5 wt.%), PBD (40 wt.%) and **52** (2.5 wt.%), (b) PF (67.5 wt.%), PBD (30 wt.%) and 2.5 (wt.%) of **52**. The device based on the PF-PBD matrix (b) showed dominant emission from the host. This host emission was absent in the case of PVK (a) where the maximum emission was observed at 627 nm. However, compared to the OLED made of PF without PBD the efficiency is fivefold increased in device (b) (Figure 57).

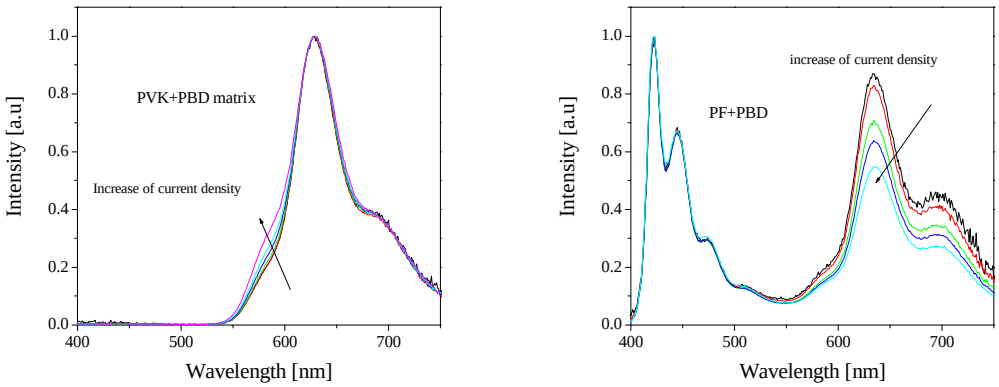

Figure 56. EL spectra of (a) PVK+PBD(0.4)+ **52** (2,5%) left and (b) PF+PBD(0.3)+ **52** (2,5%) right.

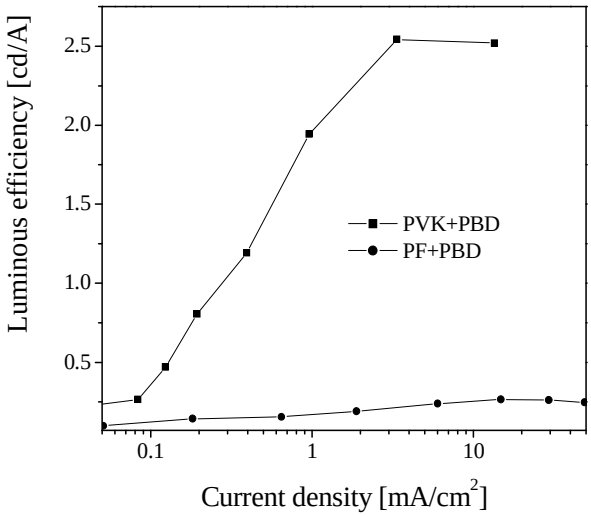

Figure 57. Luminous efficiency – current density curves of (a) PVK+PBD (0.4) + **52** (2.5% by weight) and (b) PF+PBD (0.3) + **52** (2.5 % by weight).

The EL spectrum of (b) shows a strong contribution from the PF host whereas in (a) no emission from PVK was observed (Figure 56). This shows that the energy transfer to the phosphorescent guest is increased in the case of the PVK host. This finding is supported by the increased luminous efficiency (Figure 57).

PL spectra of thin films with a similar composition were also recorded. The films were optically excited at 380 or 450 nm. The emission from **52** was more dominant in the PL with the PVK host (a) than with the PF host (b) (Figure 58). This finding supports the assumption, that the energy transfer to the phosphor is enhanced for the PVK host.

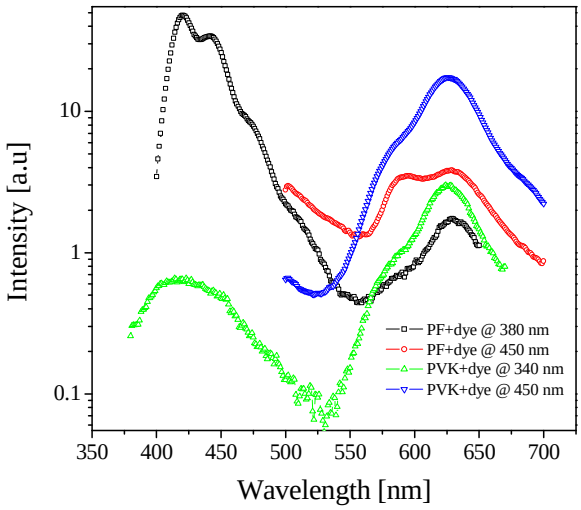

Figure 58. PL spectra of PVK (green and blue) and PF (black and red) doped with 4% of **52** at different excitation wavelengths.

The EL efficiency of the devices made from **53** (2%) blended into a matrix based on PVK and PBD (40%) are also only moderate (ca. 2.0 cd/A, Figure 59).

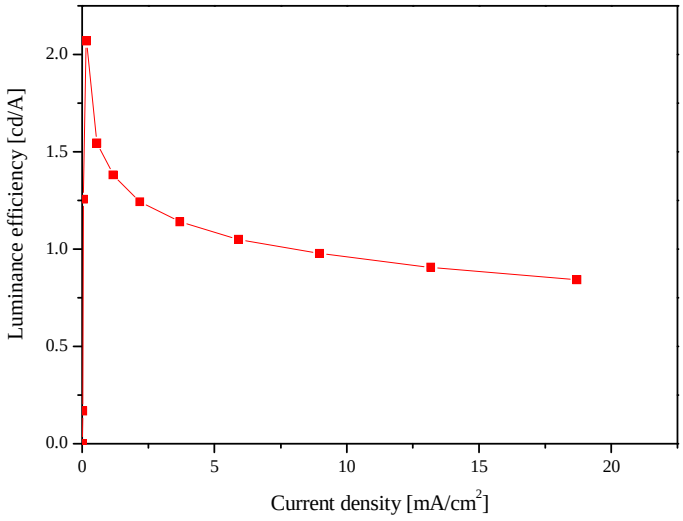

Figure 59. Efficiency of an OLED made from **53** [PVK/PBD(40%)/**53**(2%)].

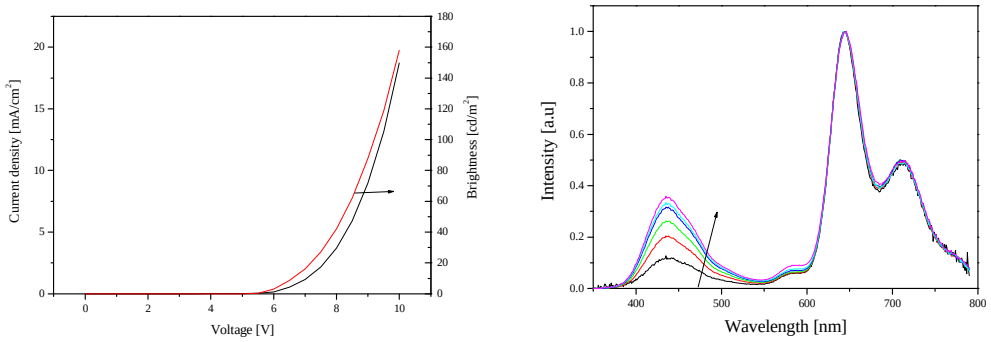

Figure 60. I-V characteristics and EL spectrum of a device made by **53** [PVK/PBD(40%)/**53**(2%)].

The EL spectrum hereby shows increasing host emission (from PVK) with increasing current density (Figure 60). This is most probably caused by the low concentration of the triplet emitter and subsequently inefficient energy transfer from the host.[171] Good efficiencies of up to 12.5 Cd/A were achieved using **51** as guest (Figure 61). Again, the matrix was based on PVK/PBD (40%).

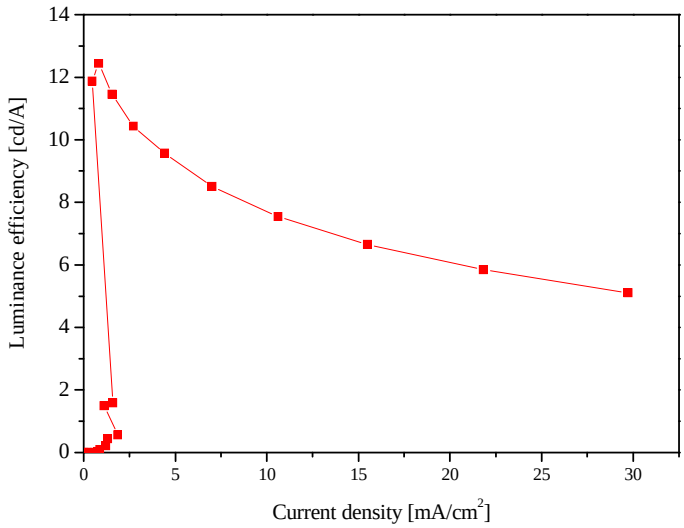

Figure 61. Efficiency of a device based on **51** [PVK/PBD(40%)/**51**(2%)].

The device showed high brightness (ca. 1500 Cd/m²) and again increasing host emission with increasing current density (Figure 62).

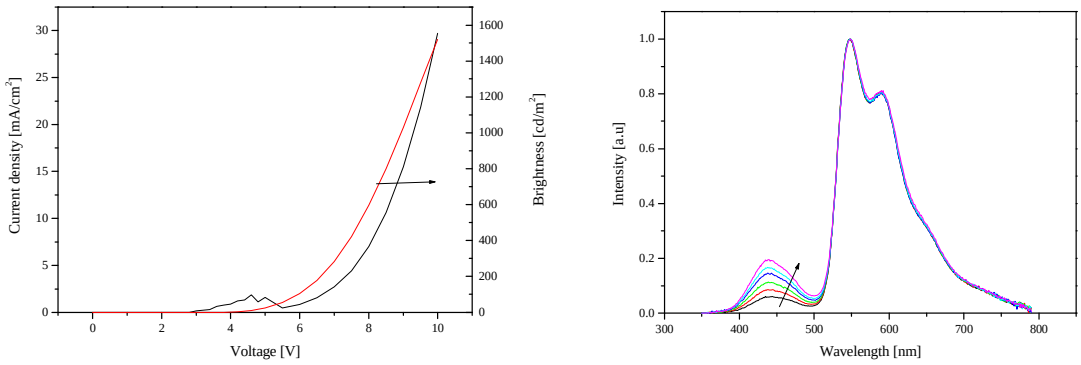

Figure 62. I-V characteristics (left) and EL spectrum (right) of a device based on **51**.

In order to avoid phase separation and to increase the energy transfer to the guest, Pt(II)-salen containing copolymers were subsequently synthesized.

3.2.3. Platinum containing Copolymers

3.2.3.1. Synthesis

The copolymers were synthesized by statistical incorporation of the phosphors applying a Yamamoto-type coupling procedure, which is well introduced in our group. Conventional heating as well as microwave assisted synthesis was used to prepare these copolymers.[146;172]

We concentrated our investigations on the incorporation of the Pt-salen complexes **41**, **42** and **43** into the backbone of solution-processed semiconducting polymers because the emission maxima of the other complexes are similar. As proof of concept we choose to incorporate the phosphors into a polyfluorene backbone. The copolymers were synthesized using different feed ratios of the Pt-salen monomer to 2,7-dibromo-9,9-dialkylfluorene (Figure 63). In the case of microwaves as the heat source short reaction times of ca. 12 minutes were applied.[147;173] A maximum temperature of 115°C was applied which was reached in less than thirty seconds. The reaction mixture was heated for three days at 80°C in the case of conventional heating. The crude polymers were Soxhlet extracted using ethyl acetate for 2 days to remove oligomeric by-products and yielded copolymers **P13, P14, P16, P17** and **P18** (Table 9).

Table 9. Reaction conditions and polymer analysis for **P13**-**P18**.

Incorporated complex	Polymer	Solvent	Molar amount of metal complex[d]	Reaction time	M_w[a]	M_n[a]	M_w/M_n
42	**P13**[b]	THF	2.1 %	12 min.	357,400	169,500	2.11
42	**P14**[b]	DMF/ toluene	8%	12 min	65,400	24,300	2.70
-	**P15**[a,c,e]	THF	-	3 d	222,200	125,700	1.77
41	**P16**[a,c]	THF	2.1 %	3 d	237,600	108,000	2.2
43	**P17**[a,c]	THF	n.d.	3 d	102,900	60,500	1.7
43	**P18**[a,c]	THF	n.d.	3 d	16,000	7,600	2.1

[a] after Soxhlet extraction with ethyl acetate. [b] microwave as heat source (**P13** = 115°C, **P14** = 220°C). [c] conventional heating at 80°C. [d] Determined by ^{1}HNR spectroscopy. [e] PF2/6 without metal complex for comparison.

The actual percentage of the Pt(II) **42** phosphor incorporated into the main chain of **P13** (2.1%) and **P14** (8.0%) was calculated from the relative ^{1}H-NMR intensities of the ethylene bridge protons of the salen ligand at $\delta \sim 3.8$ ppm relative to the sum of the aryl protons (Table 10). It was found that the metal complex was incorporated in different molar amounts into **P13** and **P14**. This suggest that the reactivity of the complex depends on the polarity of the solvent. **P13** was synthesized using THF as the solvent whereas a mixture of DMF/toluene (1:3) was used for **P14**.

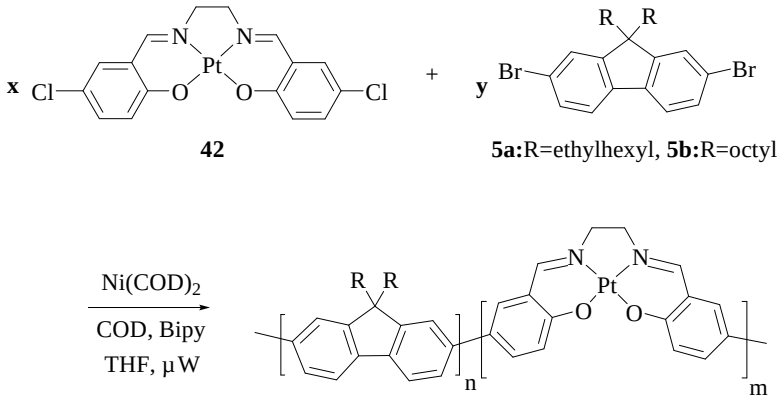

42 **5a:**R=ethylhexyl, **5b:**R=octyl

Figure 63. Synthesis of copolymers **P13** and **P14** via microwave-assisted Yamamoto-type coupling.

Copolymer **P16** (based on complex **41**), **P17** and **P18** (based on complex **43**) were synthesized utilizing conventional heating for three days (Figure 64).

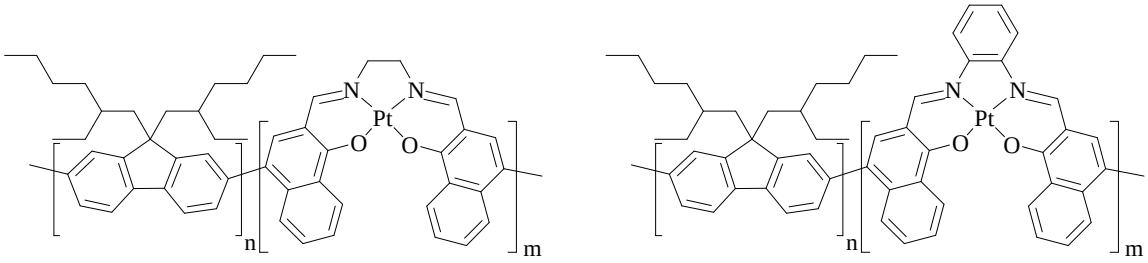

Figure 64. Chemical structure of Pt(II)-salen containing copolymer **P16 (**left) and **P17** and **P18** (right).

Extraction of the crude polymer with ethyl acetate yielded the polymers with the molecular weights summarized in Table 9. The actual percentage of incorporated Pt(II)-salen into the polymer backbone was again determined by ^{1}H NMR for **P16** (Table 10). This method was not applicable in the case of **P17** and **P18**. The ^{1}H NMR of **P16** is exemplarily presented in Figure 65.

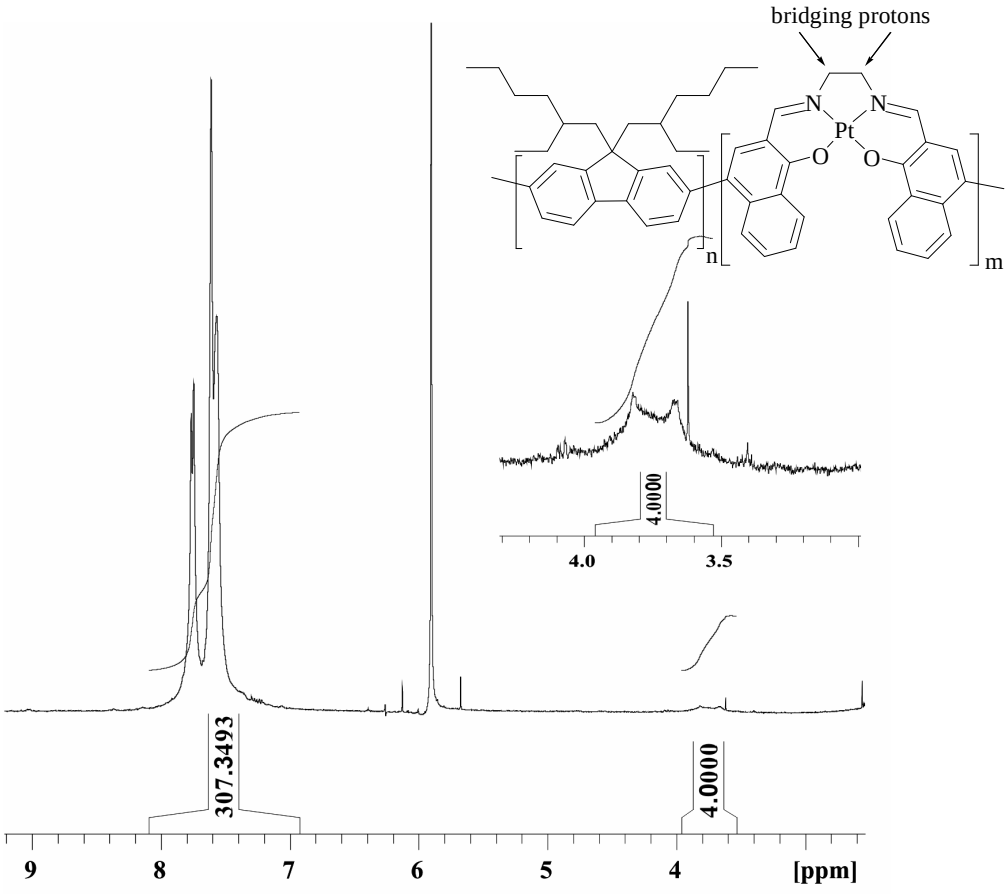

Figure 65. ^{1}H NMR spectrum of **P16**. The inset shows the protons of the ethylene bridge**.**

Table 10. Molar feed ratio of monomers and incorporated Pt-salen units determined from the integrated ^{1}H NMR spectra**.**

Polymer	Dibromofluorene	Pt(II)-salen [Mol%]	m [Mol%]
P13	1	15	2.1
P14	1	20	8.0
P16	0.98	2	2.1
P17	0.9	10	--
P18	0.95	5	--

The ratio of the intensities of the aromatic protons compared to the ethylene protons of the diimino bridge were determined to be 285.4 : 4 which means 47.6 fluorene units per one phosphor (**41**) unit. Accordingly, 2.1 % of the Pt-salen (**41**) was incorporated into the main-chain of **P16**. Interestingly, the feed ratio in the synthesis and the actual amount of complex **41** in **P16** is nearly the same whereas the incorporation of **42** in **P13** is only 2.1% with a feed ratio of 15 mol%. Whether these different reactivities are caused by the different reaction conditions (conventional heating vs microwave heating) or due to different reactivities of the complexes is not clear.

3.2.3.2. Optical Properties

Copolymer **P13** displays an intense absorption band at 383 nm in solution due to the polyfluorene chromophore and a low intensity absorption shoulder at ca. 450 nm due to the incorporated Pt-salen phosphors (Figure 66). The PL spectrum in solution is dominated by the PF emission with a maximum at 413 nm.

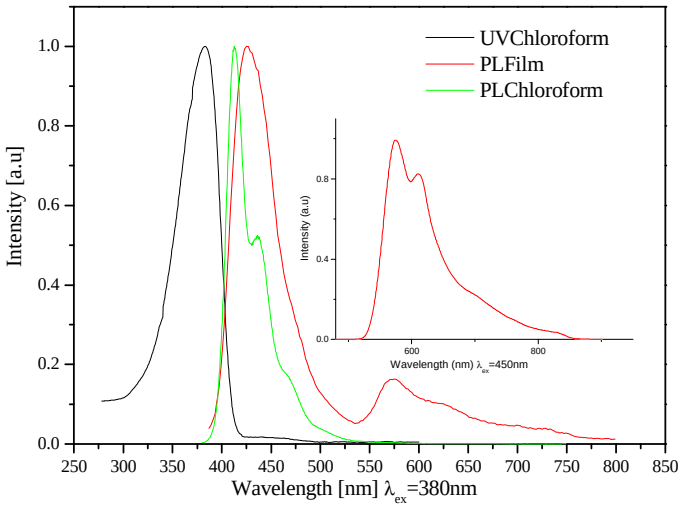

Figure 66. Absorption and emission (λ_{ex}=380 nm) spectra of **P13** in chloroform and as thin spin-coated film at 298 K. The inset shows the luminescence of the film excited at 450 nm.

The PL spectrum of the copolymer **P13** in the solid state displays a slightly red-shifted PF emission (428 nm) and an additional lower energy emission with appreciable intensity peaking at 575 nm (excitation at λ_{ex}=380 nm) (Figure 66). The lower energy peak is attributed to the green emitting Pt-salen phosphor. When the copolymer **P13** is directly excited at 450 nm, i.e. at the λ_{max} of the Pt-salen complex, the emission at 575 nm is dominantly confirming the origin of the green emission since the absorption of PF is negligible at this wavelength.

Organic light emitting diodes with a device structure ITO/PEDOT:PSS/**P13**/Ca/Al show a rather broad emission in the EL spectrum. The most prominent peak is at ca. 640 nm, with a shoulder at ca. 580 nm (Figure 67). The band at 580 nm is also observed in the solid state PL spectrum of a film of the copolymer **P13** and is attributed to the phosphorescence of the Pt-salen chromophore (Figure 66). The additional emission peak at 640 nm can be attributed to an emission from excimers of the Pt-salen phosphors.

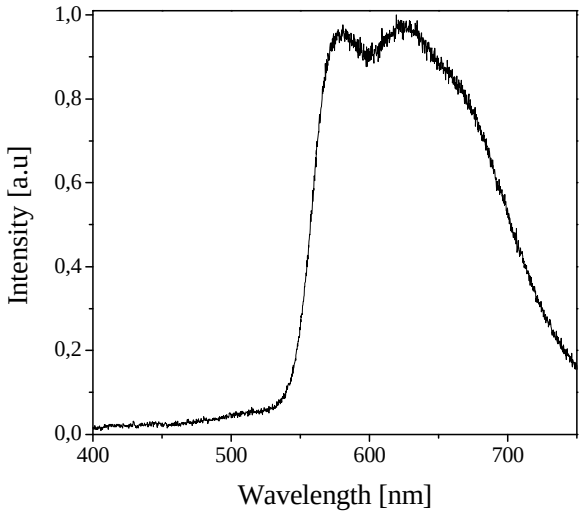

Figure 67. EL spectra of the device in the configuration ITO/PEDOT:PSS/**P13**/Ca/Al.

The formation of phosphorescent excimers has also been observed in OLEDs constructed from platinum(II)-(2-(4´,6´-difluorophenyl)pyridinato-N,$C^{2´}$)(2,4-pentanedionato).[174] The EL efficiencies of the devices based on pure copolymer **P13** are quite low (ca. 0.1-0.3 cd/A), depending on the amount of Pt-salen phosphor in the copolymer and most probably influenced by aggregate quenching. In order to reduce or suppress such concentration effects, copolymer **P14** was blended into a matrix based on poly(vinylcarbazol) (PVK) and (2-(4-biphenyl)-5-(4-*tert*-butylphenyl)-1,3,4-oxadiazole) (PBD) with a weight ratio PVK:PBD of 4:1. In this case, the 640 nm contribution to the EL spectrum is largely suppressed and the phosphorescence closely resembles the PL of the Pt-salen chromophore (Figure 69). Interestingly, the EL spectrum of the copolymer **P14** blended into the PVK:PBD matrix is slightly red-shifted by about 0.1 eV compared to that of a device containing the monomeric Pt-salen complex **54** (Figure 68) in the same matrix.

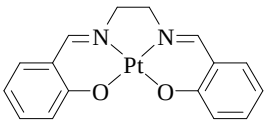

54

Figure 68. Chemical structure of complex **54.**

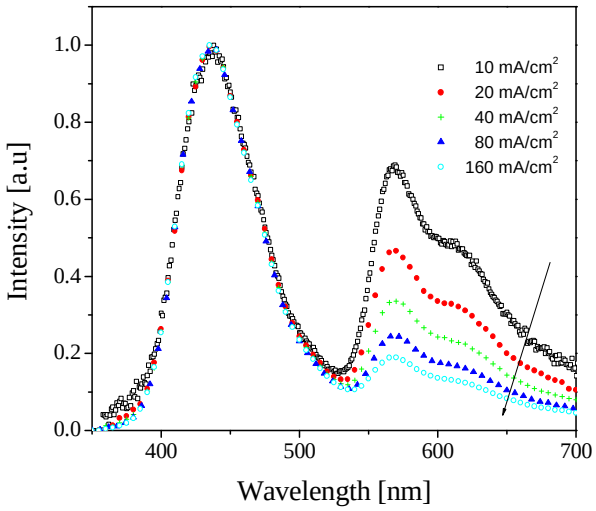

Figure 69. EL spectra of ITO/PEDT:PSS/PVK-**P14**/Ca/Al-devices (5% **P14** in PVK w/w).

However, the energy transfer between PVK and **P14** is rather inefficient and the EL contribution of the PVK matrix at 438 nm is dominant. Therefore, poly[9,9-bis(2-ethylhexyl)fluorene] (PF2/6) (**P15**) was used as an alternate matrix polymer. Devices based on a blend of the copolymer **P14** in PF2/6 (5% and 10% by weight) show a much more efficient energy transfer (Figure 70).

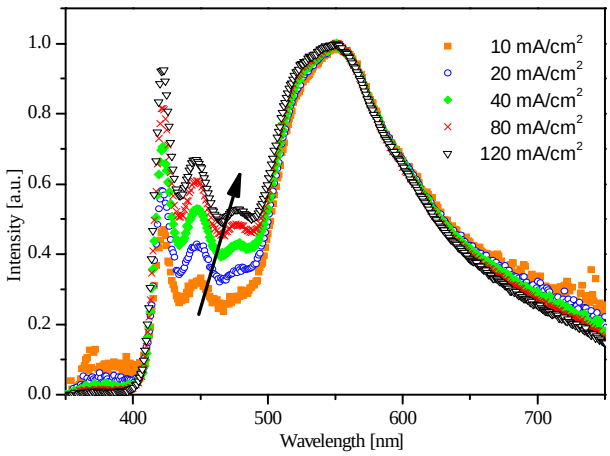

Figure 70. EL spectra of copolymer **P14** doped into PF2/6 (**P15**) (10% **P14** in PF2/6 w/w) at different current densities (device configuration: ITO/PEDT:PSS/PF2/6-**P14**/Ca/Al).

Based on recent findings on polyfluorenes with covalently-attached Ir-complexes, the occurrence of a mixed triplet state in these novel copolymers is proposed. The mixing of

triplet levels of the fluorene and cyclometalating ligand gives a hybrid mixed triplet state as the lowest energy level.[114] The efficiency of the devices were substantially improved to ca. 3-6 cd/A with the copolymer **P14** / PF2/6 blends as emissive layer (Figure 71). This improvement is attributed to the reduction of the electronic interaction between Pt-salen phosphors (excimer formation) in the device.

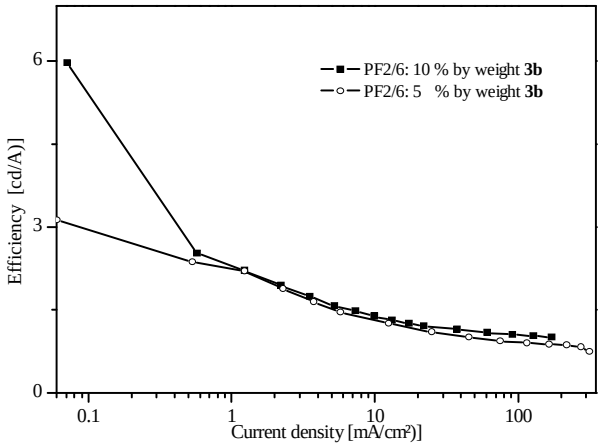

Figure 71. Efficiency of OLEDs based on (PF2/6)/**P14** blends as a function of current density**.**

Good device performances regarding the device efficiency and the colour purity were achieved in the case of **P16** as the emitting layer without additional host polymer (whereas only **P14** / PF2/6 blends showed similar efficiencies). The device configuration was ITO/PEDOT:PSS/**P16**/Ca/Al. The device revealed high brightness (ca. 1700 cd/m²) (Figure 72) at reasonable high efficiency of ca. 4 cd/A (Figure 73). Only the orange emission from the Pt-salen phosphor at 600 nm was observed indicating an optimum charge trapping at the phosphorescent guest (Figure 74).

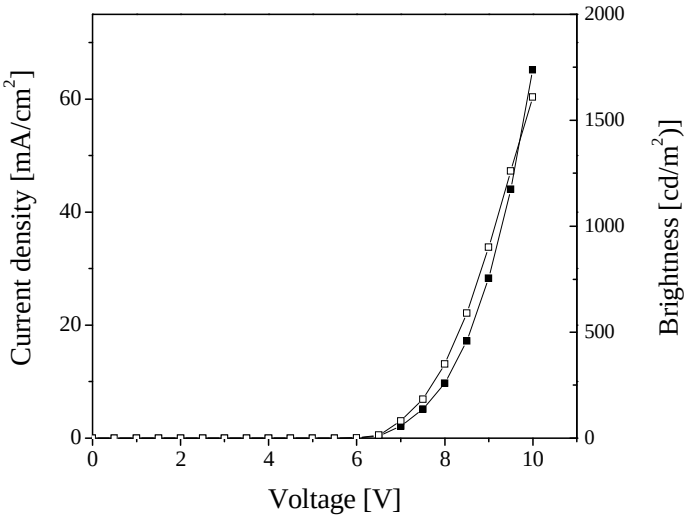

Figure 72. I-V characteristics of an OLED based on (ITO/PEDOT:PSS/**P16**/Ca/Al).

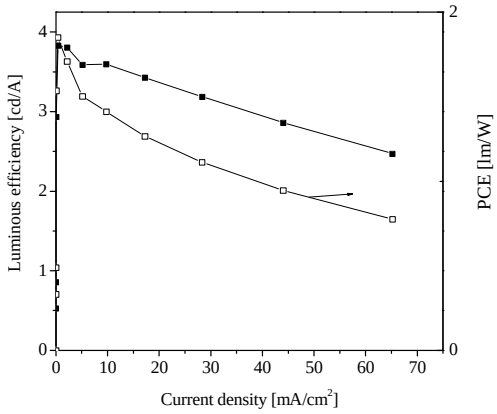

Figure 73. Efficiency of an OLED device ITO/PEDOT:PSS/**P16**/Ca/Al**.**

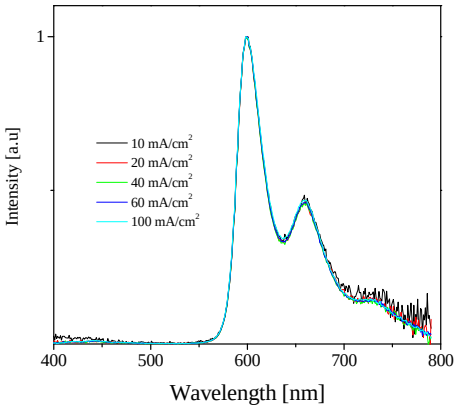

Figure 74. EL Spectrum (ITO/PEDOT:PSS/**P16**/Ca/Al)**.**

After a period of 3 hours the device based on **P16** showed a decrease of more than 50% regarding the brightness starting from 100 cd/m² to <45 cd/m² with constant current (Figure 75).

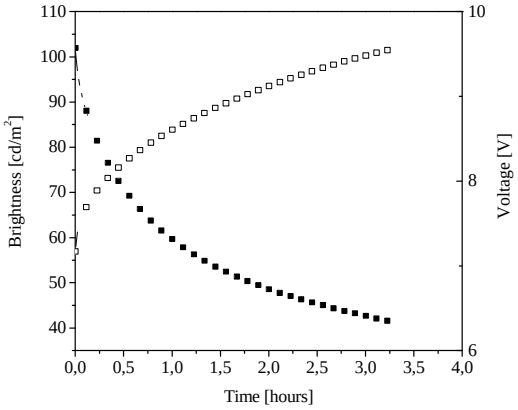

Figure 75. Lifetime characteristics of the device based on **P16**.

OLED devices based on **P17** and **P18** were not fabricated at the completion of this thesis. Their optical properties are summarized in Table 11 and the optical spectra of **P17** is shown in the experimental part. The PL emission is as expected dominated by the polyfluorene emission if excited into the PF absorption band. When excited at 507 nm, into the absorption band of the metal complex, the PL emission of **P17** shows a maximum at 659 nm for the Pt(II)-salen complex. **P18** (with a lower feed ratio of the Pt-dye) displays only a very weak emission of the phosphorescent complex.

Table 11. Optical properties of **P17** and **P18.**

Polymer	Absorption ($CHCl_3$) λ_{max} [nm]	Emission ($CHCl_3$) λ_{max} [nm] λ_{ex}=507nm
P17	381, 500-570 (broad)	659, 725
P18	380, 500-580 (broad)	654

3.3. Matrix Materials for Triplet Emitters

Synthesis and application of polymers and small molecules as a matrix for triplet emitters for OLED devices has been intensified in the last decade.[134;175-177] For suitable host materials it is mandatory to tune its band-gap so that the energy-levels match to those of the neighbouring layers or electrodes for efficient charge injections and with the guest for effective energy transfer of singlet excitons. At the same time the triplet energy (E_T) has to be higher than that of the guest to avoid triplet back transfer from accumulated triplet excitons at the guest. Because of this assumption, many hosts are only suitable for red and yellow phosphors, mostly based on PPV or PF derivatives (which have a low E_T). Polyvinylcarbazole (PVK) is commonly used as the host polymer for green and blue phosphorescent guests. OLEDs based on the PVK host and blue phosphors show low efficiencies compared to those made by small molecule hosts.[178] The triplet energy for PVK was estimated as 2.50 eV.[179] One disadvantage of PVK is that it only transports holes and OLEDs based on PVK needs therefore an electron transporting dopant for balanced charge transport. For blue emitters (which general have a $E_T < 2.62$) E_T of the host has to be higher compared to hosts for red or green emitters.[180;181] That is the reason

why it is difficult to design host materials for blue emitters. Brunner *et al.* investigated small molecules as host materials based on carbazole moieties.[175] An important finding was that the triplet energy is mainly determined by the maximum length of conjugated oligo(*para*-phenylene) segments. The triplet energy can be therefore influenced by controlling the length of conjugated oligophenylene segment.

Another task is to optimize the host materials regarding their lifetime in working devices. The focus in this section is set on the use of substituted benzophenones as comonomer in the preparation of novel host materials for triplet emitters for an application in OLEDs. Benzophenone is known as a phosphorescent organic molecule and has intensively been characterized.[182;183] Hoshino and Suzuki reported on the electroluminescence originating from triplet excited states of benzophenone in a poly(methylmethacrylate) (PMMA) matrix.[184] They observed an increase in the EL intensity caused by phosphorescence at 100 K which was negligible at room temperature. Incorporating benzophenone (Figure 76) into a polymer chain should lower the effective conjugation length (by interrupting the conjugation) as well as in a reduction of the degree of order in the polymer chains.

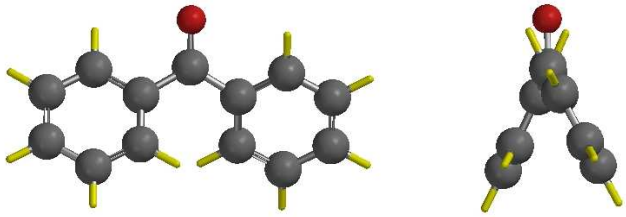

Figure 76. On top and side view of benzophenone. Structure taken from the Spartan ´04 database**.**

Benzophenone should also act as a charge trap (like fluorenone) and should consequently influence the energy and charge transfer processes in OLEDs.

3.3.1. Results and Discussion

3.3.1.1. Synthesis

During this work different copolymers with benzophenone building blocks were synthesized applying a Yamamoto-type coupling procedure with 1,4´-dibromobenzophenone as comonomer. Another comonomer which was tested is 1,4-bis(4´,4´´-decylbenzoyl)-2,5-dibromobenzene (**57**).[185-187] The synthesis of the diketone **57** is outlined in Figure 77.

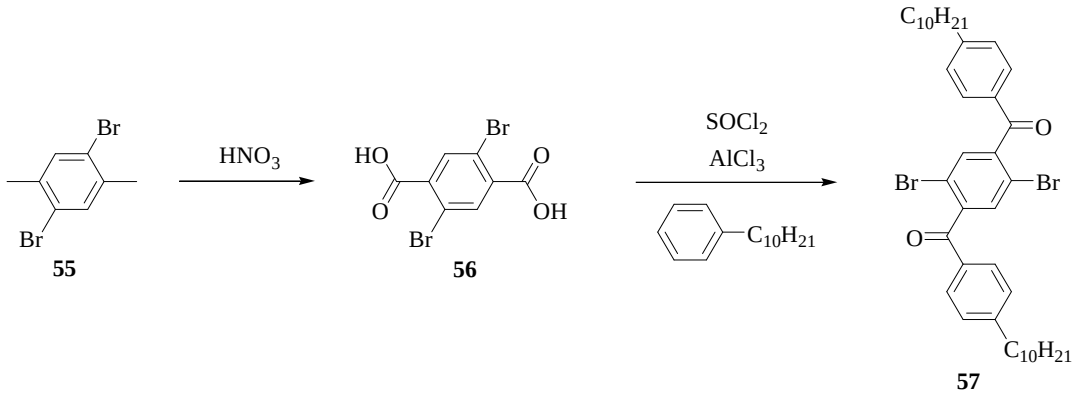

Figure 77. Synthesis of diketone monomer **57**.

The first step is the oxidation of 2,5-dibromo-1,4-dimethylbenzene (**55**) to the corresponding 2,5-dibromoterephthalic acid (**56**). The acid was converted to the corresponding diacid dichloride with the use of thionyl chloride and *in sit*u converted in a Friedel-Crafts-type acylation to give **57**.

Five different ratios of dibromobenzophenone and fluorene (**5b**) were used to synthesize the corresponding random copolymers **P19**-**P24** (Figure 78.) An overview of the feed ratios and the copolymer molecular weights is given in Table 12.

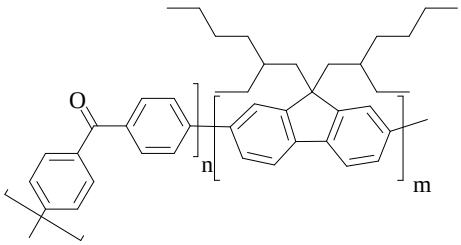

Figure 78. Chemical structure of copolymers **P19**-**P24**.

Table 12. Composition and molecular weights of **P19**-**P24**.

Polymer	Benzophenone [%]	M_n [g/mol]	M_w [g/mol]	PD
P19	5	168,00	322,000	1,9
P20	6.5	145,000	272,000	1,9
P21	10	147,000	307,000	2,1
P22	20	111,000	242,000	2,2
P23	33	187,000	291,000	1,6
P24	50	69,000	142,000	2,1

Lifetime tests utilizing **P19**-**P24** as host polymer of phosphorescent OLEDs were performed at the Samsung SDI European Research Centre in Berlin. They found that the best lifetimes of OLED devices were obtained for **P21** (10% benzophenone units). With this knowledge also the synthesis of the fluorene-based copolymer containing 10% of the diketone **57** (**P25**) was accomplished and the polymer tested as a host material for triplet emitters (Figure 79).

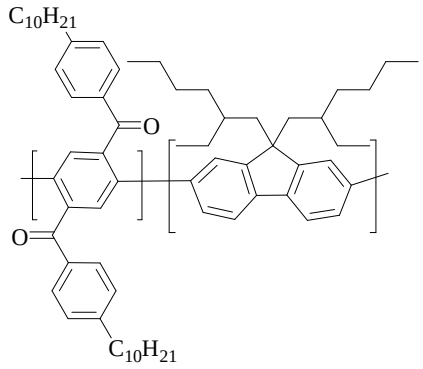

Figure 79. Chemical structure of copolymer **P25.**

In order to combine the benefits of such copolymers with the already described Pt(II)-salen-containing copolymers, a statistical copolymer (Figure 80) was synthesized containing both Pt(II)-salen and 10% benzophenone units (**P26**). The amount of Pt-salen chromophors was determined by ^{1}H NMR to 1.7%.

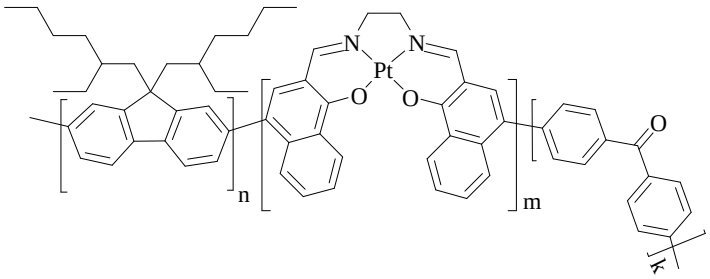

Figure 80. Chemical structure of copolymer **P26.**

On the journey towards suitable host polymers also monomeric building blocks with a pentaphenyl as longest conjugated unit were prepared.[188] Brunner *et al.* have described copolymers with different lengths of conjugated oligophenylene segments.[134] Copolymers containing only short oligophenylene segments have been found to be mandatory for being a suitable host for green or blue triplet emitters. Monomers **58** and **59** (Figure 81) consists of a central 1,4-phenylene core and two fluorenyls attached in para-position. The central

core allows for attaching different substituents, e.g. in 2,3,5,6-tetrafluoro-1,4-phenylene (**58)** or 2,5-bis(trifluoromethyl)-1,4-phenylene (**59)**.

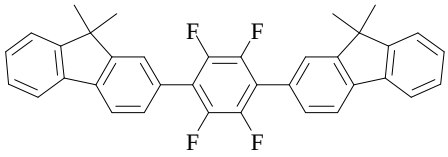

58

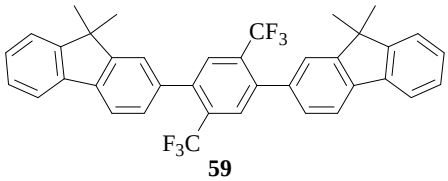

59

Figure 81. Chemical structure of **58** and **59**.

The synthesis of **58** is outlined in Figure 82. The commercially available 1,4-dibromo-2,3,5,6-tetrafluorobenzene (**60**) was converted in a Suzuki-type reaction with the corresponding 9,9-dimethyl-fluorene-2-boronic ester to **58**.[140]

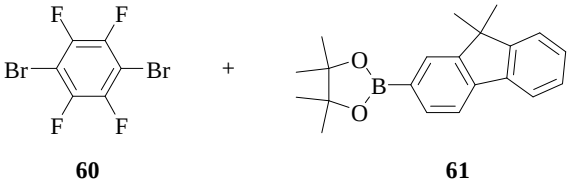

60 **61**

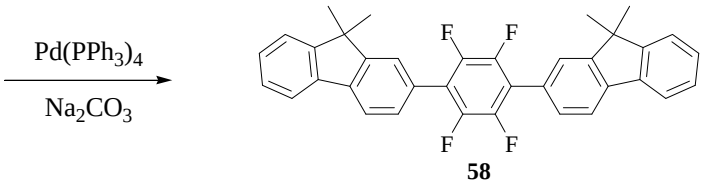

58

Figure 82. Synthesis of 1,4-Bis[2´-(9´,9´-dimethyl)fluorenyl]tetrafluorobenzene (**58**).

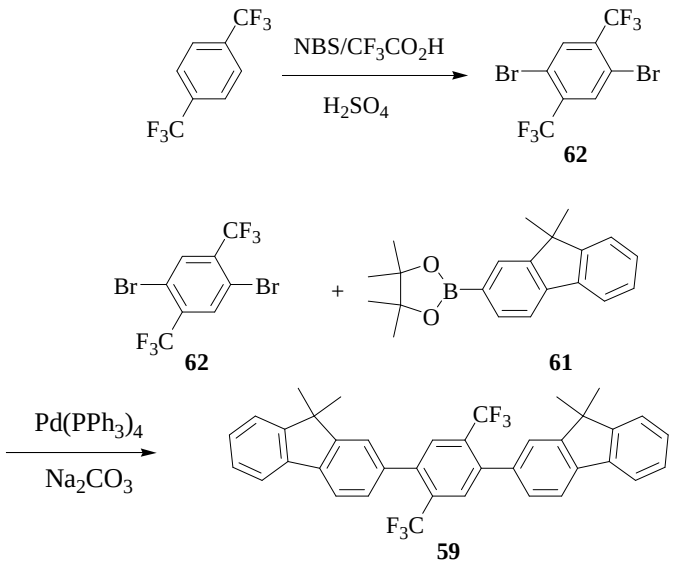

Figure 83. Synthesis of 1,4-Bis(2´-9´,9´-dimethylfluorenyl)-2,5-bis(trifluoromethyl)benzene (**59**).

1,4-Dibromo-2,5-bis(trifluoromethyl)benzene (**62**) was obtained from 1,4-bis(trifluoromethyl)-benzene in a bromination reaction. A mild bromination reported by Dolbier *et al*. was chosen for the synthesis of **62** (Figure 83) to avoid hydrolysis of the trifluoromethyl groups.[189] The Suzuki-type reaction with the boronic ester **61** gave **59** in good yields (82%).

Crystals of **58** and **59** were grown and the X-ray structures were resolved which are shown in Figures 84 and 85, respectively.

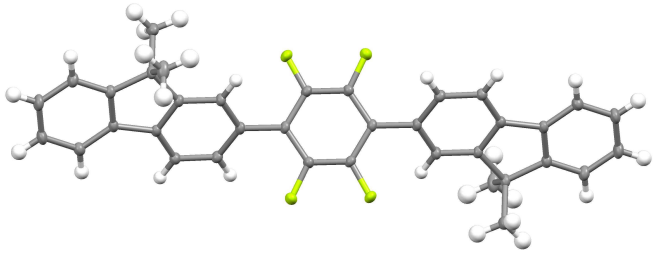

Figure 84. Chrystal structure of **58.**

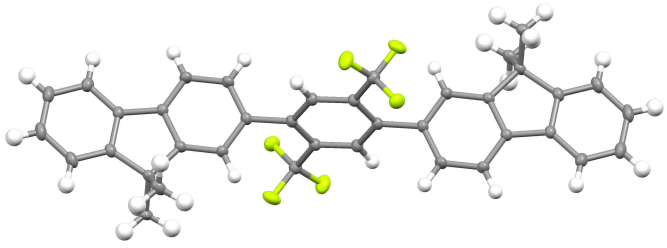

Figure 85. Crystal structure of **59**.

58 and **59** both crystallize with a crystallographic inversion centre. Only half of the molecule is crystallographically independent. Subsequently, for **58** only one torsion angle of 43.8° is observed between the central tetrafluoro benzene core and the terminal fluorenyl system. Both fluorenyls are nearly planar with a maximum variation of 0.08 Å. An significant π-π interaction in the lattice is probably hindered by the torque of the oligomer. The oligomer **59** reveals an increased torsion angle between the central benzene-core and the fluorenyl group of 73°.

An electrophilic Friedel-Crafts-type polymerisation of monomers **58** and **59** with N-methylisatine was carried out in the group of Prof. Zolotukhin (national university of Mexico, UNAM) in Mexico-City. Figure 86 shows the synthesis of the investigated polyarylene **P27**.[190] In a typical electrophilic polymerisation performed by Zolotukhin *et al.* N-methylisatine (N-methylindoline-2,3-dione) and **58** are stirred with trifluoromethane sulfonic acid under dry nitrogen for 9 hours. The resulting viscous solution is then poured into water. The resulting polymer is extracted with methanol and acetone.

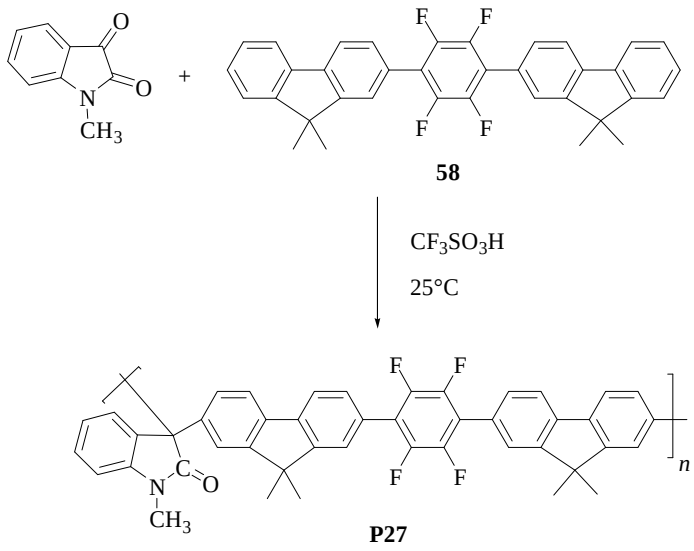

Figure 86. Chemical structure of the copolymer **P27**.

P27 was achieved as a white polymer with the molecular weight of M_w=178.000 g/mol and a high polydispersity of 10.4.

3.3.1.2. Optical Properties

The benzophenone/fluorene copolymers **P19**-**P24** were tested as hosts for triplet emitters in phosphorescent OLEDs. These measurements were done at the Samsung SDI European Research Center in Berlin. The 10% benzophenone-containing copolymer **P21** emerged as the best-suited copolymer concerning the lifetime and the efficiency of the OLED devices.

Figure 87 shows the EL spectra of different devices based on **P21**. Three different concentration levels of the Ir(bpi) (1%, 4% and 7%) were tested using also different ratios of host polymer blended with the hole transporting material ST1693 (supported from Sensient, Figure 88) (70:30, 90:10, and 80:20).

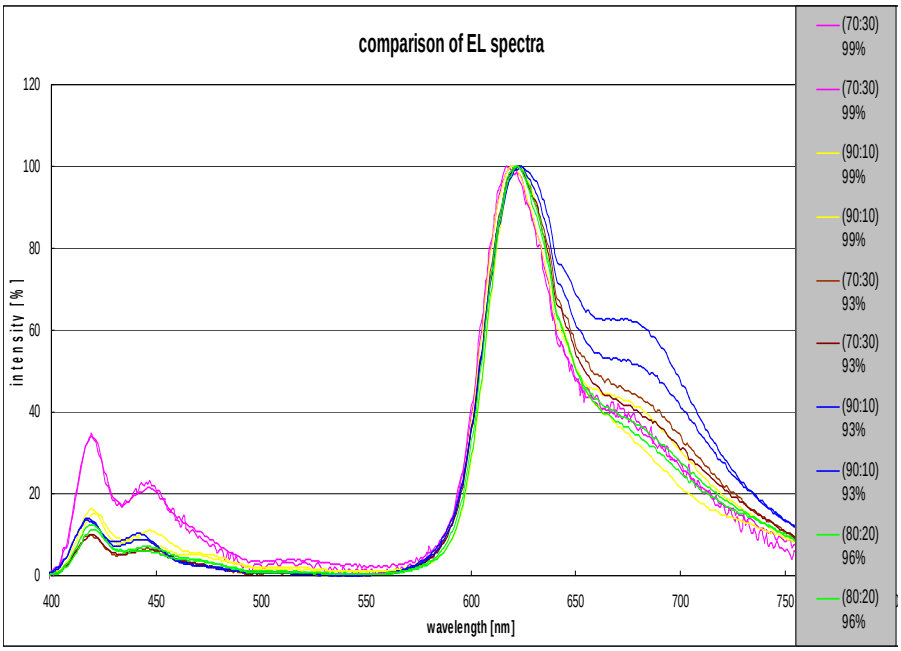

Figure 87. Comparison of EL spectra based on **P21** with different amounts of HTM (ST1693 see Figure 95) and Ir phosphor. Legend: The brackets show the ratio of **P21**/ST1693 (see Figure 88) and below the total host amount used in the OLEDs is given related to the concentration levels of the Ir(bpi) guest: 1% (99% host), 4% (96% host) 7% (93% host).

All devices showed dominant emission from Ir(bpi) but still some host emission depending on the amount of Ir-phosphor in the blend. It is difficult to determine the reason because this host emission could be caused by phase separation, inefficient energy transfer, or triplet back transfers. However, the efficiencies are still quite low depending on the amount

of Ir-phosphor and the HTM concentration varying from approx. 0.1 to 1.2 cd/A (Figure 89).

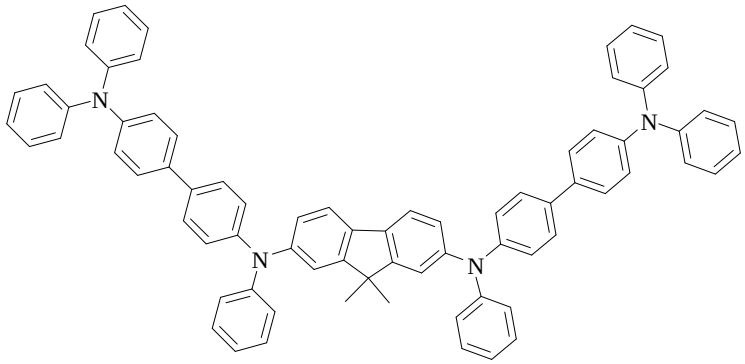

Figure 88. Chemical structure of HTM ST1693.

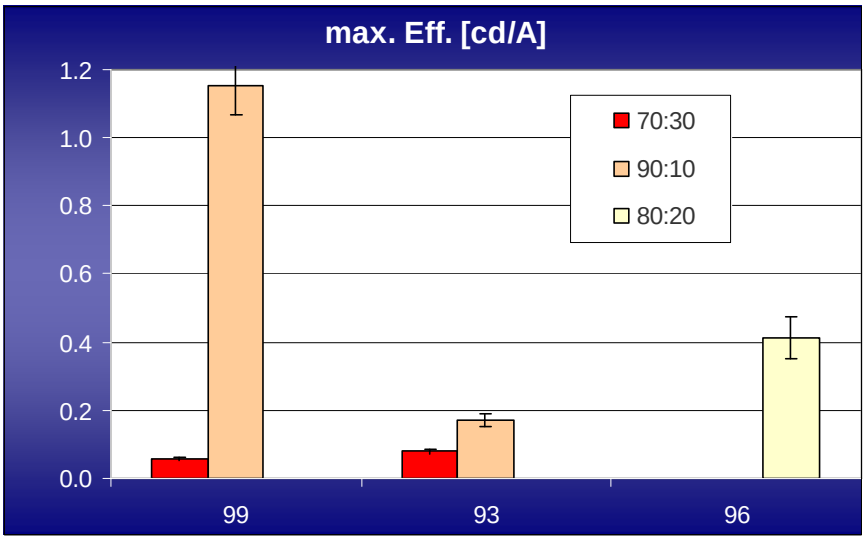

Figure 89. Efficiency of the devices based on **P21** depending on the HTM concentration and the amount of Ir-phosphor. Legend: Ratio of **P21** to HTM ST1693 (70:30; 90:10 and 80:20) Left: 1% Ir(bpi); middle 7% Ir(bpi); right 4% Ir(bpi)

Lifetime tests of the device based on **P21**, HTM (10%) and Ir dopant 0.5% showed promising lifetimes (brightness test at 100 cd/m²) of over 50% of the initial brightness after 1000 h. One remaining question was a possible spectral degradation of the emission. The comparison of the PL spectra of a thin film as shown in Figure 90 before and after aging

showed no degradation of the emission of the Ir dopant. More probably the HTM ST1693 seems to be the source of the degradation processes as the films with lower content of ST1693 shows less degradation.

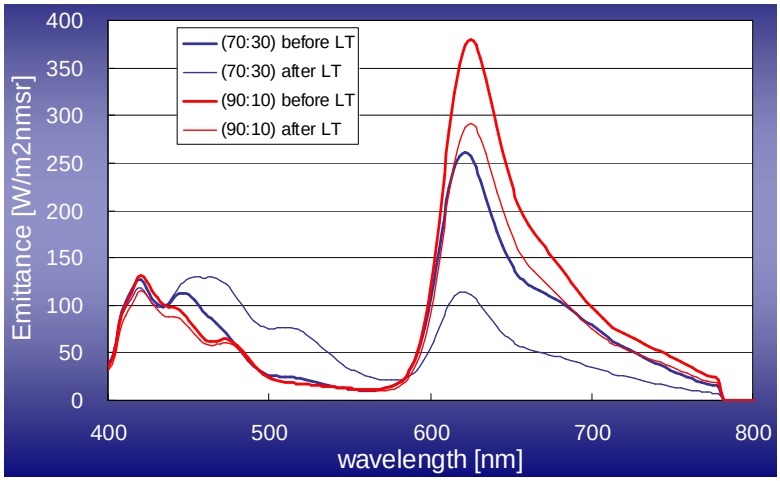

Figure 90. PL of thin films of **P19** with different ratios of HTM and 1% Ir(bpi) before and after lifetime testing.

The EL spectrum of a device based on **P25** with 10% by weight of a hole transport material (ST1693) showed very low efficiencies <0.4 cd/A for the green triplet emitter Ir(mppy). The blue emission is still dominant in EL (Figure 91).

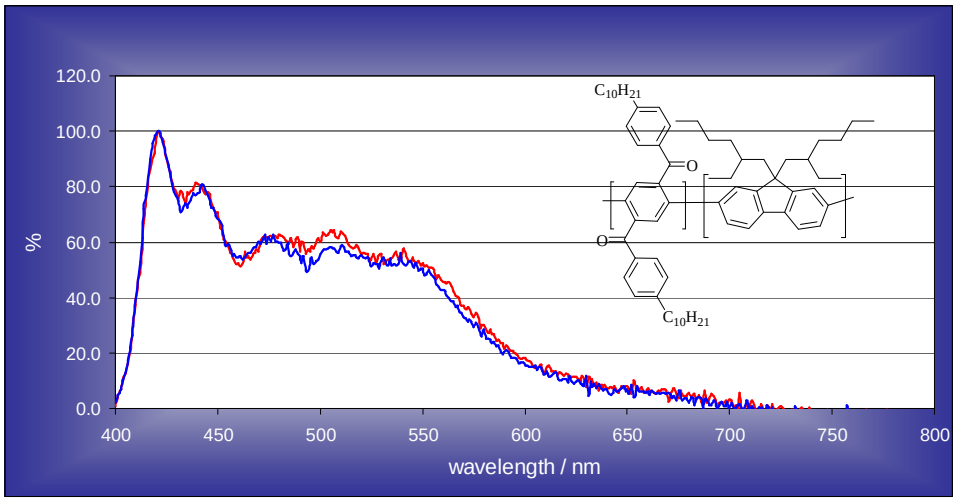

Figure 91. EL spectrum of an OLED device based on **P25** with 10% ST1693 and the Ir(mppy) emitter.

As the efficiencies for the **P25** host were smaller if compared to **P21** Pt(II)-salen-containing fluorene/benzophenone copolymers have been the next target.

The absorption spectrum of **P26** in solution is dominated by the fluorene absorption. No metal complex absorption was observed. In the solution PL spectrum the host emission is the only observed emission component. The solid state spectrum showed a moderately intense emission band of the Pt-salen phosphor even at room temperature peaking at 599 nm (Figure 92) accompanied by a vibronic side band at 657 nm with an excitation at the λ_{max} of the PF (380 nm). This indicates energy transfer to the Pt-salen phosphor.

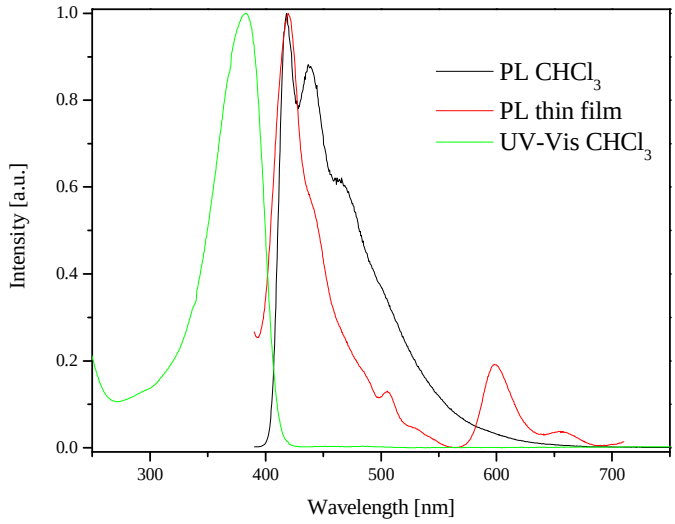

Figure 92. Absorption and emission of **P26** (λ_{ex} = 380 nm)**.**

OLED devices made of **P26** as a single layer with the device structure ITO/PEDOT:PSS/**P26** (70 nm)/CsF/Al showed high brightness of ca. 1000 cd/m² at low current densities and low onset voltages (Figure 93). The efficiency of the device was also satisfactory with 2.5 cd/A as this device was not optimized regarding the thickness of the emitting layer (Figure 94). The most important improvement of this device was observed in lifetime measurements (with constant current) showing an increased lifetime if compared to the copolymer without the benzophenone units (**P16**). The device based on **P26** showed a fivefold increased operational lifetime with >60 % of the initial brightness after 12h (Figure 95).

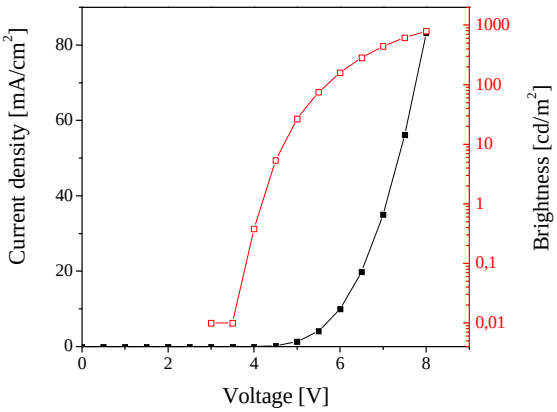

Figure 93. I-V characteristics of the device based on **P26**.

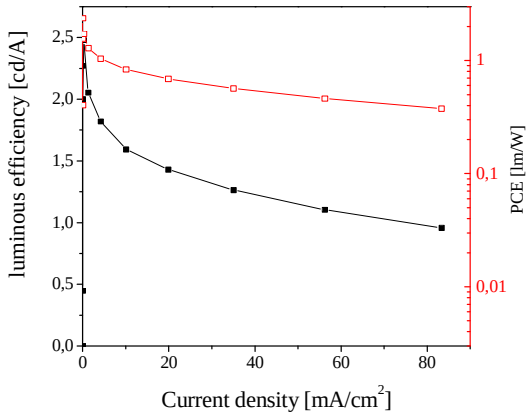

Figure 94. Efficiency of the device based on **P26**.

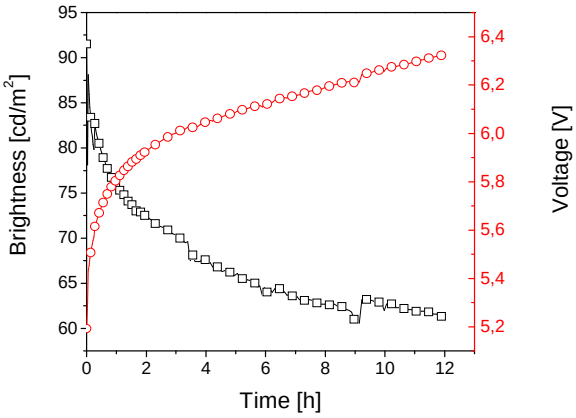

Figure 95. Lifetime characteristics of the device based on **P26**.

Devices made from copolymer **P27** gave quite low efficiencies of up to 0.7 cd/A (device structure: ITO/**P27**:6% $Ir(piq)_2acac$:8% TPD (80nm)/Ca/Al).

In order to improve the efficiency a insoluble interlayer was included into the device structure. The use of the interlayer concept has been applied in fluorescent and electrophosphorescent OLEDs.[169;191;192] Several polymers can form insoluble interlayers on a PEDOT:PSS layer after annealing, e.g. poly[2,7-(9,9-dioctylfluorene)-*alt*-(1,4-phenylene-((4-*sec*-butylphenyl)imino)-1,4-phenylene)] (TFB), poly(9,9-dioctylfluorene-2,7-diyl-*co*-bis-N,N-(4-butylphenyl)-bis-N,N'-phenyl-1,4-phenylene-diamine) (PFB).

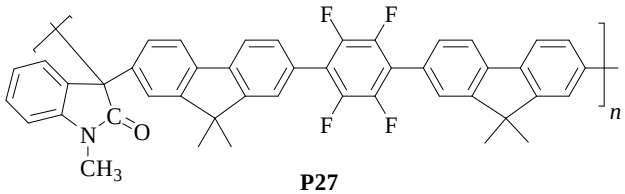

P27

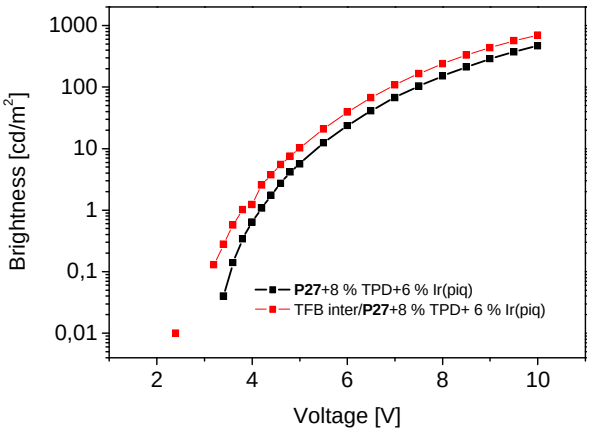

Figure 96. Brightness of OLEDs based on **P27**.

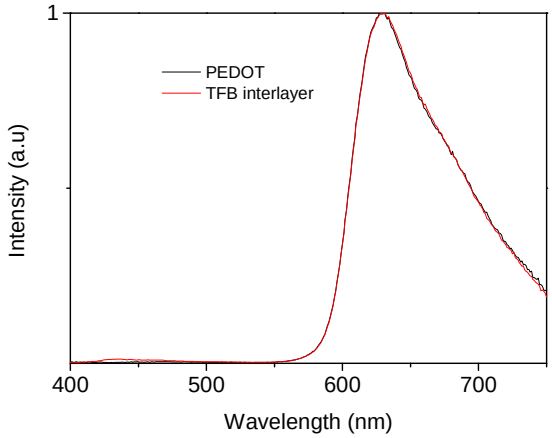

Figure 97. EL spectrum of OLEDs based on **P27.**

However, initial OLED results based on the **P27** host on top of a PFB interlayer showed slightly lower efficiencies of ca. 0.5 cd/A (device structure ITO/ PFB interlayer/**P27** : 6% $Ir(piq)_2acac$ / Ca/Al). Both devices showed high brightnesses of ca. 1000 cd/m² (Figure 96) and their emission spectra are very similar (Figure 97).

3.4. Conclusion

We have presented and introduced a novel synthetic concept towards main-chain electrophosphorescent copolymers based on Pt(II) Schiff base complexes as the phosphor. Promising results were obtained regarding the OLED efficiency of up to 3-6 cd/A for devices based on **P14** / PF2/6 blends. Devices based on **P16** as the emitting layer showed high brightness of ca. 1700 cd/m² at a reasonable high efficiency of ca. 4 cd/A.

Lifetime measurements showed less than 50% of the initial brightness after a period of ca. 3 hours. Improved operational lifetimes were obtained for novel matrix materials based on random fluorene-benzophenone copolymers (e.g. **P21**) A novel fluorene/benzophenone copolymer **P26** with on-chain Pt(II)-salen phosphor showed also an extended lifetime with still 60% of the initial brightness after an operational period of 12 hours.

Also other oligophenylene-based monomeric building blocks for related copolymers have been synthesized. These monomers have been incorporated into novel alternating copolymers in collaboration with the group of Prof. Mikhail Zolotukhin (national university of Mexico, Mexico-City).

4. Summary

New results on the origin of a green emission band peaking at 479/506 nm observed in OLEDs made of polyfluorene as the emitting material were discussed in chapter 2. A new defect structure – alkylidenefluorene units – in addition to fluorenone defects (keto defects) was proposed and taken into account. Model Copolymers consisting of dialkylfluorene and alkylidenefluorene units in different ratios were synthesized. The optical properties were recorded and solid state emission bands at 481/510 nm observed. Very similar defect emission bands in degraded OLED devices based on PF emitters are probably caused by such alkylidene defects.

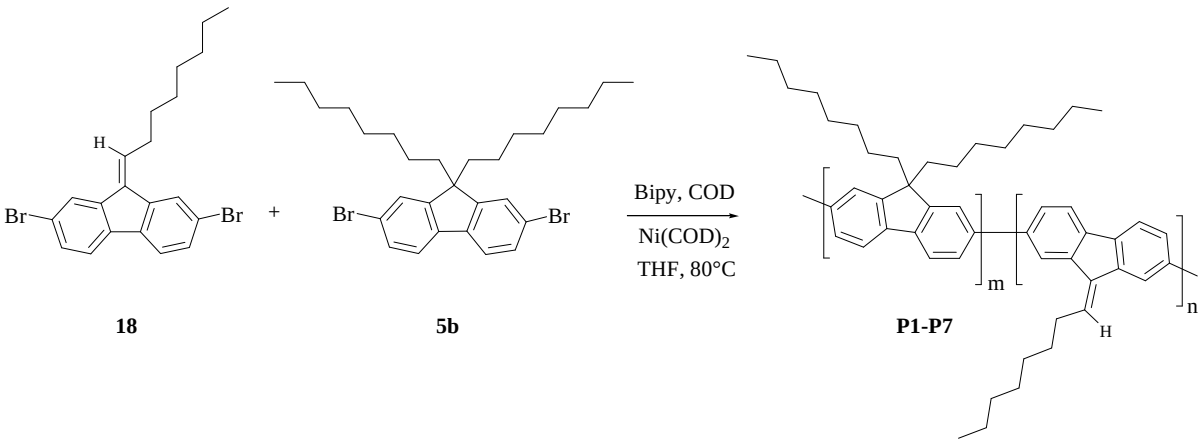

Figure 98. Model copolymers containing alkylidene defects**.**

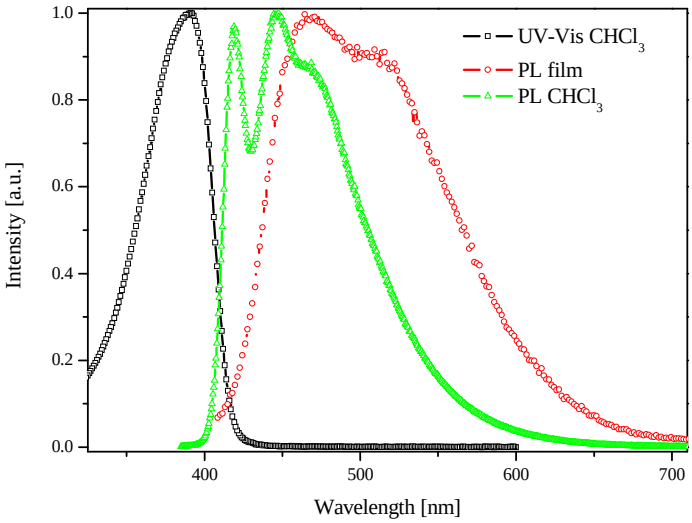

Figure 99. Photoluminescence and absorption of 5% alkylidene containing polyfluorene **P7**.

Moreover, binaphthyl spacers were introduced into the main chain of polyfluorenes fluorene/fluorenone copolymers. OLED investigations showed that the incorporation of binaphthyl spacers leads to an increase of the green emission in the fluorene/fluorenone copolymer **P10**. This suggests an accelerated energy transfer to the defect sites in the copolymer **P10**.

In the second part of this work novel electrophosphorescent main-chain copolymers and novel matrix materials for OLED devices were synthesized and investigated. In particular, copolymers with main-chain Pt(II)-salen triplet emitters were synthesized and tested in solution-processed OLED devices. Their structure is shown in Figure 100 examplarily for the copolymers **P16** and **P18**.

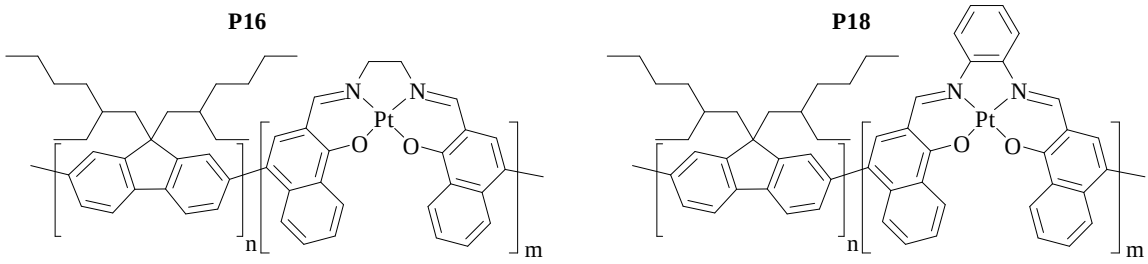

Figure 100. Chemical structure of Pt(II)-salen-containing copolymers **P16 (**left) and **P18** (right).

Devices based on blends of the copolymers with PF2/6 as emissive layer showed a red emission with high brightnesses of 1000-1700 cd/m² at a reasonable high efficiency of 3-6 cd/A. The emission colour of the synthesized platinum(II) complexes (see chapter 3.2.2.) can be tuned by a variation of the salen ligands (from yellow to red phosphorescence).

Different novel copolymers (random benzophenone/fluorene) copolymers as potential OLED matrix materials are presented in chapter 3.3. (Figure 101). The lifetime of the corresponding OLEDs could be improved in comparison to a PVK matrix.

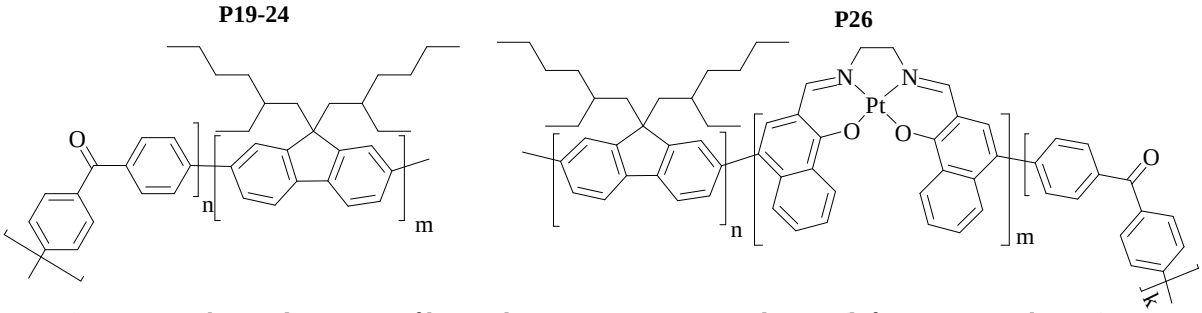

Figure 101. Chemical structure of benzophenone-containing copolymers (left **P19**-**P24,** right **P26)**.

For a molar content of 10% benzophenone (**P21)** very promising operational lifetimes (for 50% of the initial brightness) were reported (up to 1000 h). A main-chain phosphorescent copolymer **P26** containing 10% benzophenone units (Figure 101) also showed improved operational lifetimes (as compared to a copolymer without benzophenone units) at reasonable high brightness (1000 cd/m²) and OLED efficiency of ca. 2.5 cd/A.

5. Outlook

5.1. Oligofluorenes

To investigate structure-property relationships in more detail, monodisperse oligofluorenes with a central alkylidenefluorene could lead to a better understanding of the green emission components in degraded polyfluorenes. Similar investigations regarding fluorenone defects are described in the literature.[76;149;150;193]

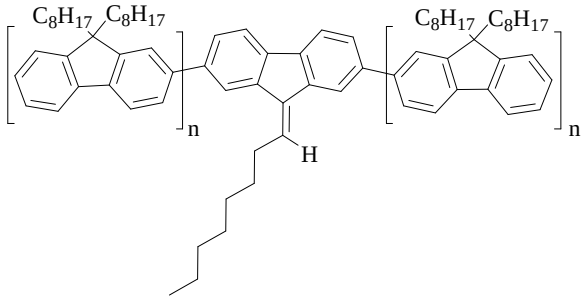

Figure 102. Chemical structure of alkylidenefluorene-containing oligofluorenes.

Figure 102 shows the structures of alkylidene-containing oligofluorenes, whereby the length of oligofluorene units can vary.

5.2. New Polymers for Organic Light Emitting Diodes (OLEDs)

The electrophilic Friedel-Crafts-type polymerizations as developed in the group of Prof. Mikhail Zolotukhin (national university of Mexico) may be suitable to prepare several other copolymers as promising candidates for host polymers of phosphorescent OLEDs.

Suitable monomers can be prepared by Suzuki-type coupling of the dimethylfluorene-boronic ester monomer with dihalide compounds.

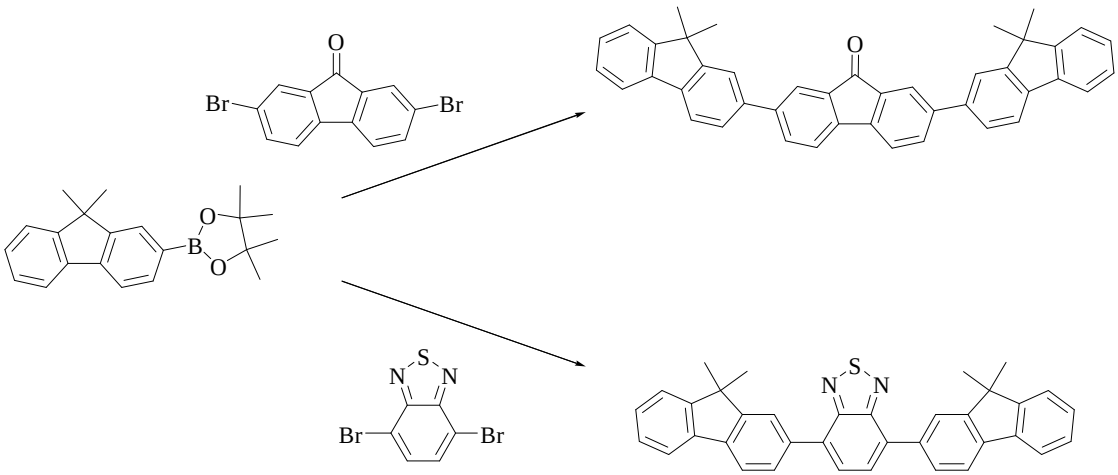

Figure 103. Chemical structures of monomers suitable for electrophilic polymerization.

Some chemical structures are shown in Figure 103 and will be used in the synthesis of the corresponding copolymers. Similar copolymers have been applied for electronic applications such as polymers lasers (fluorene-*alt*-benzothidiazole (PFBT) copolymers) or OLEDs.[140;194]

5.3. Electrophosphorescent Dyes

Initial results on the synthesis and the application of pyrrol-based platinum Schiff base complexes show promising efficiencies even for solution-processed devices. While working on the synthesis of these pyrrole based complexes, Che and co-workers described the application of a series of vacuum-deposited pyrrol-based Pt(II) complexes in OLEDs.[195] The synthesis was performed in a similar fashion to the Schiff base complexes described in chapter 3.

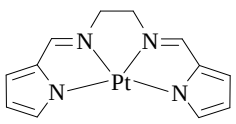

63

Figure 104. Chemical structure of a pyrrol-based Pt(II) phosphor **63.**

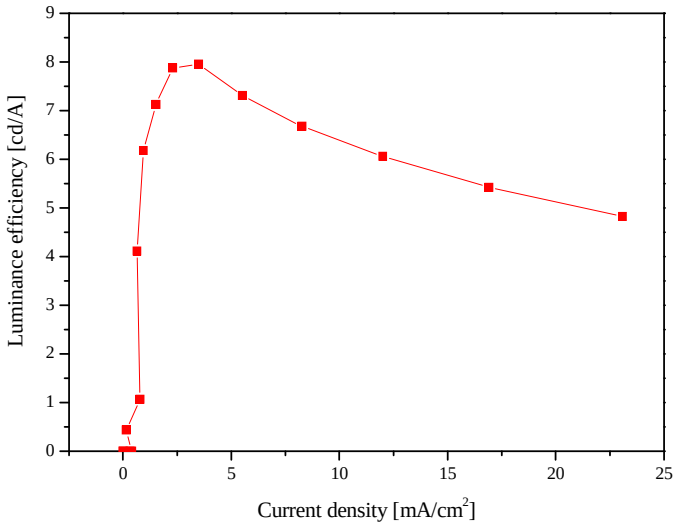

Figure 105. Efficiency of an OLED device based on **63**.

However, we will apply solution-processing to fabricate OLED devices based on a pyrrole Pt(II) Schiff base complex. A first example shown in Figure 104 (device structure: PEDOT/PVK+PBD (40%)+ **63** (2%)/Ca/Al). A maximum luminescence efficiency of 8 Cd/A at a reasonable high brightness of ca. 1100 cd/m^2 was achieved by blending the phosphor into a PVK matrix (Figures 105 and 106). Applying the described strategy to incorporate the phosphor into the main-chain of a semiconducting polymer, the ligand sphere has to be modified resulting in an AA- or AB-type monomer (Figure 107). As the first device results are very promising, pyrrole-based Pt(II) phosphors are interesting candidates for solution-processed, phosphorescent OLEDs.

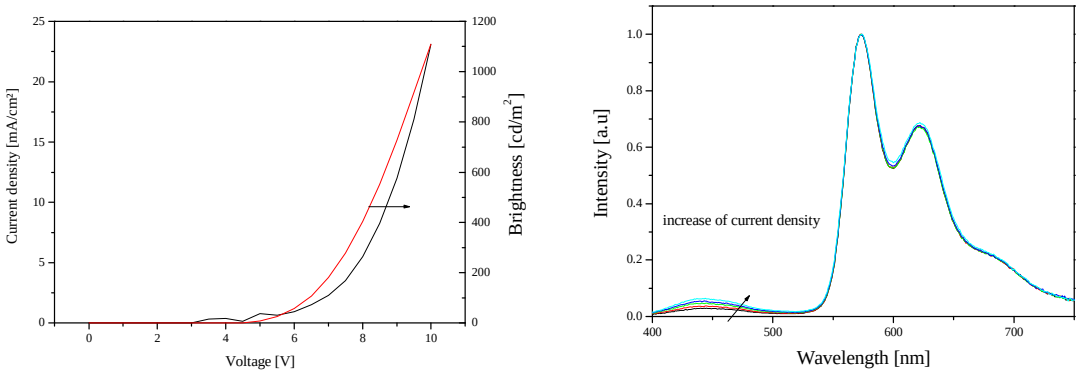

Figure 106. I-V characteristics and EL spectrum of a device prepared from **63**.

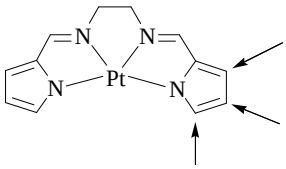

Figure 107. Possible variations of the ligand sphere at three different substitution positions.

5.4. Matrix Materials

Further improvements of copolymers with on-chain phosphors are expected from the synthesis of carbazole-based copolymers (Figure 108). The use of carbazole-based oligomers and polymers as hosts for phosphorescent guests has been described by Brunner *et al*., wherein the fine tuning of the energy levels can lead to improved energy transfer and results in higher OLED efficiencies.[175]

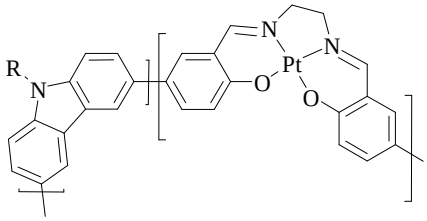

Figure 108. Carbazole-based copolymers with on-chain Pt-salen phosphors.

Cao *et al*. reported the synthesis and characterization of fluorene-*alt*-carbazole copolymers with on-chain iridium complexes.[196] Such a synthetic strategy could be transferred to the synthesis of related copolymers containing Pt(II)-salen complexes (Figure 109).

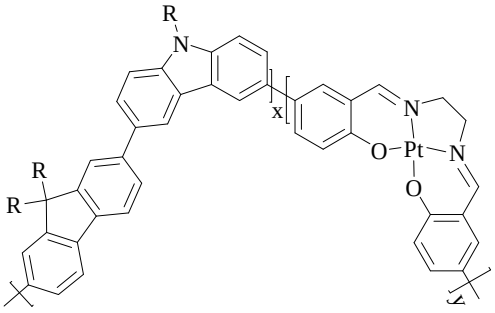

Figure 109. Fluorene-*alt*-carbazole based copolymers with on-chain Pt(II)-salen phosphors.

6. Experimental Section

6.1. General Methods

Unless otherwise indicated, all starting materials were obtained from commercial suppliers (Aldrich, Fischer, EM Science, Lancaster, ABCR, Strem) and were used without further purification. All reactions were carried out under an argon atmosphere. Analytical thin-layer chromatography (TLC) was performed on silicagel F-254 pre-coated TLC plates. Visualization was performed with a 254 nm ultraviolet lamp. Silica gel column chromatography was carried out with Silica Gel (230-400 mesh) from EM Science. The ^{1}H- and ^{13}C-NMR spectra were recorded on a Bruker ARX 400 spectrometer with deuterated tetrachloroethane or dimethylsulfoxide as the solvents. Low-resolution mass spectroscopy was obtained on a Varian MAT 311A operating at 70 eV (electron impact) and reported as m/z. FD masses were obtained on a ZAB 2-SE-FDP. Elemental analyses were done on a Vario EL II (CHNS) instrument. UV-Vis absorption spectra were recorded on a Jasco V550 spectrophotometer. Fluorescence measurements were carried out on a Varian Cary Eclipse instrument. Gel permeation chromatographic analysis (GPC) utilized PS columns (three columns, 5 µm gel, pore widths 103, 105 and 106 Å) connected with UV-Vis and RI detection. All GPC analyses were performed on solutions of the polymer in THF or toluene at 30°C with a flow rate of 1 mL/min (concentration of the polymer ca. 1.5 g/L). The calibration was based on polystyrene standards with narrow molecular weight distribution. Phase transitions were studied by differential scanning calorimetry (DSC) with a Perkin Elmer DSC6 thermosystem at a scanning rate of 10 K min^{-1} for both heating and cooling cycles. Microwave assisted syntheses were performed using a CEM – Discovery monomode microwave utilizing a IR-temperature sensor, magnetic stirrer and sealed 10 mL glass vials. All reactions were monitored and controlled using a personal computer.

6.2. General Procedures

6.2.1. Procedure A: Alkylation of Dibromofluorene

According to Nothofer[144]

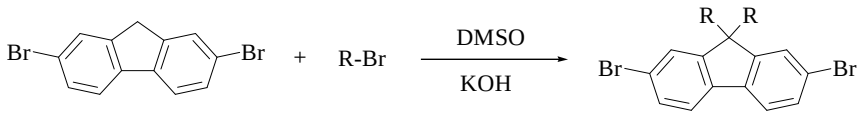

An aqueous sodium hydroxide solution (40 mL, 50%) and the alkylbromide (225 mmol) were added to a solution of 2,7-dibromofluorene (33 g, 102 mmol) and tetrabutylammonium bromide (9.9 g, 31 mmol) in DMSO (75 mL) at 80°C. The mixture was stirred at 80°C for 2 h and then poured into water (100 mL). The mixture was extracted two times with diethylether and the combined organic phases were washed with brine, water and dried over Na_2SO_4. Upon evaporating off the solvent the residue was purified via column chromatography with hexane as eluent to receive a colourless oil, which was stirred under high vacuum and subsequently solidified to gain the dialkylated compound in an average yield of ca. 80-90 %.

6.2.2. Procedure B: Polymerisation According to Yamamoto

According to Nothofer[144]

The polymers were synthesized following this general procedure. Unless otherwise indicated, exactly this procedure was used. To remove solvent traces, the monomers as well as the bipyridyl were first also heated under high vacuum to 40-80°C. To remove bromine as endgroups of the polymers, an excess of bromobenzene (0.1 eq) was added at the end of the reaction and the mixture was stirred for additional 24 h at 80°C.

To a 100 mL flame-dried Schlenk tube containing $Ni(COD)_2$ (2.4 equiv), bipyridyl (2.2 eqiuv) and dihalogenated monomer (1 equiv), THF (30 mL) and COD (2.2 equiv) were added via a syringe. The tube was heated for 5 d at 80°C. The reaction was quenched with

HCl in 1,4-dioxane (c = 4 mol/l)and extracted with chloroform. The solution was washed 2 times with 2N aqueous HCl, $NaHCO_3$, Na-EDTA solution and brine. The solvent was removed and the residue was dissolved in chloroform. The polymer was precipitated into methanol and extracted with ethyl acetate to give the desired polymer.

In the case of statistical copolymers, the sum of the molar equivalents of all monomers were used for the calculation as 1 equiv. Only the amount of the monomer(s) is given in the following procedures.

6.3. Monomers

6.3.1. 2,7-Dibromo-9,9-bis(2-ethylhexyl)fluorene (5a)

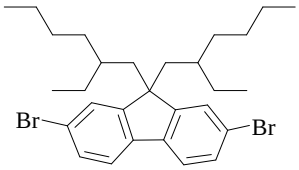

The synthesis was done according to procedure A. Yield 50 g (89%) white product.

^{1}H NMR (400 MHz, $C_2D_2Cl_4$, 80°C): δ = 7.37 – 7.45 (m, 6 H, Ar-H), 1.91 (d, 4 H, *J* = 4.8 Hz, Ar-CH_2), 0.38 – 0.89 (m, 30 H, alkyl-H) ppm.
^{13}C NMR (100 MHz, $C_2D_2Cl_4$, 80 °C): δ = 152.7, 139.4, 130.3, 127.6, 121.4, 121.1, 55.6, 44.5, 35.0, 33.9, 28.3, 27.4, 23.0, 14.4, 10.7 ppm.
LR-MS (EI, m/z): 57 (100.0), 43 (43.7), 41 (23.7), 548 [M^+] (22.5).
Mp.: 52-53°C

6.3.2. 2,7-Dibromo-9,9-di-*n*-octyl-fluorene (5b)

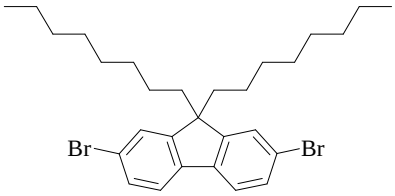

The synthesis was done according to procedure A. Yield 48 g (85%) white crystals.
^{1}H NMR (400 MHz, $C_2D_2Cl_4$, 80°C): δ = 7.4 – 7.55 (m, 6 H, Ar-H), 1.82 – 1.97 (m, 4 H, Ar-CH_2), 1.10 (q, 4 H, CH_2), 0.97 – 1.05 (m, 8 H, γ/δ CH_2), 0.76 (t, 6 H, CH_3), 0.52 – 0.61 (m, 4 H, ß-CH_2-) ppm.
^{13}C NMR (100 MHz, $C_2D_2Cl_4$, 80 °C): δ = 152.3, 138.8, 129.8, 125.9, 121.0, 120.9, 54.2, 39.9, 31.1, 29.9, 29.2, 28.9, 23.2, 22.2, 13.5 ppm.
LR-MS (EI, m/z): 57 (100.0), 323 (22.2), 546 (22.2), 548 [M^+] (28.0).
Mp: 55-56°C

6.3.3. 2,7-Dibromo-9,9-di-*n*-octyl-fluorene

Purified according to Meijer *et al.*[88]

To a solution of 14.3 g (26.1 mmol) 2,7-dibromo-9,9-di-*n*-octylfluorene in 150 mL of dry THF, a solution of 8.8 g (78.2 mmol) potassium *tert*-butoxide in 40 mL of THF was added. The mixture was stirred for 20 min. The slightly coloured solution was filtered with the use of the Schlenktechnique through a short column packed with activated basic aluminium oxide. The purified product was washed off the column with 200 mL dry of THF. This procedure was repeated 2 times. Recrystallization from ethanol gave 13.8 g (25.2 mmol) colourless crystals. Standard analytical methods (HPLC, GCMS, NMR, IR and Elemental Anaylsis) showed no difference from the "non-purified" product.[88]

6.3.4. 2,7-Dibromofluorene (17)

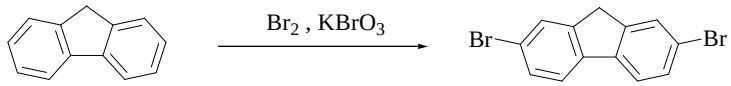

20.0 g (0.120 mol) fine grinded fluorene were dissolved in 100 mL of acetic acid at ca. 70°C. To this solution 3 mL of concentrated sulphuric acid was slowly added. Afterward 40 mL of a 5 M bromine solution (0.20 mol) in acetic acid was added over a period of 30 min so that the temperature was kept at ca. 60°C. When half of the bromine solution has dropped in, 6.7 g (40 mmol) $KBrO_3$ was carefully added in small portions. The reaction was stirred for additional 30 min at 70°C. After cooling down to room temperature the suspension was cooled down to -10°C and the solid was collected by filtration. The solid was washed twice with 70 mL of 70% aqueous acetic acid and 70 mL of water. The crude product was recrystallized two times from toluene followed by an addition of 120 mL ethanol to the heat solution. Additional recrystallization may be necessary if some mono-brominated product is detected by GC-MS. 25 g (64%) of colourless crystals were achieved with a melting point of 158-161°C.

^{1}H NMR (400 MHz, $CDCl_3$): δ = 7.64 (d, J = 0.8 Hz, 2 H), 7.57 (d, 2 H, J = 8.1 Hz), 7.49 (dd, 2 H, J = 1.4 Hz, J = 8.1 Hz), 3.84 (s, 2 H) ppm

^{13}C NMR (100 MHz, $CDCl_3$): δ = 144.8, 139.7, 130.1, 128.3, 121.1, 120.9, 35.5 ppm.

LR-MS (EI, m/z): 243 (100.0), 163 (95.8), 324 [M^+] (81.2).

GC-MS : Retention time: 8.425 min, 100% M^+ : 324.

6.3.5. 2,7-Dibromo-9-octylidene-fluorene (18)

6.3.5.1. A) Octyl-triphenylphosphonium bromide (20)

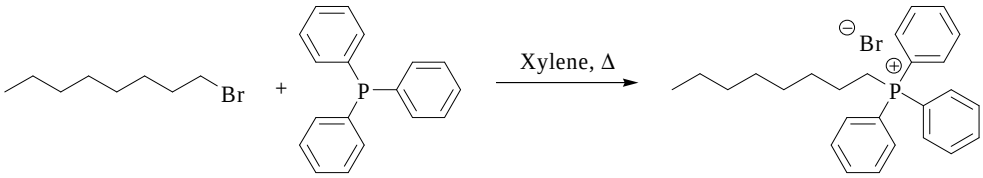

A mixture of 1-bromooctane (5.04 g, 26.1 mmol) and triphenylphosphine (6.85 g, 26.1 mmol) in xylene (25 mL) was heated to reflux for 3d. The solvent was removed under reduced pressure and the high viscous oil was used in the next step without further purification.

6.3.5.2. B) 2,7-Dibromo-9-octylidene-fluorene (18)

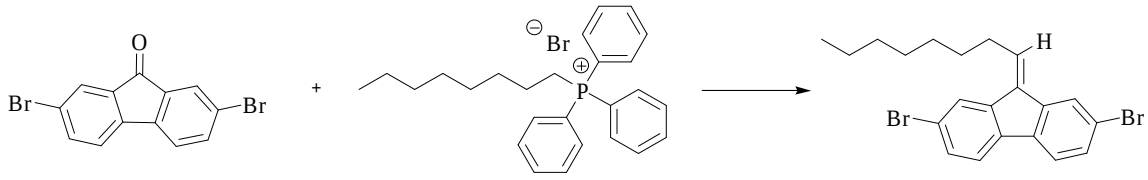

0.199 g (8.30 mmol) sodium hydride were dissolved in 20 mL of DMSO. After 45 min this mixture was cooled down to 0°C and 3.78 g (8.30 mmol) *n*-octyl-triphenylphosphoniumbromide were added. The solution was allowed to warm up to r.t. and stirred for additional 10 min. A solution of 2,7-dibromofluoren-9-one (2.81 g, 8.30 mmol) in 30 mL of DMSO was added to this mixture. The mixture was stirred for 30 min at 80°C, poured into water and extracted with chloroform. The organic layer was washed two times with water, dried over Na_2SO_4 and the solvent removed under reduced pressure. Chromatography with hexane as the eluent gave 273 mg of **18** (15%) as slightly yellow solid.

^{1}H-NMR (400 MHz, $C_2D_2Cl_4$, 25°C): δ = 7.87 (d, 1H, *J* = 1.2 Hz), 7.69 (d, 1H, *J* = 1.4Hz), 7.50 (d, 1H, *J* = 8.1 Hz), 7.45 (d, 1H, *J* = 8.3 Hz), 7.43 (dd, 1H, *J* = 8.6, 1.9 Hz), 7.37 (dd, H, *J* = 8.1, 1.5 Hz), 6.69 (t, 1H, *J* = 7.3 Hz), 2.70 (q, 2H, *J* = 7.4 Hz), 1.60 (m, 2H), 1.10 – 1.41 (m, 8H), 0.83 (t, 3H, *J* = 6.8 Hz);

^{13}C-NMR (100 MHz, $C_2D_2Cl_4$, 25°C) δ = 141.2, 139.2, 138.8, 136.6, 135.1, 133.7, 131.0, 130.7, 128.3, 123.4, 121.5, 121.4, 121.3, 121.3, 32.1, 29.8, 29.8, 29.7, 29.5, 23.0, 14.5

Anal. Calcd. for $C_{22}H_{24}Br_2$: C, 58.95

Found: C, 58.36

(The hydrogen could not be detected correctly due to problems with the elemental analysis apparatus)

6.3.6. (R/S)-2,2´-Dioctyloxy-6,6´-dibromo-1,1´-binaphthyl [(R/S)-22]

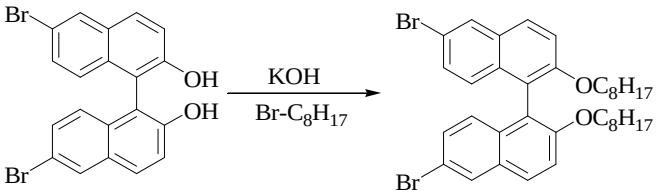

A solution of 6,6´-dibromo-1,1´-binaphthol (1) (10.0 g, 22.6 mmol) and KOH (3.6 g, 65 mmol) in anhydrous ethanol (200 mL) was degassed with argon and heated to reflux. Octylbromide (12.5 g, 65 mmol) was slowly added and the solution refluxed for 12 hours. The reaction mixture was cooled down and filtered. The solid was then recrystallized from ethanol, filtered and dried under vacuum to afford **22** in 92 % yield.[197]

^{1}H NMR (400 MHz, $C_2D_2Cl_4$, 25°C): δ = 7.94 (d, 2H, *J* = 1.9 Hz), 7.76 (d, 2H, *J* = 9.0 Hz), 7.34 (d, 2H, *J* = 9.0 Hz), 7.19 (dd, 2H, *J* = 1.9 Hz, *J* = 9.1 Hz), 6.92 (d, 2H, *J* = 9.0 Hz), 3.85 (m, 4H), 1.32 (m, 4H), 1.17 (m, 4H), 0.92 (m, 22H) ppm.

^{13}C NMR (100 MHz, $C_2D_2Cl_4$, 25 °C): δ = 155.1, 132.8, 130.3, 130.0, 129.5, 128.6, 127.5, 120.2, 117.3, 116.9, 69.8, 31.9, 29.5, 29.4, 29.3, 25.9, 22.9, 14.5 ppm.

LR-MS (EI, 70eV): m/z = 44 (54.3), 444 (68.8), 668 [M^+] (100.0), 669 (38.3), 670 (46.2).

Anal. Calcd. for $C_{36}H_{44}Br_2O_2$: C, 64.68; Found: C, 64.68 (The hydrogen could not be detected correctly due to problems with the elemental analysis apparatus).

6.3.7. 4-Chloro-1-hydroxy-naphth-2-aldehyde (26)

According to Royer and Buisson[168]

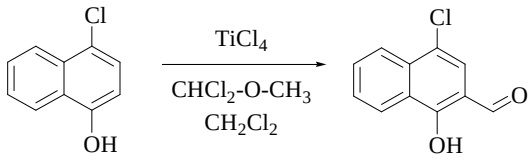

1,1-Dichloromethyl-methylether (0.123 mol) and Ti(IV)chloride (0.235 mol) were dissolved in 500 mL of dichloromethane and cooled down to 0°C. To this solution a mixture of 4-chlor-1-naphthol (20.0 g, 0.112 mol) in 500 mL of dichloromethane was slowly added keeping a maximum temperature of <5°C. Afterward the mixture was stirred additional 2 h at 5°C and 1 h at room temperature. The reaction was carefully quenched with 2N aqueous HCl and extracted with chloroform. The solvent was removed under reduced pressure and the residue chromatrographed with a THF/hexane mixture (10:90) as the eluent. Recrystallization of the greenish-yellow product from ethanol yielded 15.0 g (65%) of yellow product.[168]

^{1}H-NMR (400 MHz, DMSO-D_6, 32 °C): δ = 12.14 (s, 1H, -OH), 10.16 (s, 1H, aldehyde), 8.40 (d, 1H, *J* = 8.7 Hz), 8.10 (d, 1H, *J* = 8.7 Hz), 7.85 (t, 1H, *J* = 7.6 Hz), 7.82 (s, 1H), 7.69 (t, 1H, *J* = 7.6 Hz).

^{13}C-NMR (100 MHz, $C_2D_2Cl_4$, 80°C): δ = 195.7, 160.9, 134.7, 132.1, 127.4, 126.0, 125.8, 125.0, 124.9, 122.7, 114.4.

LR-MS (EI, 70eV): m/z = 206 [M^+] (100), 205 (48.7), 208 (37.6).

Anal. Calcd. for $C_{11}H_7ClO_2$: C, 63.94; H, 3.41.

Found: C, 63.98; H, 3.17

6.3.8. N,N´-Bis(5-chlorosalicylidene)-1,2-ethylenediamine (30)

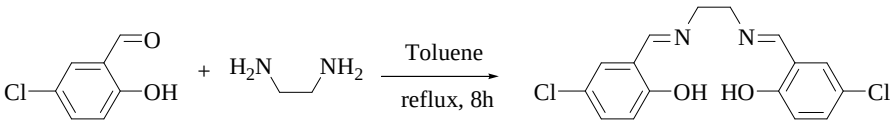

To a solution of 5-chloro-2-hydroxybenzaldehyde (5.5 g, 0.04 mol) in 250 mL of toluene ethylenediamine (1.0 g, 0.02 mol) was slowly added. The mixture was stirred under reflux with a Dean Stark apparatus for 8 h. The resulting yellow precipitate was filtered and washed several times with THF and hexane. Yield 4.9 g (87 %).

^{1}H-NMR (400 MHz, DMSO-D_6, 32 °C): δ = 13.35 (s, 2H, OH), 8.55 (s, 2H, HC=N), 7.50 (d, 2H, *J* = 2.0 Hz, Ph), 7.31 (ddd, 2H, *J* = 0.8 Hz, *J* = 2.7 Hz, *J* = 8.8 Hz, Ph), 6.86 (d, 2H, *J* = 8.7 Hz, Ph) 3.91 (s, 4H) ppm.

^{13}C-NMR (100 MHz, DMSO-D_6, 32 °C): δ = 165.7, 159.5, 132.0, 130.4, 121.8, 119.6, 118.5, 58.4 ppm.

FD-MS: m/z = 336.6 [M^+] (100), 338.6 (71), 337.6 (23), 339.6 (16).

Anal. Calcd for $C_{16}H_{14}Cl_2N_2O_2$: C, 56.99; H, 4.18; N, 8.31

Found: C, 57.06; H, 4.07; N, 8.30.

6.3.9. N,N´-Bis(5-chlorosalicylidene)-1,2-phenylenediamine (31)

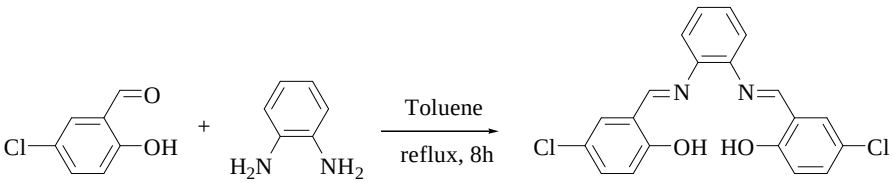

To a solution of 5-chloro-2-hydroxybenzaldehyde (5.78 g, 37 mmol) in 250 mL of toluene 1.9 g (17.6 mmol) *o*-phenylenediamine were slowly added. The mixture was stirred under reflux with a Dean Stark apparatus for 24 h. The resulting intensively coloured precipitate was filtered and washed several times with THF and hexane. Yield 5.7 g (84 %).

^{1}H-NMR (400 MHz, DMSO-D_6, 32°C): δ = 12.83 (s, 2H), 8.89 (s, 2H), 7.74 (d, 2H, *J* = 2.7 Hz), 7.40 (m, 6H), 6.97 (d, 2H, *J* = 8.9 Hz).

^{13}C-NMR (100 MHz, DMSO-D_6, 32°C): δ = 162.2, 159.0, 142.0, 132.8, 130.7, 128.0, 122.5, 120.8, 119.6, 118.7 ppm.

LR-MS (EI, 70eV): m/z = 384 [M^+] (100), 386 (88), 385 (47).

6.3.10. N,N´-Bis(5-chlorosalicylidene)-1,2-cyclohexenediamine (32)

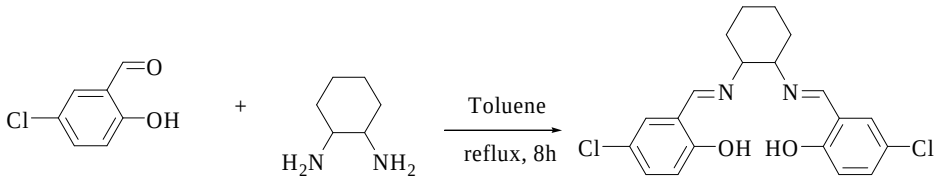

To a solution of 5-chloro-2-hydroxybenzaldehyde (8.64 g, 55 mmol) in 500 mL of toluene 1,2-cyclohexyldiamine (3.0 g, 26 mmol) were slowly added. The mixture was stirred under reflux with a Dean Stark apparatus for 24 h. The resulting yellow precipitate was filtered and recrystallized from hexane yielding 6.6 g (64%) of **32**.

^{1}H-NMR (400 MHz, DMSO-D_6, 32°C): δ = 13.20-13.40 (m, 2H, OH), 8.12-8.20 (m, 2H), 7.08-7.20 (m, 4H), 6.76-6.82 (m, 2H), 3.20-3.52 (m, 2H), 1.36-1.89 (m, 8H).

^{13}C-NMR (100 MHz, DMSO-D_6, 32°C): δ = 163.7, 159.7, 132.4, 130.9, 123.4, 119.7, 118.7, 72.7, 33.2, 24.4 ppm.

LR-MS (EI, m/z): 235 (100), 390 [M^+] (97), 392 (93), 391 (74).

Anal. Calcd for $C_{16}H_{14}Cl_2N_2O_2$: C, 61.39; H, 5.15; N, 7.16;

Found: C, 61.09; H, 4.81, N, 7.22.

6.3.11. N,N´-Bis(4-chloro-2-naphthylmethylene-1-ol)-1,2-ethylenediamine (33)

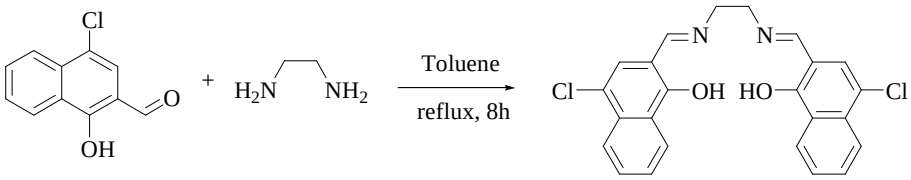

To a solution of 1 g (4.84 mmol) of **26** in 250 mL toluene, ethylenediamine (0.116 g, 1.94 mmol) was slowly added. The mixture was stirred under reflux with a Dean Stark apparatus for 24 h. The resulting intensively coloured precipitate was filtered and recrystallized from ligroin/DMSO. Yield: 1.42 g (67%) of yellow needles.

^{1}H-NMR (400 MHz, DMSO-D_6, 80°C): δ = 8.33 (d, 2H, *J* = 8.0 Hz), 8.18 (s, 2H), 7.86 (d, 2H, *J* = 8.2 Hz), 7.68 (t, 2H, *J* = 7.6 Hz), 7.48 (t, 2H, *J* = 7.6 Hz), 7.20 (s, 2H), 3.91 (s, 2H) ppm.

^{13}C-NMR (100 MHz, DMSO-D_6, 80°C): δ = 175.3, 161.8, 133.6, 130.7, 130.6, 127.5, 125.2, 125.1, 123.1, 113.8, 107.8, 50.1 ppm.

LR-MS (EI, 70eV): m/z = 218 (100), 436 [M^+] (65), 438 (44), 437 (17).

6.3.12. N,N´-Bis(4-chloro-2-naphthylmethylene-1-ol)-1,2-benzenediamine (34)

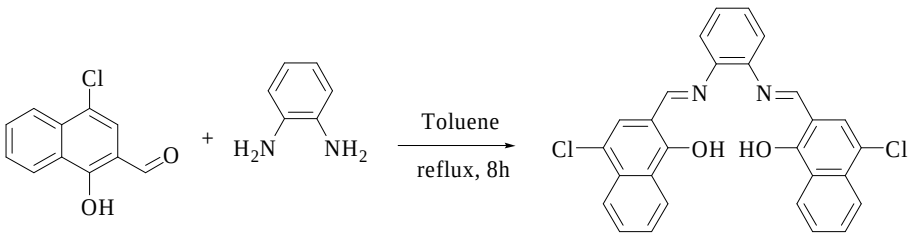

To a solution of 5-chloro-2-hydroxybenzaldehyde (1.00g, 4.84 mmol) in 250 mL of toluene 1,2-phenylenediamine (0.209 g, 1.94 mmol) was slowly added. The mixture was stirred under reflux with a Dean Stark apparatus for 8 h. The resulting yellow precipitate

was filtered and recrystallized from ligroin/DMSO. Yield 0.83 g (88 %) of an orange powder.

Due to the low solubility a NMR analysis failed. The corresponding platinum complex was better soluble most probably because hydrogen bonds were absent.

LC-MS: RT 11.5 min; (ESI, m/z) 485.08 [M^+] (100%), 486.09 (33%), 487.08 (68%), 488.08 (14%), 489.08 (13%), 969.15 (20%), 970.16 [MH^{2+}] (12%), 971.15 (29%), 972.15 (16%), 973.15 (16%).

6.3.13. N,N´-Bis(4-chloro-2-naphthylmethylene-1-ol)-1,2-cyclohexanediamine (35)

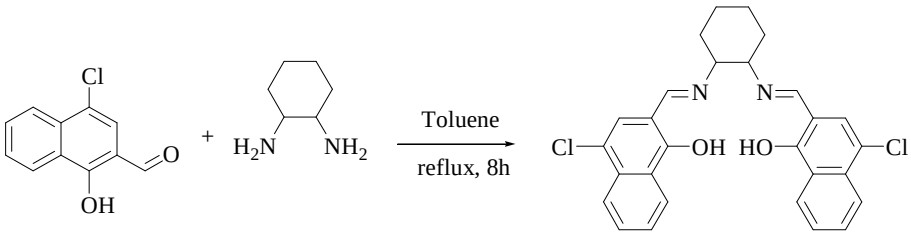

To a solution of 5-chloro-2-hydroxybenzaldehyde (1.640g, 10.475mmol) in 250 mL of toluene 1,2-cyclohexane-diamine (0.363g, 3.18 mmol) was slowly added. The mixture was stirred under reflux with a Dean Stark apparatus for 8 h. The resulting yellow precipitate was filtered and washed several times with THF and hexane. Yield 0.84 g (54 %) of **35**.

^{1}H-NMR (400 MHz, DMSO-D_6, 80°C): δ = 12.99 (s, 2H, OH), 8.28 (d, 2H, *J* = 8.1 Hz), 8.17 (s, 2H), 7.80 (d, 2H, *J* = 8.1 Hz), 7.66 (t, 2H, *J* = 7.6 Hz), 7.47 (t, 2H, *J* = 7.5 Hz), 7.12 (s, 2H) ppm.

^{13}C-NMR (100 MHz, DMSO-D_6, 80°C): δ = 175.6, 160.9, 133.7, 131.1, 130.8, 127.9, 125.7, 125.4, 123.5, 114.0, 107.8, 63.3, 31.7, 23.6 ppm.

LR-MS (EI, m/z): 490 [M^+]

6.3.14. N,N´-Bis(5-chlorosalicylidene)-2,3-naphthalenediamine (36)

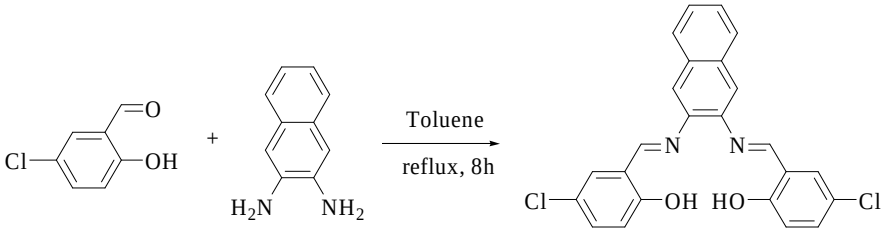

5-Chloro-2-hydroxybenzaldehyde (10.4 g, 66 mmol) and 2,3-diamino-naphthalene (5.0 g, 32 mmol) were dissolved in 350 mL of toluene. The mixture was stirred under reflux with a Dean Stark apparatus for 24 h. The resulting precipitate was filtered and recrystallized from ligroin/DMSO. Yield 6.6 g (48 %) of an orange powder.

^{1}H-NMR (400 MHz, DMSO-D_6, 80°C): δ = 12.55 (s (broad), 2H, OH), 9.00 (s, 2H), 7.93 (dd, 2H, *J* = 3.3 Hz, *J* = 6.1 Hz), 7.85 (s, 2H), 7.77 (d, 2H, *J* = 2.6 Hz), 7.51 (dd, 2H, *J* = 3.3 Hz, *J* = 6.2 Hz), 7.40 (dd, *J* = 2.7 Hz, *J* = 8.8 Hz), 6.98 (d, 2H, *J* = 8.8 Hz) ppm.
Due to the low solubility a ^{13}C NMR analysis failed
LR-MS (EI, m/z): 434 [M^+] (100), 436 (93), 435 (57).

6.3.15. [N,N´-Bis(5-chlorosalicylidene)-2,3-naphthalene-diaminato-N,N´,O,O´] platinum(II) (37)

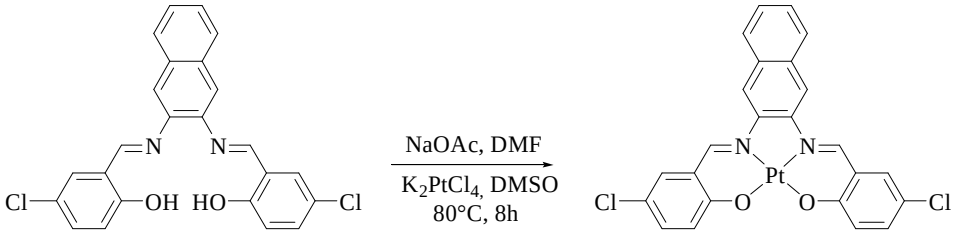

2.0 g (4.4 mmol) **36** and 0.8 g (9.7 mmol) NaOAc were dissolved in 30 mL of DMF. A solution of 1.831 g (4.4 mmol) K_2PtCl_4 in 15 mL of DMSO was added at 80°C via a syringe. The mixture was stirred for 8 h at 80°C. The mixture was cooled down to room temperature and the crude product filtered off and washed with water and methanol. Recrystallization from acetonitrile/DMSO gave 1.75 g (63%) of **37** as a purple solid.

^{1}H NMR (400 MHz, DMSO-D_6, 80°C): δ = 9.54 (m, 2H), 8.78 (m, 2H), 7.88 (m, 4H), 7.54 (m, 4H), 7.04 (m, 2H) ppm.
Due to the low solubility a ^{13}C NMR analysis failed
LC-MS: RT 9.3 min; (ESI, m/z) 629.02 [M^+] (100%), 628.02 (80%), 627.01 (67%), 631.01 (66%), 630.02 (65%)

6.3.16. [N,N´-Bis(5-chlorosalicylidene)-1,2-phenylene-diaminato-N,N´,O,O´] platinum(II) (40)

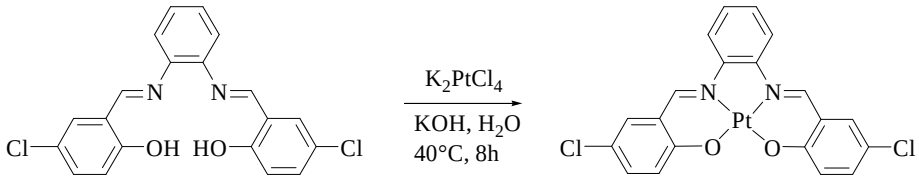

0.8 g (2.08 mmol) FG102 and 0.5 g (6.10 mmol) NaOAc were dissolved in 30 mL of DMF. A solution of 0.862 g (2.08 mmol) K_2PtCl_4 in 10 mL of DMSO was added at 80°C via a syringe. The mixture was stirred for 8 h at 80°C. The mixture was cooled down to room temperature and the crude product filtered off and washed with water and methanol. Recrystallization from acetonitrile gave 0.51 g (61%) of **40** as a dark red solid.

^{1}H-NMR (400 MHz, DMSO-D_6, 80 °C): δ = 9.46 (s, 2H), 8.35 (dd, 2H, *J* = 3.3 Hz, *J* = 6.3 Hz), 7.92 (d, 2H, *J* = 2.8 Hz), 7.52 (dd, 2H, *J* = 2.7 Hz, *J* = 9.2 Hz), 7.46 (dd, 2H, *J* = 3.3 Hz, *J* = 6.2 Hz), 7.11 (d, 2H, *J* = 9.3 Hz) ppm.
Due to the low solubility a ^{13}C NMR analysis failed

6.3.17. N,N´-Bis(4-chloro-2-iminomethyl-naphthalene-1-ol)-1,2-ethylenediaminato-N,N´,O,O´] platinum(II) (41)

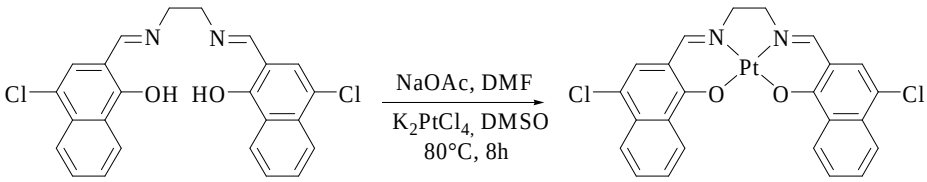

0.5 g (1.14 mmol) **33** and 0.206 g (2.52 mmol) NaOAc were dissolved in 30 mL of DMF. A solution of 0.475 g (1.14 mmol) K_2PtCl_4 in 5 mL of DMSO was added at 80°C via a syringe. The mixture was stirred for 8 h at 80°C. The mixture was cooled down to room temperature and the crude product filtered off and washed with water and methanol. Recrystallization from acetonitrile gave 0.39 g (54%) of **41** as an orange solid.

^{1}H-NMR (400 MHz, DMSO-D_6, 80 °C): δ = 8.76 (m, 2H), 8.55 (m, 2H), 7.64-8.00 (m, 8H), 3.90 (s, 4H).

Due to the low solubility a ^{13}C NMR analysis failed

LC-MS: RT 8.8 min; (ESI, m/z) 630.98 (100%), 629.99 [MH^+] (91%), 628.98 (62%), 632.98 (59%), 631.98 (58%).

Anal. Calcd for $C_{24}H_{16}Cl_2N_2O_2Pt$: C, 45.73; N, 4.44;

Found: C, 45.60; N, 4.51.

(The hydrogen could not be detected correctly due to problems with the elemental analysis apparatus).

6.3.18. [N,N´-Bis(5-chlorosalicylidene)-1,2-ethylenediaminato-N,N´,O,O´] platinum(II) (42)

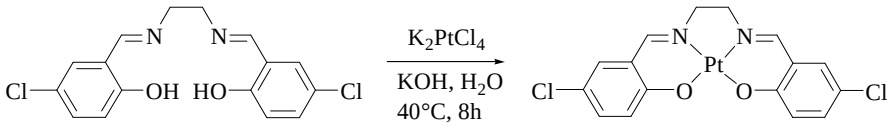

An aqueous solution of KOH (50 mL, 1M), the ligand (**30**) (200 mg, 0.59 mmol) and K_2PtCl_4 (246 mg, 0.59 mmol) were stirred for 8 hours at 40°C. The orange precipitate was

filtered off and extensively washed with aqueous KOH (1M), water and finally with methanol. The solid was recrystallized from acetonitril and filtered to give an orange powder. Yield: 0.15 g (54 %).

^{1}H-NMR (400 MHz, DMSO-D_6, 80 °C): δ = 8.42 (s, 2H, $^3J_{H\text{-}Pt}$ = 34.3 Hz, HC=N), 7.38 (d, 2H, *J* = 9.2 Hz, Ph), 6.2 (d, 2H, *J* = 9.2 Hz, Ph), 3.81 (s, 4H, CH_2) ppm.
^{13}C-NMR (100 MHz, DMSO-D_6, 80 °C): δ = 161.0, 155.1, 132.5, 131.3, 122.7, 122.4, 118.3, 60.7.
MS (EI, 70 eV) : m/z = 530.
Anal. Calcd for $C_{16}H_{12}C_{l2}N_2O_2Pt$: C, 36.24; H, 2.28; N, 5.28;
Found: C, 35.90; H, 2.26; N, 5.33.

6.3.19. [N,N´-Bis(4-chloro-2-iminomethyl-naphthalene-1-ol)-1,2-phenylenediaminato-N,N´,O,O´] platinum(II) (43)

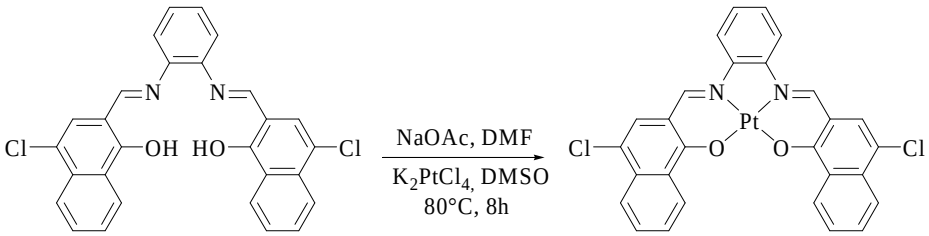

0.8 g (1.65 mmol) **34** and 0.298 g (3.6 mmol) NaOAc were dissolved in 30 mL of DMF. A solution of 0.684 g (1.65 mmol) K_2PtCl_4 in 10 mL of DMSO were added at 80°C via a syringe. The mixture was stirred for 8 h at 80°C. The mixture was cooled down to room temperature and the crude product filtered off and washed with water and methanol. Recrystallization from acetonitrile/DMSO gave 0.35 g (34%) of **43**.

^{1}H NMR (400 MHz, DMSO-D_6, 80°C): δ = 9,40 (m, 2H), 8.34 (s, 2H), 8.06 (d, 2H *J* = 8.0 Hz), 7.94 (m, 2H), 7.88 (t, 2H, *J* = 7.4 Hz), 7.72 (t, 2H, *J* = 7.3 Hz), 7.39 (s, 2H) ppm.
Due to the low solubility a ^{13}C NMR analysis failed
LR-MS (EI, m/z): 72.9 (100), 676 (2), 677 [M^+] (1).

6.3.20. [N,N´-Bis(5-chlorosalicylidene)-1,2-cyclohexane-diaminato-N,N´,O,O´] platinum(II) (44)

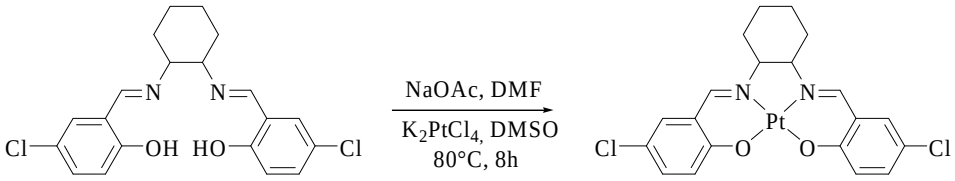

2.5 g (6.39 mmol) **32** and 1.15 g (14.1 mmol) NaOAc were dissolved in 30 mL of DMF. A solution of 2.65 g (6.39 mmol) K_2PtCl_4 in 15 mL of DMSO was added at 80°C via a syringe. The mixture was stirred for 8 h at 80°C. The mixture was cooled down to room temperature and the crude product filtered off and washed with water and methanol. Recrystallization from acetonitrile/DMSO gave 2.02 g (54%) of **44** as an orange solid.

^{1}H-NMR (400 MHz, DMSO-D_6, 32°C): δ = 8.39-8.46 (m, 2H), 7.63-4.69 (m, 2H), 7.36-7.40 (m, 2H), 6.89-6.91 (m, 2H), 3.53-3.55 (m, 2H), 2.71-2.74 (m, 2H), 1.36-1.84 (m, 6H). A ^{13}C NMR analysis failed most probably due to solubility problems.

Anal. Calcd for $C_{20}H_{18}Cl_2N_2O_2Pt$: C, 41.11; N,4.79;

Found: C, 41.08; N, 4.88.

(The hydrogen could not be detected correctly due to problems with the elemental analysis apparatus).

6.3.21. [N,N´-Bis(4-chloro-2-iminomethyl-naphthalene-1-ol)-1,2-cyclohexanediaminato-N,N´,O,O´] platinum(II) (45)

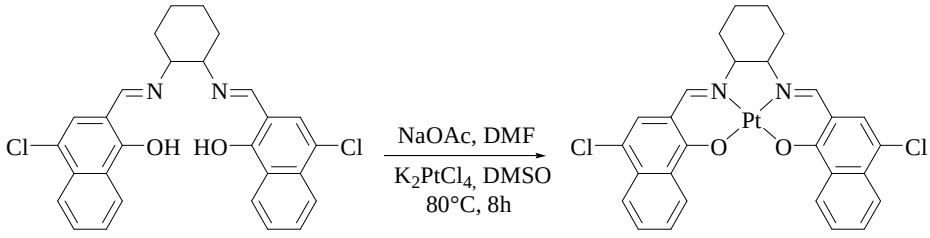

0.6 g (1.22 mmol) **35** and 0.220 g (2.69 mmol) NaOAc were dissolved in 30 mL ofDMF. A solution of 0.507 g (1.22 mmol) K_2PtCl_4 in 10 mL of DMSO was added at 80°C via a syringe. The mixture was stirred for 8 h at 80°C. The mixture was cooled down to room

temperature and the crude product filtered off and washed with water and methanol. Recrystallization from acetonitrile/DMSO gave 0.411 g (49%) of **45** as a orange solid.

^{1}H-NMR (400 MHz, DMSO-D_6, 80°C): δ = 8.76 (d, 2H, *J* = 8.1 Hz), 8.40 (t, 2H, J_{HPt} = Hz), 7.99 (d, 2H, *J* = 8.2 Hz), 7.94 (s, 2H), 7.80 (ddd, 2H, *J* = 1.2 Hz, *J* = 6.9 Hz, *J* = 8.2 Hz), 7.74 (s, 2H), 7.63 (ddd, 2H, *J* = 1.2 Hz, *J* = 7.1 Hz, *J* = 8.2 Hz), 3.63 (d, 2H, *J* = 9.7 Hz), 1.85 (d, 2H, *J* = 8.7 Hz), 1.58 (m, 2H), 1.41 (t, 2H, *J* = 9.7 Hz), 1.25 (s, 2H) ppm.
Due to the low solubility a ^{13}C NMR failed
LR-MS (EI, m/z): 490 [M^+]
Anal. Calcd for $C_{28}H_{22}Cl_2N_2O_2Pt$: C, 49.13; N, 4.09;
Found: C, 48.91; N, 4.30.
(The hydrogen could not be detected correctly due to problems with the elemental analysis apparatus).

6.3.22. Bis(5-chlorosalicylidene)-1,2-cyclohexanediamine (48)

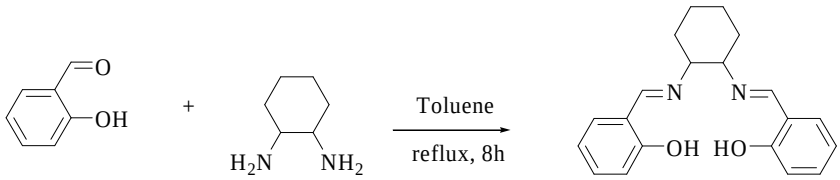

To a solution of 2-hydroxybenzaldehyde (8.98 g, 73.5 mmol) in 250 mL of toluene 1,2-cyclohexyldiamine (4.0 g, 35.0 mmol) was slowly added. The mixture was stirred under reflux with a Dean Stark apparatus for 8 h. The resulting yellow precipitate was filtered and recrystallized from acetonitrile yielding 8.69 g (77 %) of a yellow powder.
^{1}H-NMR (400 MHz, $C_2D_2Cl_4$, 32°C): δ = 13.29-13.47 (m, 2H, OH), 8.20-8.28 (m, 2H), 6.73-7.51 (m, 8H), 3.20-3.51 (m, 2H), 1.18-1.91 (m, 8H) ppm.
^{13}C-NMR (100 MHz, $C_2D_2Cl_4$, 32°C): δ = 164.8, 161.0, 132.5, 131.8, 119.0, 117.2, 117.0, 72.7, 33.4, 24.5 ppm.
LC-MS: RT 4.5 min; (ESI, m/z) 323.17 [MH^+] (100%), 324.17 (20%), 325.18 (2%)
Anal. Calcd for $C_{20}H_{22}N_2O_2$: C, 74.51; H, 6.88; N, 8.69;
Found: C, 74.40; H, 6.34; N, 8.82.

6.3.23. N,N´-Bis(salicylidene)-1,2-phenylenediamine (49)

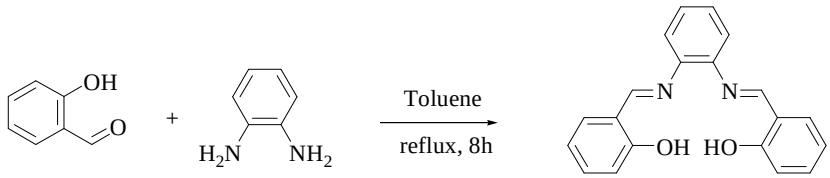

To a solution of 2-hydroxybenzaldehyde (37.97 g, 0.311 mol) in 150 mL of toluene a solution of 1,2-phenylenediamine (16.0 g, 0.148 mol) in 150 mL of toluene was slowly added. The mixture was stirred under reflux with a Dean Stark apparatus for 24 h. The resulting precipitate was filtered and recrystallized from ligroin. Yield: 45.03 g (79%) of **49**.

^{1}H-NMR (400 MHz, DMSO-D_6, 32°C): δ = 12.89 (s, 2H), 8.90 (s, 2H), 7.46 (dd, 2H, *J* = 1.5 Hz, *J* = 8.0 Hz), 7.38-7.44 (m, 6H), 6.93-6.96 (m, 4H) ppm.
^{13}C-NMR (100 MHz, DMSO-D_6, 32°C): δ = 163.9, 160.3, 142.2, 133.3, 132.4, 127.7, 119.7, 119.4, 119.0, 116.6 ppm.
LR-MS (EI, 70eV): m/z = 316 [M^+] (100), 317 (21), 315 (18).

6.3.24. N,N´-Bis(salicylidene)-2,3-naphthalenediamine (50)

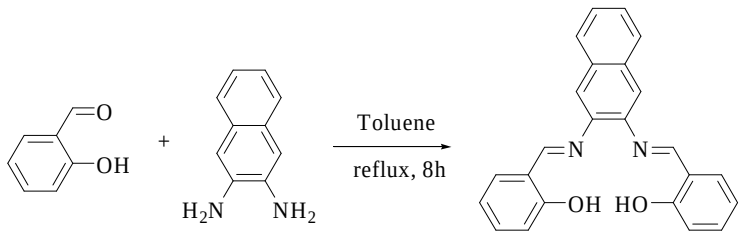

To a solution of 2,3-diamine-naphthalene (2.0 g, 12.6 mmol) in 150 mL of toluene 5-chloro-2-hydroxybenzaldehyde (3.86 g, 31.6 mmol) was slowly added. The mixture was stirred under reflux with a Dean Stark apparatus for 24 h. The resulting precipitate was filtered and recrystallized from ligroin. Yield 3.6 g (78 %) of a red solid.

^{1}H-NMR (400 MHz, DMSO-D_6, 32 °C): δ = 12.86 (s, 2H), 9.02 (s, 2H), 7.93 (dd, 2H, *J* = 3.3 Hz, *J* = 6.2 Hz), 7.88 (s, 2H), 7.70 (dd, 2H, *J* = 1.6 Hz, *J* = 8.0 Hz), 7.49 (dd, 2H, *J* = 3.3 Hz, *J* = 6.2 Hz), 7.41 (m, 2H), 6.97 (m, 4H) ppm.

^{13}C-NMR (100 MHz, DMSO-D_6, 32 °C): δ = 164.0, 160.4, 142.3, 133.4, 132.3, 132.2, 127.6, 126.2, 119.5, 119.1, 116.6, 116.5 ppm.

LR-MS (EI, 70eV): m/z = 366 [M^+] (100), 367 (28), 368 (4).

6.3.25. [N,N´-Bis(salicylidene)-1,2-cyclohexanediaminato-N,N´,O,O´] platinum(II) (51)

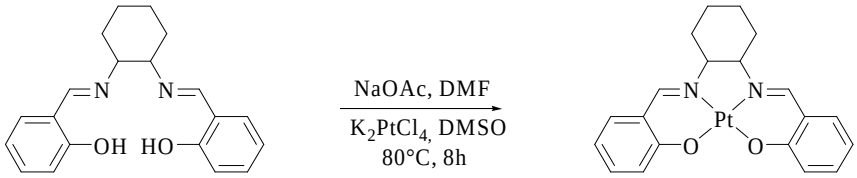

2.0 g (6.2 mmol) **49** and 1.1 g (13.7 mmol) NaOAc were dissolved in 30 mL of DMF. A solution of 2.58 g (6.2 mmol) K_2PtCl_4 in 20 mL of DMSO was added at 80°C via a syringe. The mixture was stirred for 8 h at 80°C. The mixture was cooled down to room temperature and the crude product filtered off and washed with water and methanol. Recrystallization from acetonitrile/DMSO gave 1.53 g (48%) of **51** as orange solid.

^{1}H NMR (400 MHz, DMSO-D_6, 25 °C): δ = 8.42 (bs, 2H), 7.48-7.55 (m, 2H), 7.33-7.44 (m, 2H), 6.80-6.94 (m, 2H), 6.52-6.63 (m, 2H), 3.81-4.06 (m, 2H), 2.14-2.33 (m, 2H), 1.72-1.93 (m, 2H), 1.36-1.54 (m, 4H) ppm.

^{13}C NMR (100 MHz, DMSO-D_6, 25 °C): δ = 162.3, 154.4, 134.1, 133.5, 122.4, 120.8, 115.3, 70.2, 24.0, 20.8 ppm.

LC-MS: RT 2.3 min; (ESI, m/z) 516.13 (100%), 517.13 (83%), 515.13 [M^+] (82%), 519.13 (19%), 518.13 (16%).

Anal. Calcd for $C_{20}H_{20}N_2O_2Pt$: C, 46.60; N, 5.43;

Found: C, 46.75; N, 5.56.

(The hydrogen could not be detected correctly due to problems with the elemental analysis apparatus).

6.3.26. [N,N´-Bis(salicylidene)-1,2-phenylenediaminato-N,N´,O,O´] platinum(II) (52)

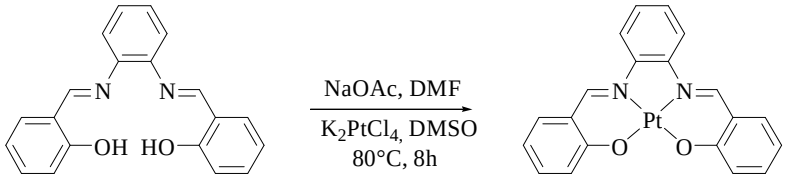

0.5 g (1.14 mmol) **49** and 0.206 g (2.52 mmol) NaOAc were dissolved in 30 mL of DMF. A solution of 0.475 g (1.14 mmol) K_2PtCl_4 in 5 mL of DMSO was added at 80°C via a syringe. The mixture was stirred for 8 h at 80°C. The mixture was cooled down to room temperature and the crude product filtered off and washed with water and methanol. Recrystallization from acetonitrile gave 0.39 g (54%) of **52** as a dark red solid.

^{1}H-NMR (400 MHz, DMSO-D_6, 80°C): δ = 9.41 (t, 2H, *J* = 34.5 Hz)), 8.39 (td, 2 H, *J* = 3.5 Hz, *J* = 6.9 Hz), 7.83 (d, 2H, *J* = 8.0 Hz), 7.54 (t, 2H, *J* = 7.8 Hz), 7.41 (td, 2 H, *J* = 3.4 Hz, *J* = 6.8 Hz), 7.10 (d, 2H, *J* = 8.7 Hz), 6.75 (t, 2H, *J* = 7.4 Hz) ppm.

^{13}C-NMR (100 MHz, DMSO-D_6, 80°C): δ = 150.7, 144.3, 135.1, 134.9, 127.4, 121.6, 121.6, 120.8, 116.2, 115.7 ppm.

LC-MS: RT 3.6 min; (ESI, m/z) 510.08 [MH^+] (100%), 509.8 [M^+] (81%), 511.08 (81%), 512.08 (16%), 513.08 (19%).

Anal. Calcd for $C_{20}H14N_2O_2Pt$: C, 47.15; N, 5.50;

Found: C, 46.93; N, 5.60.

(The hydrogen could not be detected correctly due to problems with the elemental analysis apparatus).

6.3.27. [N,N´-Bis(salicylidene)-2,3-naphthalenediaminato-N,N´,O,O´] platinum(II) (53)

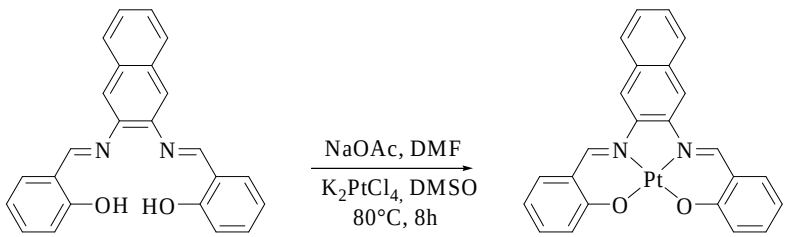

0.8 g (2.2 mmol) **50** and 0.394 g (4.8 mmol) NaOAc were dissolved in 30 mL of DMF. A solution of 0.906 g (2.2 mmol) K_2PtCl_4 in 10 mL of DMSO was added at 80°C via a syringe. The mixture was stirred for 8 h at 80°C. The mixture was cooled down to room temperature and the crude product filtered off and washed with water and methanol. Recrystallization from acetonitrile/DMSO gave 0.62 g (56%) of **53** as a dark red solid.

^{1}H NMR (400 MHz, DMSO-D_6, 80°C): δ = 9.64 (s, 2H), 8.91 (s, 2H), 7.97 (dd, 2H, J = 3.3 Hz, J = 6.2 Hz), 7.84 (d, 2H, J = 8.0 Hz), 7.54-7.60 (m, 4H), 7.07 (d, 2H, J = 8.6 Hz), 6.77 (t, 2H, J = 7.3 Hz)ppm.

^{13}C NMR (100 MHz, DMSO-D_6, 80°C): δ =164.3, 150.5, 143.2, 134.9, 134.8, 131.4, 127.6, 126.9, 121.9, 120.9, 115.9, 113.8 ppm.

LC-MS: RT 7.0 min; (ESI, m/z) 560.10 [MH^+] (100%), 559.10 [M^+] (75%), 561.10 (76%), 562.10 (20%), 563.10 (20%)

Anal. Calcd for $C_{24}H_{16}N_2O_2Pt$: C, 51.52; N, 5.01;

Found: C, 51.44; N, 5.13.

(The hydrogen could not be detected correctly due to problems with the elemental analysis apparatus).

6.3.28. [N,N´-Bis(salicylidene)-1,2-ethylenediaminato-N,N´,O,O´] platinum(II) (54)

6.3.28.1. N,N´-Bis(salicylidene)-1,2-ethylenediamine

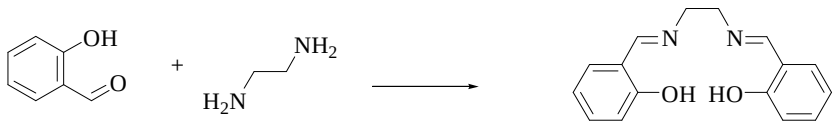

To a solution of 2-hydroxybenzaldehyde (12.8 g, 0.105 mol) in 200 mL of toluene ethylenediamine (3.0 g, 0.050 mol) was slowly added. The mixture was stirred under reflux with a Dean Stark apparatus for 24 h. The resulting precipitate was filtered and recrystallized from ligroin/DMSO. Yield 8.85 g (66 %) of the salen intermediate.

^{1}H-NMR (400 MHz, $C_2D_2Cl_4$, 32 °C): δ = 13.24 (s, 2H, OH), 8.28 (s, 2H), 7.24 (t, 2H, *J* = 7.8 Hz), 7.19 (d, 2H, *J* = 7.6 Hz), 6.88 (d, 2H, *J* = 8.3 Hz), 3.82 (s, 4H) ppm.

^{13}C-NMR (100 MHz, DMSO-D_6, 32 °C): δ = 166.7, 161.1, 132.7, 131.8, 119.1, 118.9, 117.2, 59.9 ppm.

LC-MS: RT 1.8 min; (ESI, m/z) 269.13 [MH^+] (100%), 270.14 (17%), 271.14 (2%)

6.3.28.2. [N,N´-Bis(salicylidene)-1,2-ethylenediaminato-N,N´,O,O´] platinum(II) (**54**)

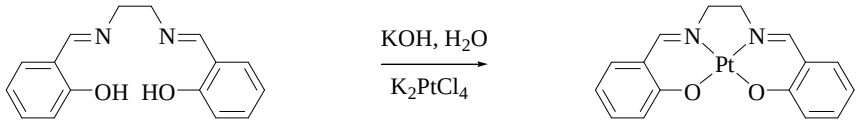

An aqueous solution of KOH (20 mL, 1M), the Schiff base ligand (200 mg, 0.75 mmol) and K_2PtCl_4 (310 mg, 0.75 mmol) were stirred for 8 hours at 40°C. The orange precipitate was filtered and extensively washed with aqueous KOH (1M), water and finally with methanol. The solid was recrystallized from acetonitrile and filtered to give an orange powder. Yield: 0.249 g (72 %) of **54**.

^{1}H-NMR (400 MHz, DMSO-D_6, 80 °C): δ = 7.81 (s, 2H, $^{3}J_{H\text{-}Pt}$ = 65.4 Hz), 7.41 (t, 2H, J = 7.6 Hz), 7.11 (d, 2H, J = 7.8 Hz), 7.05 (d, 2H, J = 8.5 Hz), 6.53 (t, 2H, J = 7.2 Hz), 3.68 (s, 4H) ppm.

^{13}C-NMR (100 MHz, DMSO-D_6, 80 °C): δ = 161.0, 155.1, 132.5, 131.3, 122.7, 122.4, 118.3, 60.7.

6.3.29. 4´,4´´-Didecyl-2,5-dibromoterephthalophenone (57)

According to Scherf and Müllen[185]

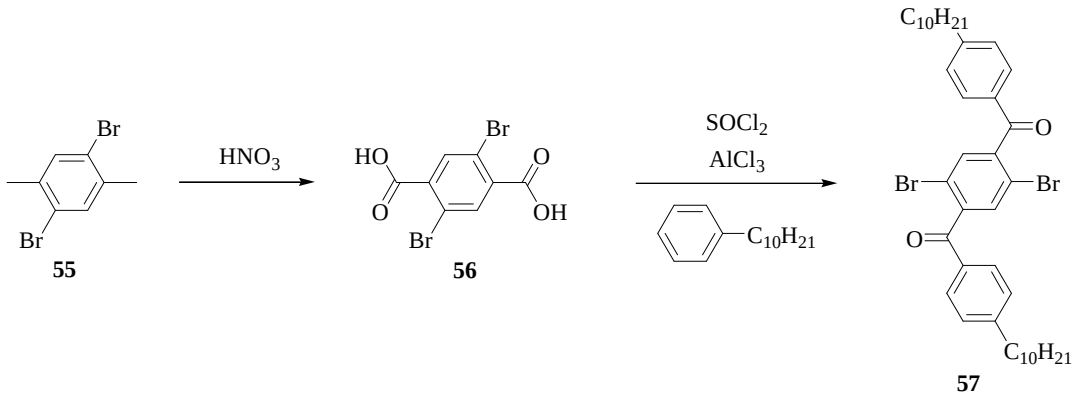

6.3.29.1. A) 2,5-Dibromoterephthalic acid (**56**)

2,5-Dibromo-1,4-dimethylbenzene (100 g, 0.38 mol) was stirred in 300 mL of HNO_3 (~ 40%) and refluxed for 5 days. The reaction was cooled to room temperature and neutralized with aqueous KOH solution. $KMnO_4$ (150 g, 0.95 mmol) was added and the mixture refluxed for further 24 h. Then another portion of $KMnO_4$ (50 g, 0.32 mmol) was added and the mixture refluxed for additional 24 h. The reaction mixture was cooled down to room temperature and acidified with sulphuric acid (pH = 1). After adding aqueous Na_2SO_3 solution to dissolve the MnO_2 the colourless precipitate could be separated, washed and dried. Yield: (74 %)[185]

^{1}H NMR (400 MHz, d_6-DMSO, 80 °C): δ = 15.3-12.7 (bs, 2H), 7.98 (s, 2H) ppm.
^{13}C NMR (50 MHz, d_6-DMSO, 80 °C): δ = 165.8, 137.3, 135.2, 119.0 ppm.
LR-MS (EI, m/z): 307 (43.4), 322 (50.8), 324 [M^+] (100.0), 326 (47.5).

6.3.29.2. B) 4´,4´´-Didecyl-2,5-dibromoterephthalophenone (**57**)

2,5-Dibromoterephthalic acid (20 g, 0.046 mol) was refluxed in thionyl chloride (30 g, 0.25 mol) for 8 h. The excess of thionyl chloride was distilled off and the residue recrystallized from heptane, filtered and dried. The dichloride was used for the next step without any further purification. To a solution of 2,5-dibromoterephthaloyl dichloride (3.6g, 10 mmol) in dichlormethane (100 mL) aluminiumtrichloride (3.4 g, 26 mmol) was added at 0°C. After 15 min a solution of *n* - decylbenzene (9 g, 41 mmol) in

dichloromethane (25 mL) was added and stirred for 24 h at room temperature. The reaction mixture was quenched with aqueous HCl and extracted into dichlormethane. The organic phase was washed with water, brine, dried over Na_2SO_4, and the solvent evaporated till dryness. The crude product was recrystallized from acetone. Yield: 75 %.

^{1}H NMR (400 MHz, $C_2D_2Cl_4$, 25 °C): δ = 7.67 (d, 2H, *J* = 8.2Hz), 7.52 (s, 2H), 7.25 (d, 2H, *J* = 8.2Hz), 2.62 (t, 4H, *J* = 8.86), 1.56 (m, 32H), 0.80 (t, 6H, *J* = 6.8Hz) ppm.
^{13}C NMR (100 MHz, $C_2D_2Cl_4$, 25 °C): δ = 193.62 (C=O), 151.01, 143.53, 133.27, 133.06, 130.74, 129.32, 118.75, 36.47, 32.19, 32.15, 31.24, 29.90, 29.84, 29.74, 29.61, 23.01, 14.52 ppm.
LR-MS (EI, m/z): 245 (100.0), 507 (21.5), 724 [M^+] (53.2), 725 (20.5).

6.3.30. 1,4-Bis[2´-(9´,9´-dimethyl)fluorenyl]tetrafluorobenzene (58)

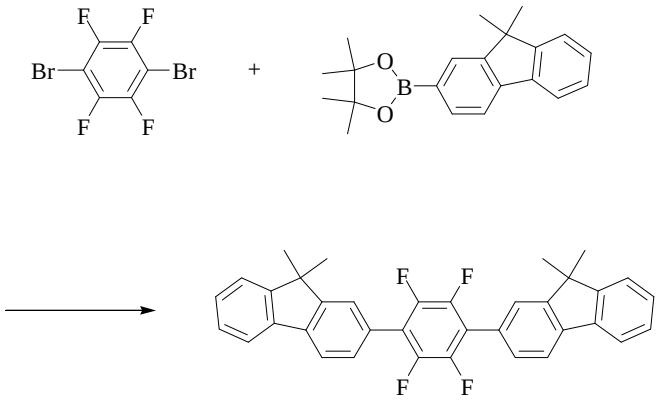

1.0 g (3.25 mmol) of 1,4-dibromo-tetrafluorobenzene, 3.33 g (10.4 mmol) of the boronic ester **61,** 13.8 g (0.130 mol) sodium carbonate and 0.404 g (1.30 mmol) aliquat 336 were dissolved in a mixture of toluene (90 mL) and water (60 mL) under argon. The $Pd(PPh_3)_4$ catalyst (188 mg, 0.162 mmol) was added to the mixture. This solution was stirred for 48 hours at 100°C. The mixture was extracted with dichloromethane and washed with aqueous 2N HCl, $NaHCO_3$-solution and brine. The organic phase was dried over Na_2SO_4 and the solvent removed under reduced pressure. The white solid was recrystallized from heptane/dichlormethane to give 1.36 g (78%) of **58** as white crystals.

^{1}H NMR (400 MHz, $CDCl_3$, 25 °C): δ = 7.83-7.91 (m, 2H), 7.75-7.83 (m, 2H), 7.57-7.63 (m, 2H), 7.44-7.56 (m, 4H), 7.32-7.42 (m, 4H), 1.56 (s, 12H) ppm.

^{13}C NMR (100 MHz, $CDCl_3$, 25 °C): δ = 168.6, 154.0, 153.9, 140.3, 138.5, 129.2, 127.9, 127.3, 127.2, 126.2, 124.6, 122.7, 120.4, 120.1, 47.1, 27.1 (2C) ppm.

FD-MS: 534.1 [M^+]

Anal. Calcd for $C_{36}H_{26}F_4$: C, 80.88; H, 4.90;

Found: C, 80.43; H, 4.93.

6.3.31. 1,4-Bis[2´-(9´,9´-dimethyl)fluorenyl]-2,5-bis(trifluoromethyl)benzene (59)

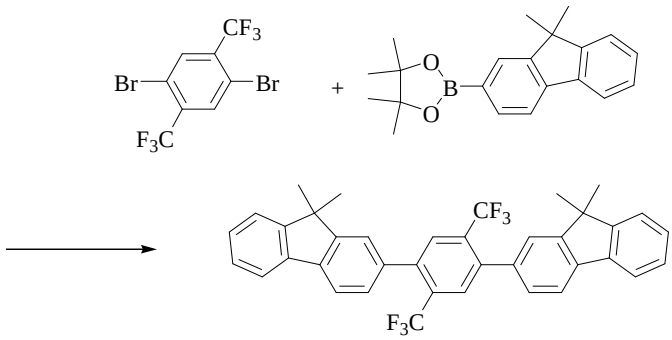

1.0 g (2.69 mmol) of **60**, 2.76 g (8.60 mmol) of the boronic ester **61,** 11.4 g (0.108 mol) sodium carbonate and 0.44 g (1.08 mmol) aliquat 336 were dissolved in a mixture of toluene (90 mL) and water (54 mL) under argon. The $Pd(PPh_3)_4$ catalyst (155 mg, 0.134 mmol) was added to the mixture. This solution was stirred for 48 hours at 100°C. The mixture was extracted with dichloromethane and washed with aqueous 2N HCl, $NaHCO_3$-solution and brine. The organic phase was dried over Na_2SO_4 and the solvent removed under reduced pressure. The white solid was recrystallized from heptane/dichlormethane to give 1.32 g (82%) of **59** as white crystals.

^{1}H NMR (400 MHz, $CDCl_3$, 25 °C): δ = 7.78-7.86 (m, 6H) 7.46-7.51 (m, 4H) 7.35-7.41 (m, 6H), 1.56 (s, 12H) ppm.

^{13}C NMR (100 MHz, $CDCl_3$, 25 °C): δ = 153.9, 153.5, 141.1, 139.4, 138.6, 137.1, 131.2 (q, $^2J_{CF}$ = 29.6 Hz), 130.2, 130.2, 127.8, 127.7, 127.1, 123.5, 122.7, 120.3, 119.6, 47.0, 27.1 (2C) ppm.

FD-MS: 597.9 [M^+]

Anal. Calcd for $C_{38}H_{29}F_6$: C, 76.24; H, 4.71;

Found: C, 76.76; H, 4.55.

6.3.32. 1,4-Dibromo-2,5-bis(trifluoromethyl)benzene (60)

According to Dolbier *et al.*[189]

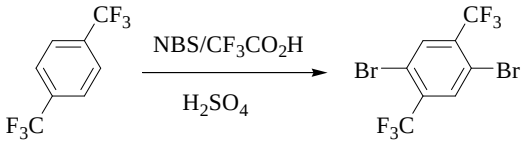

20.0 g (0.093 mol) 1,4-bis(trifluoromethyl)benzene were dissolved in 150 ml of trifluoroacetic acid (TFA) / H_2SO_4 (v/v H_2SO_4/TFA ~0.3). 49.9 g (0.28 mol) NBS were added in portions during a period of 2 h. The mixture was heated for 48 h at 60°C. Afterwards the mixture was poured into ice-water. The product was extracted with dichlormethane, washed with brine and dried over Na_2SO_4. The organic layer was concentrated to ca. 30 mL and the white product filtered off. Recrystallization from dichlormethane gave 15.6 g (45 %) of white crystals.[189]

^{1}H NMR (400 MHz, $CDCl_3$, 25 °C): δ = 8.01 (s, 2H) ppm.
^{13}C NMR (100 MHz, $CDCl_3$, 25 °C): δ = 134.5 (q, $^{2}J_{CF}$ = 32.1 Hz) 134.1-134.4 (m), 121.4 (q, $^{1}J_{CF}$ = 274.4 Hz), 119.1 ppm.
^{19}F NMR (376 MHz, $CDCl_3$, 25 °C): δ = -64.06 (s, 6F) ppm.
Anal. Calcd for $C_8H_2Br_2F_6$: C, 25.84; H, 0.54;
Found: C, 25.63; H, 0.97.

6.3.33. 9,9-Dimethyl-2-(4,4´,5,5´-tetramethyl-1,3,2-dioxaborolato)fluorene (61)

6.3.33.1. A) 2-Bromo-9,9-dimethylfluorene

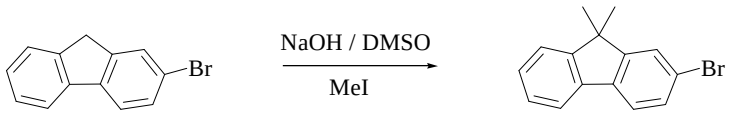

The synthesis was done following procedure A. The temperature was lowered to 45°C before iodomethane was added.

^{1}H NMR (400 MHz, $CDCl_3$): δ = 7.3 – 7.7 (m, 6 H, Ar-H), 1.49 (s, 6 H, CH_3) ppm.

^{13}C NMR (100 MHz, $CDCl_3$): δ= 155.7, 153.3, 138.2, 138.2, 130.1, 127.7, 127.2, 126.1, 122.6, 121.4, 121.0, 120.0, 47.1, 27.0 ppm.

LR-MS (EI, m/z): 178 (100.0), 272 [M^+] (93), 274 (93), 273 (45), 274 (43).

6.3.33.2. B) 9,9-Dimethyl-2-(4,4´,5,5´-tetramethyl-1,3,2-dioxaborolato)fluorene (**61)**

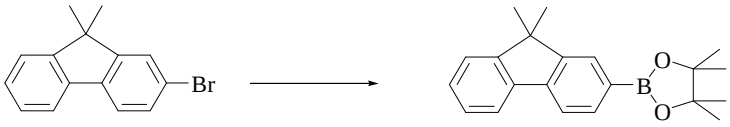

A flame dried 500 mL flask was charged with 2-bromo-9,9-dimethylfluorene (15 g, 55 mmol) and sealed under argon. Dry hexane (250 mL) and THF (50 mL) were added and the mixture cooled to -78°C. *n*-BuLi (55 mmol) was added, the mixture stirred for 10 min and allowed to warm up to 0°C. The solution was cooled again to - 78°C, and 2-isopropoxy-4,4´,5,5´-tetramethyl-1,3,2-dioxaborolane (71 mmol) added at once. The reaction was stirred at room temperature for 12 h. The mixture was poured into water and extracted with chloroform. The organic layer was washed with water and brine and dried over Na_2SO_4. The solution was evaporated to dryness and the residue purified by column chromatography using hexane/ethyl acetate (95:5) as eluent. After the solvent was removed, the remaining solid was recrystallized from hexane to afford 12.5 g of **61** as a white solid in 71 % yield.

^{1}H NMR (400 MHz, $CDCl_3$, 25 °C): δ = 7.73-7.90 (m, 4H), 7.32-7.47 (m, 3H), 1.52 (s, 6H, CH_3), 1.39 (s, 12H, CH_3) ppm.

^{13}C NMR (100 MHz, $CDCl_3$, 25 °C): δ = 154.3, 152.8, 142.2, 139.0, 133.9, 127.8, 127.7, 126.9, 122.6, 120.4, 119.3, 83.7, 46.8, 27.1, 24.9 ppm.

LR-MS (EI, m/z): 319.9 [M^+] (100.0), 304.6 (90.0).

6.4. Polymer Synthesis

6.4.1. Polyfluorenes containing alkylidene building blocks (P1-P7)

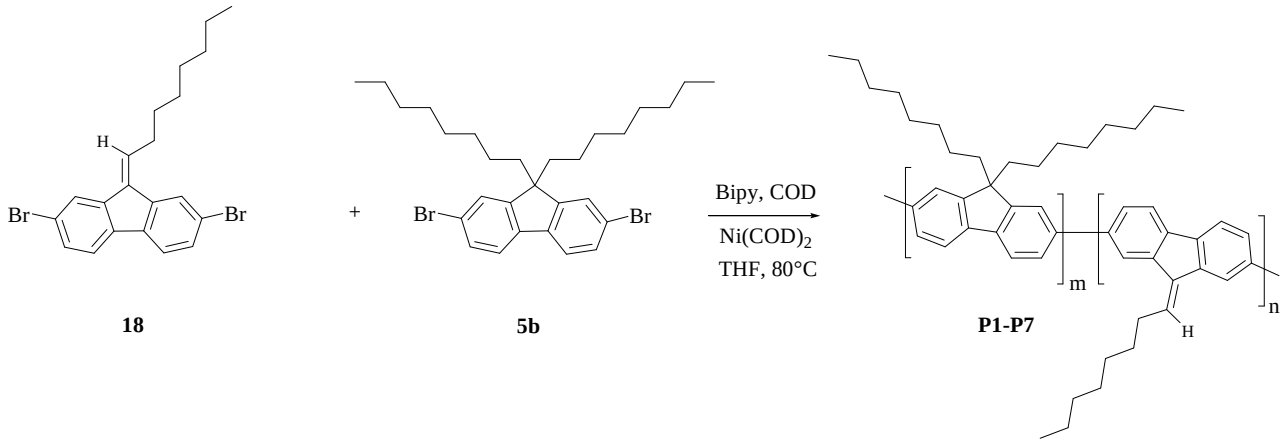

18 **5b** **P1-P7**

The polymers were prepared following procedure B:

Polymer	**5c**	**18**	Mn	Mw/Mn	Yield [mg]
P1 (1.1%)	0.5 g (0.91 mmol)	4.6 mg ($1.0 \cdot 10^{-5}$ mol)	63,700	2.0	263 (74%)
P2 (2.1%)	0.5 g (0.91 mmol)	8.3 mg ($1.9 \cdot 10^{-5}$ mol)	59,800	1.9	135 (38%)
P3 (4.8%)	0.5 g (0.91 mmol)	20.1 mg ($4.6 \cdot 10^{-5}$ mol)	58,200	1.9	245 (69%)
P4[a] (0.5%)	0.504 g (0.92 mmol)	2.0 mg ($4.6 \cdot 10^{-6}$ mol)	44,000	2.3	185 (52%)
P5[a] (1.0%)	0.504 g (0.92 mmol)	4.0 mg ($9.2 \cdot 10^{-6}$ mol)	28,700	2.1	156 (44%)
P6[a] (2.0%)	0.502 g (0.92 mmol)	8.1 mg ($1.9 \cdot 10^{-5}$ mol)	58,700	3.8	224 (63%)
P7[a] (4.7%)	0.5 g (0.91 mmol)	19.7 mg ($4.5 \cdot 10^{-5}$ mol)	91,300	3.1	278 (78%)

a) prepared from **5b**

No significant differences were observed in the ^{1}H and ^{13}C NMR spectra. The concentration of the alkylidene units is too low for a detection of alkylidene-related signals. Only the significant signals of the fluorene units could be detected. Exemplarily, the NMR analysis of **P1** is given here:

^{1}H-NMR (400 MHz, $C_2D_2Cl_4$, 80°C): δ = 7.23 – 8.11 (m, 6H), 1.79 – 2.46 (bs, 4H), 0.36-0.93 (m, 30 H) ppm. (all signals are rather broad)

^{13}C-NMR (100 MHz, $C_2D_2Cl_4$, 80°C) δ = 151.6, 140.6, 140.4, 126.3, 123.4, 120.0, 55.4, 35.3, 34.6, 28.8, 27.6, 23.0, 16.5, 14.1, 10.7 ppm.

Due to the low content of alkylidenefluorene units only signals from fluorene units are observed.

6.4.2. Random Copolymers P8-P10 (Fluorene/Fluorenone/Binaphthyl)

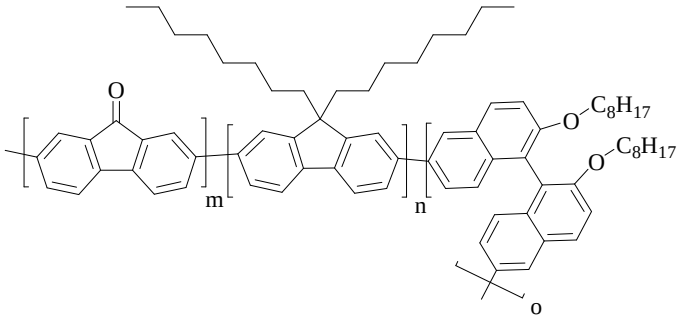

These polymers were synthesized following procedure B.

Polymer	Binaphthyl Monomer **22**	Fluorenone Monomer **19**	Fluorene Monomer **5b**
P8	0.201 g (0.301 mmol)	0.5 mg ($1.48 \cdot 10^{-6}$ mol)	1.10 g (2.01 mmol)
P9	0.297 g (0.445 mmol)	1.0 mg ($2.96 \cdot 10^{-6}$ mol)	1.38 g (2.52 mmol)
P10	0.299 g (0.447 mmol)	5.0 mg ($14.89 \cdot 10^{-6}$ mol)	1.38 g (2.52 mmol)

GPC: **P8**: M_n=164,000 g/mol D = 2.2; **P9**: M_n=172,000 g/mol D = 2.1; **P10**: M_n=169,000 g/mol D = 2.6;

P8:

^{1}H-NMR (400 MHz, $C_2D_2Cl_4$, 80°C) .: δ = 7.26 – 8.10 (m), 3.93 (bs, O-CH_2), 2.06 (bs), 1.42 (bs) , 0.68-1.26 (m) ppm. (all signals are rather broad)

^{13}C-NMR (100 MHz, $C_2D_2Cl_4$, 80°C) δ = 195.2, 169.7, 163.9, 157.0, 156.4, 137.2, 136.6, 134.0, 133.2, 133.1, 131.3, 120.3, 120.3, 119.0, 118.5, 117.4, 111.0, 67.8, 54.9, 40.5, 29.2, 29.2, 22.6, 14.0 ppm.

No clear assignment of the signals is possible. The fluorene signals are dominant due to the low content of the other monomeric units.

P9:

^{1}H-NMR (400 MHz, $C_2D_2Cl_4$, 80°C) : δ = 7.15 – 8.13 (m), 3.93 (bs, O-CH_2), 2.07 (bs), 1.42 (bs) , 0.62-1.27 (m) ppm. (all signals are rather broad)

^{13}C-NMR (100 MHz, $C_2D_2Cl_4$, 80°C) δ = 152.2, 140.7, 140.4, 140.3, 126.4, 121.9, 120.2, 120.0, 55.6, 40.4, 31.9, 30.2, 29.9, 29.7, 29.3, 25.9, 24.3, 22.7, 14.2 ppm. No clear assignment of the signals is possible. The fluorene signals are dominant due to the low content of the other monomeric units.

P10:

^{1}H-NMR (400 MHz, $C_2D_2Cl_4$, 80°C) : δ = 7.24 – 8.09 (m), 3.90 (bs, O-CH_2), 2.06 (bs), 1.41 (bs) , 0.68-1.26 (m) ppm. (all signals are rather broad)

^{13}C-NMR (100 MHz, $C_2D_2Cl_4$, 80°C) δ = 170.9, 152.2, 140.8, 140.2, 126.6, 126.3, 125.8, 121.9, 120.2, 55.6, 40.4, 31.9, 30.2, 29.8, 29.3, 25.9, 24.3, 22.7, 14.2 ppm. No clear assignment of the signals is possible. The fluorene signals are dominant due to the low content of the other monomeric units.

6.4.3. Random Fluorenone-PF2/6 Copolymer (P11)

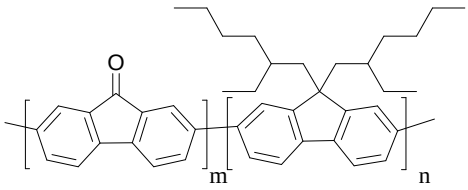

This polymer was synthesized following procedure B from 2,7-dibromo[9,9-bis(2-ethylhexyl)fluorene] (**5a**) (1.06 g, 1.93 mmol) and 2,7-dibromofluorenone 0.0066 g (0.0195 mmol) as monomers; Yield: 0.316 g of a slightly yellow solid.

GPC: M_n=177,000 PD = 2.6.

^{1}H-NMR (400 MHz, $C_2D_2Cl_4$, 25°C): δ = 7.20 – 8.06 (m, 6H), 1.72-2.31 (m, 2H), 0.53-1.02 (m, 32H) ppm. (all signals are rather broad)

^{13}C-NMR (100 MHz, $CDCl_3$, 25°C) δ = 151.5, 140.6, 140.4, 126.5, 123.3, 120.1, 55.4, 45.1, 35.3, 34.6, 28.8, 27.6, 23.1, 14.2, 10.7 ppm. No clear assignment of the signals is possible. The fluorene signals are dominant due to the low content of fluorenone units.

6.4.4. Poly[9,9-dioctylfluorene] (PFO) (P12)

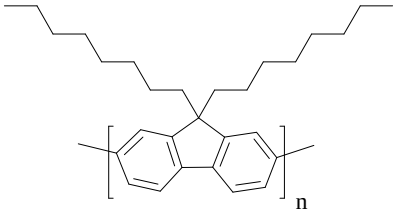

This polymer was synthesized following procedure B from 2,7-dibromo-(9,9-dioctylfluorene) (**5c**) (1.5 g, 2.74 mmol). Yield: 0.85 g (80%) of a white solid.

GPC: M_n = 116,000 g/mol, PD = 2.3.

DSC: $T_{C \rightarrow LC}$ =169°C; $T_{LC \rightarrow C}$ = 130°C

^{1}H-NMR (400 MHz, $CDCl_3$, 25°C): δ = 7.59 – 7.83 (m, 6H), 1.00-1.30 (m, 28H), 0.79 (t, 6H, *J* = 7.2 Hz) ppm. (all signals are rather broad)

^{13}C-NMR (100 MHz, $CDCl_3$, 25°C) δ = 151.9, 140.6, 140.0, 126.2, 121.4, 120.1, 55.4, 40.3, 31.9, 30.1, 29.3, 28.1, 23.9, 22.6, 14.0 ppm.

6.4.5. Random PF2/6-Pt-Salen Copolymer via a Microwave Assisted Yamamoto-type Protocol (P13)

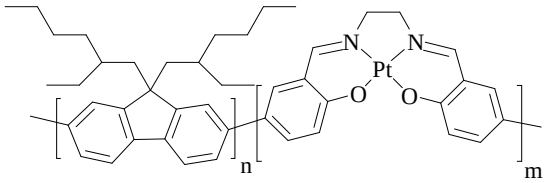

To a 10 mL reaction tube containing $Ni(COD)_2$ (143 mg, 0.52 mmol), **42** (19 mg, 0.04 mmol), bipyridyl (89 mg, 0.57 mmol) and 2,7-dibrom[9,9-bis(2-ethylhexyl)fluorene] (130 mg, 0.24 mmol) (**5a**), 5 mL of THF and COD (0.09 mL, 0.57 mmol) were added via a syringe. The tube was heated in a microwave apparatus for 12 minutes at 300 W/115°C. The solution was washed 2 times with 2N aqueous HCl, Na-EDTA solution and water. The solvent was removed and the residue was dissolved in chloroform. The polymer was

precipitated into methanol and extracted with acetone to give a yellow powder. Yield 57 mg (40%).

GPC: M_n = 169,500, PD = 2.1.

^{1}H NMR (400 MHz, $C_2D_2Cl_4$, 25°C): δ = 7.08 - 8.23 (m), 3.70 - 3.89 (m), 1.59 - 2.59 (m), 1.16 - 1.51 (m), 0.26 - 1.14 (m); (all signals are rather broad)

^{13}C NMR (100 MHz, $C_2D_2Cl_4$, 25°C) δ = 151.4, 140.7, 140.4, 126.3, 123.2, 120.0, 55.4, 50.6, 35.3, 34.6, 29.9, 28.8, 27.6, 23.0, 14.1, 10.7 (all signals are rather broad, no signal could be assigned to the platinum-complex due to the low concentration level).

6.4.6. Statistical PFO-Pt-Salen Copolymer via a Microwave Assisted Yamamoto-type Protocol (P14)

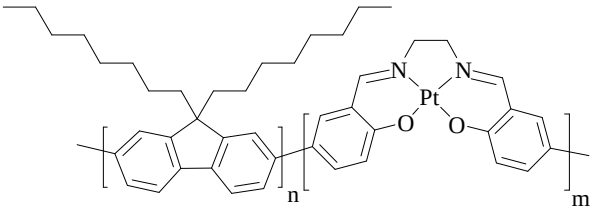

To a 10 mL reaction tube containing $Ni(COD)_2$ (110 mg, 0.4 mmol), **42** (19 mg, 0.04 mmol), bipyridyl (68 mg, 0.44 mmol) and 2,7-dibromo-9,9-dioctylfluorene (**5b**) (100 mg, 0.18 mmol), 5 mL of a mixture of toluene/DMF (4/1) and COD (0.07 mL, 0.44 mmol) were added via a syringe. The tube was heated in a microwave apparatus for 12 minutes at 300 W/220°C. The solution was washed 2 times with 2N aqueous HCl, Na-EDTA solution and water. The solvent was removed and the residue was dissolved in chloroform. The polymer was precipitated into methanol and extracted with ethyl acetate to give a yellow powder. Yield 45 mg (41%).

GPC: M_n=24,300, PD = 2.7.

^{1}H-NMR (400 MHz, $C_2D_2Cl_4$, 25°C): δ = 7.45 - 7.89 (bm), 3.75 - 3.88 (m) , 1.9-2.2 (m), 1.38-1,45 (m) , 1.05-1.25 (m), 0.85-0.95 (m), 0.75-0.8 (m) ppm. (all signals are rather broad)

^{13}C-NMR (100 MHz, $C_2D_2Cl_4$, 25°C) δ = 151.1, 140.4, 140.1, 126.2, 121.7, 120.1, 55.4, 40.3, 31.9, 30.2, 29.4, 24.1, 22.8, 14.3 ppm (all signal are rather broad, no signal could be assigned to the platinum-complex due to the low concentration level).

6.4.7. Poly[9,9-bis(2-ethylhexyl)fluorene] (PF2/6) (P15)

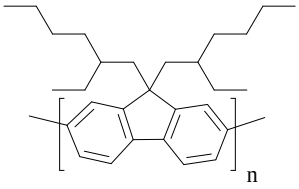

This polymer was synthesized following procedure B from 2,7-dibromo-[9,9-bis(2-ethylhexyl)fluorene] **5a** (3 g, 0.55 mmol). Yield: 1.8 g (84%) of a white solid.

GPC: M_n = 125,700, PD = 1.7.

^{1}H-NMR (400 MHz, $C_2D_2Cl_4$, 25°C): δ = 7.26 - 8.05 (m, 6H), 1.74 - 2.51 (m, 2H), 0.12 - 1.08 (m, 32 H); (all signals are rather broad)

^{13}C-NMR (100 MHz, $C_2D_2Cl_4$, 25°C) δ = 151.5, 140.6, 140.4, 126.4, 123.3, 120.0, 55.4, 45.1, 35.3, 34.6, 28.8, 27.6, 23.0, 14.2, 10.7.

6.4.8. Random PF2/6-Pt-Salen Copolymer (P16)

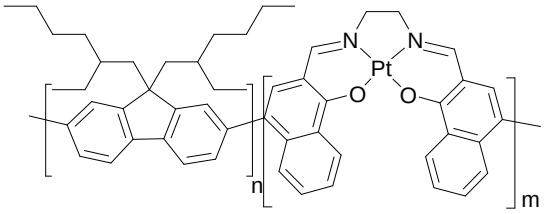

This polymer was synthesized following procedure B from 2,7-dibromo-[9,9-bis(2-ethylhexyl)fluorene] **5a** (1 g, 1.82 mmol) and the co-monomer **33** (0.024 g, 0.048 mmol). Yield: 0.35 g of an orange solid.

GPC: M_n=116,300, PD = 2.1.

^{1}H-NMR (400 MHz, $C_2D_2Cl_4$, 80°C) .: δ = 7.57 - 7.77 (bm), 1.85 – 2.30 (m) , 1.42 (bs), 1.23 (bs) , 0.57-0.93 (m) ppm. (all signals are rather broad)

^{13}C-NMR (100 MHz, $C_2D_2Cl_4$, 25°C) δ = 151.4, 140.9, 140.5, 126.3, 123.1, 112.0, 55.3, 45.0, 35.2, 34.5, 28.7, 27.5, 22.9, 14.0, 10.6 ppm. (all signals are rather broad, no clear assignment was possible)

6.4.9. Random PF2/6-Pt-Salen Copolymers (P17 and P18)

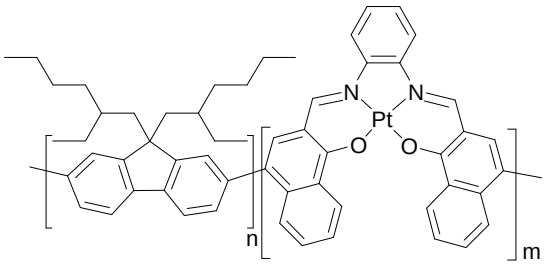

The polymers were synthesized following procedure B from:

P17: 2,7-dibromo-[9,9-bis(2-ethylhexyl)fluorene] **5a** (0.5 g, 0.912 mmol) and co-monomer **43** (0.069 g, 0.101 mmol). Yield: 0.21 g of a purple solid.

P18: 2,7-dibromo-[9,9-bis(2-ethylhexyl)fluorene] **5a** (0.5 g, 0.912 mmol) and comonomer **43** (0.033 g, 0.048 mmol). Soxhlet extraction with acetone for one 1 day yielded 0.35 g of a purple powder.

GPC: **P17**: M_n=60,500, PD = 1.7. **P18**: M_n=7,600, PD = 2.1

^{1}H-NMR (400 MHz, $C_2D_2Cl_4$, 80°C) .: δ = 8.53-9.43 (m), 6.66-8.31 (m), 1.65-2.87 (m), 0.37-1.65 (m) ppm. (all signals are rather broad)

A ^{13}C NMR analysis failed because of the low solubility of **P17** and **P18**.

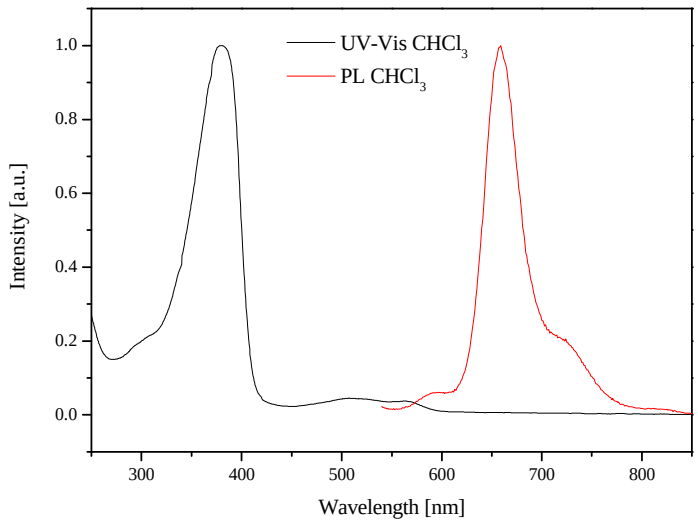

UV-Vis and absorption spectra of **P17** (λ_{ex}=505 nm)

6.4.10. Random fluorene/benzophenone copolymers P19-P24

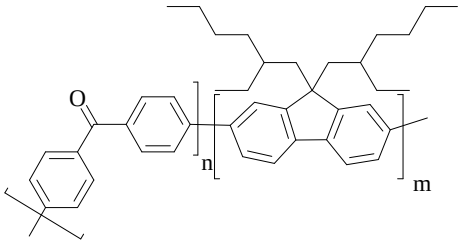

4,4´-Dibromo-benzophenone (x %) was mixed with 1.0 g (1.82 mmol) [(100-x)%] **5a** and polymerized following procedure B.

Polymer	4,4´-Dibromobenzophenone Monomer [%]	M_n [g/mol]	M_w [g/mol]	PD	Yield
P19	5	168,00	322,000	1,9	0.56 g (75%)
P20	6.5	145,000	272,000	1,9	0.51 g (68%)
P21	10	147,000	307,000	2,1	0.50 g (64%)
P22	20	111,000	242,000	2,2	0.72 g (81%)
P23	33	187,000	291,000	1,6	0.59 g (56%)
P24	50	69,000	142,000	2,1	0.51 g (36%)

Exemplarily, the NMR spectra of **P21** are presented here. However, a clear assignment of the signals was not possible. In the case of the ^{13}C NMR spectrum the signals of the fluorene units are dominant and signals of the benzophenone building blocks could not be detected.

^{1}H-NMR (400 MHz, $C_2D_2Cl_4$, 80°C).: δ = 6.98-8.14 (bm), 1.70 – 2.55 (m) , 0.40-1.08 (m) ppm. (all signals are rather broad)

^{13}C-NMR (100 MHz, $C_2D_2Cl_4$, 25°C) δ = 151.5, 140.7, 140.2, 126.4, 123.4, 120.0, 55.4, 35.3, 34.6, 28.8, 27.6, 23.0, 14.1, 10.7 ppm (all signals are rather broad, no signals originating from the benzophenone units could be detected most probably due to the relative low concentration).

6.4.11. Synthesis of Random Copolymer P25

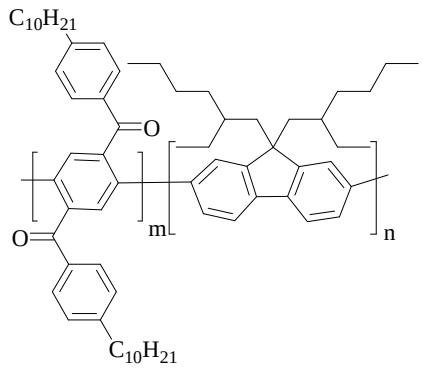

This copolymer was synthesized following procedure B from 2,7-dibromo-[9,9-bis(2-ethylhexyl)fluorene] **5a** (1.00 g, 1.82 mmol) and 4´,4´´-Didecyl-2,5-dibromo-terephthalophenone (57) (0.147 g, 0.203 mmol). Yield: 0.530 g (after Soxhlet extraction with ethyl acetate) of a slightly yellow solid.

^{1}H-NMR (400 MHz, $C_2D_2Cl_4$, 80°C) .: δ = 8.33-6.46 (bm), 2.67-0.40 (bm) ppm. (all signals are rather broad, no assignment of signals is possible due to overlapping signals).

GPC: M_n=180,000 PD = 1.7.

6.4.12. Statistical PFO-Pt-Salen Copolymer P26

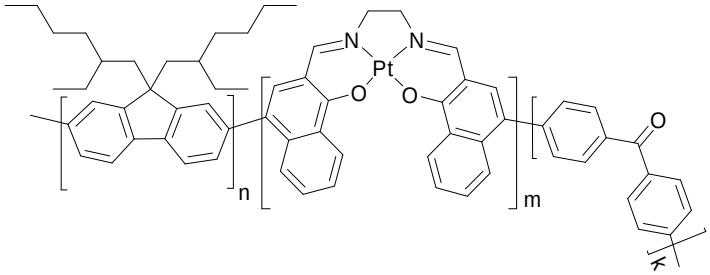

This polymer was synthesized following procedure B from 2,7-dibromo-[9,9-bis(2-ethylhexyl)fluorene] (**5a**) (2.0 g, 3.65 mmol) and the comonomers **33** (0.055 g, 0.083 mmol), and 4,4´-dibromobenzophenone (0.140 g, 0.41 mmol). Yield: 0.75 g of an orange solid.

^{1}H-NMR (400 MHz, $C_2D_2Cl_4$, 80°C) .: δ = 8.30-7.03 (bm, 6H), 2.50-1.64 (bm, 4H) , 1.55-1.28 (m, 2H), 1.14-0.14 (bm, 28H) ppm. (all signals are rather broad, no signals originating from the benzophenone units or the platinum phosphor could be detected most probably due to the relative low concentration).

^{13}C-NMR (100 MHz, $C_2D_2Cl_4$, 25°C) δ = 151.5, 140.7-140.5 (overlapping signals), 130.9, 127.0,-126.4 (overlapping signals), 123.4-123.1 (overlapping signals), 120.0 (bs), 55.4, 35.3, 34.6, 34.5, 28.8, 27.6, 23.0, 14.1, 10.7 ppm (all signals are rather broad, the fluorene signals are dominant due to the low concentration of the other monomeric units).

GPC: M_n=84,700 g/mol, PD = 1.7.

List of Symbols and Abbreviations

bipy	2,2´-bipyridyl
bm	broad multiplet
COSY	correlated spectroscopy
δ	chemical shift
DMF	*N*, *N* – dimethylformamide
d	doublet
DSC	differential scanning calorimetry
eq.	equivalent
h	hours
HOMO	highest occupied molecular orbital
IR	infrared
LUMO	lowest unoccupied molecular orbital
MeLPPP	methyl-substituted ladder poly(*para*-phenylene)
min	minutes
M_n	number average molecular weight [$g \cdot mol^{-1}$]
M_w	weight average molecular weight [$g \cdot mol^{-1}$]
NMR	nuclear magnetic resonance
n.m.	not measured
OFET	organic field effect transistor
OLED	organic light emitting diode
PD	polydispersity
PF	polyfluorene
PL	photoluminescence
ppm	parts per million
PPP	poly(*para*-phenylene)
PSS	poly(styrenesulfonate)
q	quartet
THF	tetrahydrofurane
t	triplet

7. List of Publications

1. J. Pina, J. Seixas des Melo, H.D. Burrows, F. Galbrecht, A. Bilge, C.J. Kudla, U. Scherf, Excited State Properties of Oligophenyl and Oligothienyl Swivel Cruciforms, *J. Phys. Chem. B*, **2008**, in press, DOI:10.1021/jp0773280
2. A. Tsami, X. Yang, F. Galbrecht, T. Farrell, H. Li, S. Adamczyk, R. Heiderhoff, L.J. Balk, D. Neher, E. Holder, Random fluorene copolymers with on-chain quinoxaline acceptor units, *J. Polym. Sci., Part A: Polym. Chem*., **2007**, 45, 4773
3. M. Knaapila, F.B. Dias, V.M. Garamus, L. Almásy, M. Torkkeli, K. Leppänen, F. Galbrecht, E. Preis, H.D. Burrows. U. Scherf, A.P. Monkman, Influence of Side Chain Length on the Self-Assembly of Hairy-Rod-Poly(9,9-dialkylfluorene)s in the Poor Solvent Methylcyclohexane, *Macromolecules*, **2007**, 40, 9398
4. J. Pina, J. Seixas de Melo, H.D. Burrows, F. Galbrecht, B.S. Nehls, T. Farrell, U. Scherf, Spectral and Photophysical Studies of Poly[2,6-(1,5-dioctylnaphthalene)]thiophenes, *J. Phys. Chem. C*., **2007**, 7185
5. F. Galbrecht, T.W. Bünnagel, U. Scherf, T. Farrell, Microwave-Assisted Preparation of Semiconducting Polymers, (Review), *Macromol. Rapid Commun*. **2007**, 28, 387
6. A. Zen, P. Pingel, F. Jaiser, D. Neher, J. Grenzer, W. Zhuang, J.P. Rabe, A. Bilge, F. Galbrecht, B.S. Nehls, T. Farrell, U. Scherf, R.D. Abellon, F.C. Grozema, L.D.A. Siebbeles, Organic Field-Effect Transistors Utilizing Solution-Deposited Oligothiophene-Based Swivel-Cruciforms, *Chem. Mater*. **2007**, 1267
7. M. Arif, S. Guha, M.S. Yun, S. Gangopadhyay, K. Ghosh, L. Fadiga, F. Galbrecht, and U. Scherf, Polyfluorene as a model system for space-charge-limited conduction, *Phys. Rev. B 75*, **2007**, 195202
8. P. Prins, F.C. Grozema, F. Galbrecht, U. Scherf, L.D.A. Siebbeles, Charge Transport along Coiled Conjugated Polymer Chains, *J. Phys. Chem. C.* **2007**, 11104
9. P. Görrn T. Rabe, T. Riedl, W. Kowalsky, F. Galbrecht, U. Scherf, Low loss contacts for organic semiconductor lasers, *Appl. Phys. Lett*. **2006**, 89, 161113
10. T. Rabe, K. Gerlach, T. Riedl, H. H. Johannes, W. Kowalsky, J. Niederhofer, W. Gries, J. Wang, T. Weimann, P. Hinze, F. Galbrecht, U. Scherf, Quasi-continuous wave operation of an organic thin-film distributed feedback laser, *Appl. Phys. Lett.* **2006**, 89,161113
11. T.W. Bünnagel, F. Galbrecht, U. Scherf, A Novel Poly[2,6-(4-dialkylmethylene-cyclopenta-dithiophene)] with "in-plane" Alkyl Substituents, *Macromolecules* **2006**, 39, 8870
12. S. K. Weber, F. Galbrecht, U. Scherf, Preferential Oxidative Addition in Suzuki Cross-Coupling Reactions across one Fluorene Unit, *Org. Lett*. **2006**, 4039

13. C. Rothe, F. Galbrecht, U. Scherf, A. Monkman, The beta-phase of poly(9,9-dioctylfluorene) (PFO) as potential system for electrically pumped organic lasing, *Adv. Mater*. **2006**, 2137
14. A. Zen, A. Bilge, F. Galbrecht, R. Alle, K. Meerholz, J. Grenzer, D. Neher, U. Scherf, T. Farrell, Solution Processable Organic Field-Effect Transistors Utilising a α, α '-Dihexylpentathiophene Based Swivel-Cruciform, *J. Amer. Chem. Soc.* **2006**, 3914
15. M.S. Yun, R. Ravindran, M. Hossain, S. Gangopadhyay, U. Scherf, T. W. Bünnagel, F. Galbrecht, M. Arif and S. Guha, Capacitance-voltage characterization of polyfluorene-based metal-insulator-semiconductor diodes, *Appl. Phys. Lett.* **2006**, 13506
16. H. Cheun, F. Galbrecht, B.S. Nehls, U. Scherf, M. J. Winokur, Temperature dependent spectroscopy of poly(9,9-(2-ethyl)-hexylfluorene)/(9,9-di-n-octylfluorene)copolymers, *J. of Lumin.* **2006**, 212
17. B.S. Nehls, F. Galbrecht, D.J. Brauer, C.W. Lehmann, U. Scherf, T. Farrell, Synthesis and Characterisation of a Helical Step-Ladder Poly(Para-Phenylene), *J Polym. Sci., Part A: Polym. Chem.* **2006**, 5533
18. B.S. Nehls, F. Galbrecht, A. Bilge, U. Scherf, T. Farrell, Synthesis and properties of oligo-/polymers based on a "flexible" swivel-cruciform structure, *Macromol. Symp.*, **2006**, 21
19. S. Galambosi, M. Knaapila, J. A. Soininen, K. Nygård, S. Huotari, F. Galbrecht, U. Scherf, A. P. Monkman, and K. Hämäläinen, X-ray Raman scattering study of aligned polyfluorene, *Macromolecules* **2006**, 9261
20. A. Bilge, A. Zen, M. Forster, F. Galbrecht, B.S. Nehls, T. Farrell, D. Neher, U. Scherf, Swivel-cruciform oligothiophene dimers, *J. Mater. Chem.* **2006**, 3177
21. M. Knaapila, V. M. Garamus, F. B. Dias, L. Almásy, F. Galbrecht, A. Charas, J. Morgado, H. D. Burrows, U. Scherf, and A. P. Monkman, Influence of Solvent Quality of Archetypical Hairy Rods - Branched and Linear Side Chain Polyfluorenes:Rodlike Chains versus "Beta-Sheets" in Solution, *Macromolecules* **2006**, 6505
22. F. Galbrecht, T. Bünnagel, A. Bilge, U. Scherf and T. Farrell, Cruciform - conjugated oligomers, in: Functional Organic Materials, Eds.: T. Müller and U. Bunz, Wiley-VCH, Heidelberg, **2006**, 81
23. X.H. Yang, F. Jaiser, B. Stiller, D. Neher, F. Galbrecht and U. Scherf, Efficient polymer electrophosphorescent devices with interfacial layers, *Adv. Funct. Mater.* **2006**, 2156
24. K. Becker, J.M. Lupton, J. Feldmann, B.S. Nehls, F. Galbrecht, D.Q. Gao, U. Scherf, On-Chain Fluorenone Defect Emission from Single Polyfluorene Molecules in the Absence of Intermolecular Interactions, *Adv. Funct. Mater.* **2006**, 364
25. F. Galbrecht, X. H. Yang, B.S. Nehls, D. Neher, T. Farrell, U. Scherf, Semiconducting polyfluorenes with electrophosphorescent on chain platinum-salen chromophores, *Chem. Commun.*, **2005**, 2378
26. B.S. Nehls, F. Galbrecht, D.J. Brauer, C.W. Lehmann, T. Farrell, U. Scherf, Synthesis and Spectroscopy of an Oligophenyl Based Cruciform with Remarkable π - π Assisted Folding, *Org. Biomol. Chem.*, **2005**, *3***,** 3213

Conference Publications

27. S. Galambosi, M. Knaapila, J. A. Soininen, K. Nygård, S. Huotari, F. Galbrecht, U. Scherf, A. P. Monkman, and K. Hämäläinen, X-ray Raman scattering study of aligned polyfluorene, *Condensed Matter*. **2006**, 0608623
28. J. Pina, J. Seixas de Melo, H.D. Burrows, F. Galbrecht, T. Bünnagel, U. Scherf, Spectral and Photophysical Studies of Poly[α,ω-1,1'-binaphthyl)]thiophenes: a New Class of Naphthalene-Thiophene Copolymers, *Colloids & Interfaces Proc. RICI2*, **2007**
29. B.S. Nehls, F. Galbrecht, A. Bilge, T. Farrell, U. Scherf, Synthesis and Properties of Poly- and Oligomers Based on a "flexible" Cruciform Structure, *Proc. ICGRE - Inter Academia*, **2005**, Vol. 2, 505.
30. F. Galbrecht, X.H. Yang, B.S. Nehls, T.W. Bünnagel, D. Neher, T. Farrell, U. Scherf, Novel Electrophosphorescent Polyfluorenes With On-Chain Platinum Salen Chromophores, *Proc. ICGRE - Inter Academia*, **2005**, Vol. 2, 511.
31. B.S. Nehls, F.Galbrecht, T. Rabe, M. Hopping, D. Schneider, E. Becker, H.H. Johannes, W. Kowalsky, T. Weimann, J. Wang, P. Hinze, T. Farrell, U. Scherf,T. Riedl, Threshold reduction in polymer lasers based on poly (9,9-dioctylfluorene) with binaphthyl spacers, *Macromol. Rapid Commun.* **2005**, 26, F7.

Talks and Posters

1. Fπ7, The seventh International Symposium on Functional π-Electron Systems, Osaka (Jp), 15.05-20.05.2006, Poster (I, II, III, IV)
2. JCF-Frühjahrskolloqium, Wuppertal (D), 11.04.2006, Poster
3. JCF-Frühjahrssymposium, Konstanz (D), 16.03-18.03.2006, Talk and Poster
4. 8th Portuguese Meeting on Photochemistry, 16.12-17.12.2005, Coimbra (P), Poster
5. 4th International Conference on Global Research and Education, Inter-Academia 2005, 19.09. – 22.09.2005, Wuppertal (D), Talk and Poster
6. European Younger Chemists , Brno (CZ), 30.08.-03.09.2005, Poster
7. 8th European Conference on Molecular Electronics (ECME8), Bologna (I), 29.06.2005-02.07.2005, Poster
8. Frühjahrskolloqium GdCh/JCF, Wuppertal (D), 26.04.2005 Talk and Poster
9. Makromolekulares Kolloquium, Freiburg (D), 24.2.-26.2.2005, Poster
10. 40th International Symposium on Macromolecules - IUPAC World Polymer Congress MACRO 2004, Paris (F), 04.07.-09.07.2004, Poster
11. Fortschritte bei der Synthese und Charakterisierung von Polymeren, Düsseldorf (D), 15.3.-16.3.2004, Poster
12. Makromolekulares Kolloquium, Freiburg (D), 26.2.-28.2.2004, Poster
13. European Younger Chemists, Grenoble (F), 27.08.-29.08.2003 Poster

8. Acknowledgment

- An erster Stelle danke ich Prof. Dr. Ullrich Scherf für die finanzielle und fachliche Unterstützung. Das sehr gute und motivierende Arbeitsklima hat sehr zum Gelingen dieser Arbeit beigetragen.

- Dr. Tony Farrell danke ich ganz besonders für die vielen Hilfestellungen und die Zusammenarbeit in zahlreichen Projekten.

- Meinen Laborkollegen aus dem „Musiklabor“ Torsten Bünnagel, Dr. Benjamin Nehls, Dr. Tony Farrell, Christof Kudla, Benjamin Souharce und Sven Weber gilt ein besonderer Dank für die enge und ergiebige Zusammenarbeit in vielen gemeinsamen Projekten, die schöne Zeit im Labor und einer Menge Spaß.

- Torsten Bünnagel, Benjamin Nehls, Christof Kudla und Nils Koenen möchte ich nochmals für die intensive Durchsicht und die Diskussionen zu meiner Arbeit danken. Doris Banäcker danke ich ganz herzlich für die sprachliche Überarbeitung.

- Bianca Enz danke ich vor allem für Ihre stets freundliche und erheiternde Art. Ohne ihr offenes Ohr für alle Arten von Problemen und Anliegen hätten viele Dinge nicht so reibungslos funktioniert.

- Dr. Deqing Gao gilt ebenfalls mein Dank für die enge Zusammenarbeit bei zahlreichen Synthesen.

- Den „Freunden“ des Musiklabors Dr. Askin Bilge und Argiri Tsami danke ich für die gute Zusammenarbeit in vielen Projekten und den großen Spaß den wir zusammen hatten.

- Ilka Polanz, Melanie Dausend und Andreas Siebert sei herzlich gedankt für die Messung von unzähligen NMR und MS Proben. Insbesondere möchte ich mich bei bei Frau Ilka Polanz für die Hilfestellungen bei der Bearbeitung der Spektren für die Publikationen bedanken.

- Jürgen Dönicke danke ich für die Messung von zahlreichen GC-MS Proben.

- Prof. Dr. David J. Brauer (Lehrstuhl für Anorganische Chemie) und Dr. ChristianW. Lehmann (MPI – Mülheim) danke ich für die Messung der Kristallstrukturen.

- Prof. Dr. Dieter Neher (Universität Potsdam) und Dr. Xiaohui Yang sei gedankt für den Bau der OLEDs und vielen fachlichen Hilfestellungen und Diskussionen.

- Prof. Dr. Emil List (Technische Universität Graz) danke ich für die sehr interessanten Messungen und fachlichen Diskussionen.

- Prof. Dr. Hugh Burrows (Universtiy of Coimbra) danke ich für viele zahlreiche Diskussionen und die sehr ergiebige Zusammenarbeit.

- Prof. Dr. Michael Winokur und H. Cheun (University of Wisconsin) danke ich für die sehr aufschlussreichen Messungen und fachlichen Diskussionen.

- Dr. Matti Knaapila danke ich für die sehr intensive und fruchtbare Zusammenarbeit.

- Prof. Dr. Andy Monkman danke ich für die gute Kooperation in interessanten Projekten.

- Prof. Dr. W. Kowalsky (TU-Braunschweig) und vor allem Dr. Thomas Riedl und Dipl. Ing. Torsten Rabe sowie Dipl. Ing. Anis Kammoun danke ich für die intensive Zusammenarbeit und den vielen Messungen.

- Dr. Markus Roggel und Dr. Carl M. Weisshuhn danke ich für die Unterstützung mit zahlreichen Synthesen durch die Studenten der OCI und OCII Praktika.

- Andreas Hufschmidt gilt mein besonderer Dank für die intensive Zusammenarbeit und die Hilfestellungen bei zahlreichen Synthesen.

- Nils Könen, Volker Wulf, Krishan Jagota und Nadine Meier haben durch Ihren unermüdlichen Einsatz im Rahmen des Forschungspraktikums etliche Verbindungen synthetisiert und mir dadurch sehr viel Zeit erspart.

- Markus Volk danke ich ganz besonders für die Durchführung von zahlreichen Synthesen und etlichen fachlichen Diskussionen.

- Andreas Türk und Jutta Schnee (MPI Mainz) danke ich für die Messung von zahlreichen Massenspektren.

- Ich möchte mich bei Samsung für die Kooperation bedanken. Insbesondere bei Herrn Dr. Michael Redecker und Herrn Dr. Jörn Pommerrehne.

- Ich danke auch allen anderen Mitarbeitern und Ehemaligen der Scherf-Gruppe: Dr. Udom Awasipirom, Dr. Bernhard Köhler, Dr. Sybille Allard, Sylwia Adamczyk, Patrick Casper, Dr. Saulius Grigalevicius, Ligita Grigaleviciene, Dr. Roland Güntner, Anke Helfer, Eduard Preis, Dr. Guoli Tu.

- Meiner Frau Nicole danke ich für das Verständnis und ihr Durchhaltevermögen während meiner Promotion. Ohne sie hätte ich diese Arbeit nicht in dieser kurzen Zeit fertigstellen können. Nun sind wir zu dritt. Unser Sohn Ben Louis („Horst-Maria“) bereichert ab jetzt unser Leben.

- Zum Schluß danke ich ganz besonders meiner Familie, die mich das ganze Studium über begleitet hat.

9. Curriculum Vitae

Frank Galbrecht wurde 1977 in Wuppertal geboren. Er studierte Chemie an der Universität Wuppertal und erwarb den Abschluss als Diplom-Chemiker im Jahr 2004. Während der Diplomarbeit befasste er sich mit der Synthese von phosphoreszenten Iridiumkomplexen. Im Juni 2004 begann er sein Promotionsstudium unter Anleitung von Prof. Dr. Ullrich Scherf und befasste sich mit der Synthese von halbleitenden Polymeren und organischen Materialien für optoelektronische Anwendungen.

Frank Galbrecht was born 1977 in Wuppertal (Germany). He studied chemistry at the University of Wuppertal and received his Diploma degree in 2004. His undergraduate research was focused on the synthesis of phosphorescent iridium complexes. In June 2004 he started his Ph.D. work under the supervision of Ullrich Scherf focusing on the synthesis of semiconducting polymers and organic materials for optoelectronic applications.

10. Reference List

[1.] A. Bernanose, P. Vouaux, *J. Chim. Phys. Phys. - Chim. Biol.* **1953,** *50,* 261.

[2.] C. W. Tang, S. A. Vanslyke, *Appl. Phys. Lett.* **1987,** *51,* 913.

[3.] H. Shirakawa, E. J. Louis, A. G. MacDiarmid, C. K. Chiang, A. J. Heeger, *Chem. Commun.* **1977,** 578.

[4.] J. H. Burroughes, D. D. C. Bradley, A. R. Brown, P. L. Burn, R. N. Marks, K. Mackey, R. H. Friend, A. B. Holmes, *Nature* **1990,** *347,* 539.

[5.] A. Kraft, A. C. Grimsdale, A. B. Holmes, *Angew. Chem. Int. Ed.* **1998,** *37,* 402.

[6.] Y. Shirota, *J. Mater. Chem.* **2000,** *10,* 1.

[7.] U. Mitschke, P. Bäuerle, *J. Mater. Chem.* **2000,** *10,* 1471.

[8.] R. H. Friend, R. W. Gymer, A. B. Holmes, J. H. Burroughes, R. N. Marks, C. Taliani, D. D. C. Bradley, D. A. Dos Santos, J. L. Bredas, M. Logdlund, W. R. Salaneck, *Nature* **1999,** *397,* 121.

[9.] Z. N. Bao, *Adv. Mater.* **2000,** *12,* 227.

[10.] G. Horowitz, *Adv. Mater*. **1998,** *10,* 365.

[11.] H. Sirringhaus, N. Tessler, R. H. Friend, *Science* **1998,** *280,* 1741.

[12.] C. D. Dimitrakopoulos, P. R. L. Malenfant, *Adv. Mater.* **2002,** *14,* 99.

[13.] H. Imahori, S. Fukuzumi, *Adv. Funct. Mater.* **2004,** *14,* 525.

[14.] D. T. McQuade, A. E. Pullen, T. M. Swager, *Chem. Rev.* **2000,** *100,* 2537.

[15.] C. Kallinger, M. Hilmer, A. Haugeneder, M. Perner, W. Spirkl, U. Lemmer, J. Feldmann, U. Scherf, K. Mullen, A. Gombert, V. Wittwer, *Adv. Mater.* **1998,** *10,* 920.

[16.] M. D. McGehee, A. J. Heeger, *Adv. Mater.* **2000,** *12,* 1655.

[17.] V. G. Kozlov, S. R. Forrest, *Curr. Opin. Solid State Mater. Sci.* **1999,** *4,* 203.

[18.] U. Scherf, S. Riechel, U. Lemmer, R. F. Mahrt, *Curr. Opin. Solid State Mater. Sci.* **2001,** *5,* 143.

[19.] N. Tessler, G. J. Denton, R. H. Friend, *Nature* **1996,** *382,* 695.

[20.] H. Hoppe, N. S. Sariciftci, *J. Mater. Res.* **2004,** *19,* 1924.

[21.] C. J. Brabec, N. S. Saricifti, J. C. Hummelen, *Adv. Funct. Mater.* **2001,** *11,* 15.

[22.] J. J. M. Halls, A. C. Arias, J. D. MacKenzie, W. S. Wu, M. Inbasekaran, E. P. Woo, R. H. Friend, *Adv. Mater.* **2000,** *12,* 498.

[23.] J. R. Sheats, *J. Mater. Res.* **2004,** *19,* 1974.

[24.] U. Scherf, E. J. W. List, *Adv. Mater.* **2002,** *14,* 477.

[25.] N. Dieter, *Macromol. Rapid Commun.* **2001,** *22,* 1365.

[26.] Q. B. Pei, Y. Yang, *J. Am. Chem. Soc.* **1996,** *118,* 7416.

[27.] A. W. Grice, D. D. C. Bradley, M. T. Bernius, M. Inbasekaran, W. W. Wu, E. P. Woo, *Appl. Phys. Lett.* **1998,** *73,* 629.

[28.] H. G. Nothofer, A. Meisel, T. Miteva, D. Neher, M. Forster, H. Oda, G. Lieser, D. Sainova, A. Yasuda, D. Lupo, W. Knoll, U. Scherf, *Macromol. Symp.* **2000,** *154,* 139.

[29.] D. Sainova, T. Miteva, H. G. Nothofer, U. Scherf, I. Glowacki, J. Ulanski, H. Fujikawa, D. Neher, *Appl. Phys. Lett.* **2000,** *76,* 1810.

[30.] M. Grell, D. D. C. Bradley, M. Inbasekaran, E. P. Woo, *Adv. Mater.* **1997,** *9,* 798.

[31.] M. Grell, W. Knoll, D. Lupo, A. Meisel, T. Miteva, D. Neher, H. G. Nothofer, U. Scherf, A. Yasuda, *Adv. Mater.* **1999,** *11,* 671.

[32.] M. Fukuda, K. Sawada, K. Yoshino, *Jpn. J. Appl. Phys. , Part 2* **1989,** *28,* L1433.

[33.] M. Leclerc, F. Martinez Diaz, G. Wegner, *Makromol. Chem.* **1989,** *190,* 3105.

[34.] R. D. Mccullough, R. D. Lowe, *Chem. Commun.* **1992,** 70.

[35.] R. D. Mccullough, *Adv. Mater.* **1998,** *10,* 93.

[36.] M. Fukuda, K. Sawada, K. Yoshino, *J. Polym. Sci. , Part A: Polym. Chem.* **1993,** *31,* 2465.

[37.] Y. Ohmori, M. Uchida, K. Muro, K. Yoshino, *Jpn. J. Appl. Phys. B* **1991,** *11,* L1941.

[38.] V. Percec, S. Okita, R. Weiss, *Macromolecules* **1992,** *25,* 1816.

[39.] V. Percec, M. Y. Zhao, J. Y. Bae, D. H. Hill, *Macromolecules* **1996,** *29,* 3727.

[40.] F. Ullmann, J. Bielecki, *Chem. Ber.* **1901,** *34,* 2174.

[41.] T. Yamamoto, *Prog. Polym. Sci.* **1992,** *17,* 1153.

[42.] A. Falcou, J. Schwaiger, A. Ritter, Patent of Covion Organic Semiconductors GmbH, [DE 102 41 814 A1 2004.03.25], **2004**.

[43.] M. Ranger, M. Leclerc, *Chem. Commun.* **1997,** 1597.

[44.] M. Ranger, D. Rondeau, M. Leclerc, *Macromolecules* **1997,** *30,* 7686.

[45.] S. K. Weber, F. Galbrecht, U. Scherf, *Org. Lett.* **2006,** 4039.

[46.] A. Yokoyama, H. Suzuki, Y. Kubota, K. Ohuchi, H. Higashimura, T. Yokozawa, *J. Am. Chem. Soc.* **2007,** *129,* 7236.

[47.] J. Liu, G. L. Tu, Q. G. Zhou, Y. X. Cheng, Y. H. Geng, L. X. Wang, D. G. Ma, X. B. Jing, F. S. Wang, *J. Mater. Chem.* **2006,** *16,* 1431.

[48.] G. L. Tu, Q. G. Zhou, Y. X. Cheng, L. X. Wang, D. G. Ma, X. B. Jing, F. S. Wang, *Appl. Phys. Lett.* **2004,** *85,* 2172.

[49.] M. Grell, D. D. C. Bradley, X. Long, T. Chamberlain, M. Inbasekaran, E. P. Woo, M. Soliman, *Acta Polym.* **1998,** *49,* 439.

[50.] S. Setayesh, A. C. Grimsdale, T. Weil, V. Enkelmann, K. Mullen, F. Meghdadi, E. J. W. List, G. Leising, *J. Am. Chem. Soc.* **2001,** *123,* 946.

[51.] M. Sims, D. D. C. Bradley, M. Ariu, M. Koeberg, A. Asimakis, M. Grell, D. G. Lidzey, *Adv. Funct. Mater.* **2004,** *14,* 765.

[52.] J. Teetsov, M. A. Fox, *J. Mater. Chem.* **1999,** *9,* 2117.

[53.] K. Becker, J. M. Lupton, J. Feldmann, B. S. Nehls, F. Galbrecht, D. Q. Gao, U. Scherf, *Adv. Funct. Mater.* **2006,** *16,* 364.

[54.] V. N. Bliznyuk, S. A. Carter, J. C. Scott, G. Klarner, R. D. Miller, D. C. Miller, *Macromolecules* **1999,** *32,* 361.

[55.] I. Franco, S. Tretiak, *Chem. Phys. Lett.* **2003,** *372,* 403.

[56.] E. J. W. List, R. Guentner, P. S. de Freitas, U. Scherf, *Adv. Mater.* **2002,** *14,* 374.

[57.] J. M. Lupton, M. R. Craig, E. W. Meijer, *Appl. Phys. Lett.* **2002,** *80,* 4489.

[58.] J. M. Lupton, *Chem. Phys. Lett.* **2002,** *365,* 366.

[59.] J. M. Lupton, J. Klein, *Synth. Met.* **2003,** *138,* 233.

[60.] J. M. Lupton, P. Schouwink, P. E. Keivanidis, A. C. Grimsdale, K. Mullen, *Adv. Funct. Mater.* **2003,** *13,* 154.

[61.] V. R. Nikitenko, J. M. Lupton, *J. Appl. Phys.* **2003,** *93,* 5973.

[62.] X. H. Yang, D. Neher, C. Spitz, E. Zojer, J. L. Bredas, R. Guntner, U. Scherf, *J. Chem. Phys.* **2003,** *119,* 6832.

[63.] E. Zojer, A. Pogantsch, E. Hennebicq, D. Beljonne, J. L. Bredas, P. S. de Freitas, U. Scherf, E. J. W. List, *J. Chem. Phys.* **2002,** *117,* 6794.

[64.] M. T. Bernius, M. Inbasekaran, J. O'Brien, W. S. Wu, *Adv. Mater.* **2000,** *12,* 1737.

[65.] T. M. Brown, F. Cacialli, *J. Polym. Sci. , Part B: Polym. Phys.* **2003,** *41,* 2649.

[66.] N. C. Greenham, R. H. Friend, D. D. C. Bradley, *Adv. Mater.* **1994,** *6,* 491.

[67.] Y. Cao, I. D. Parker, G. Yu, C. Zhang, A. J. Heeger, *Nature* **1999,** *397,* 414.

[68.] P. K. H. Ho, J. S. Kim, J. H. Burroughes, H. Becker, S. F. Y. Li, T. M. Brown, F. Cacialli, R. H. Friend, *Nature* **2000,** *404,* 481.

[69.] M. Wohlgenannt, K. Tandon, S. Mazumdar, S. Ramasesha, Z. V. Vardeny, *Nature* **2001,** *409,* 494.

[70.] M. Ariu, D. G. Lidzey, M. Sims, A. J. Cadby, P. A. Lane, D. D. C. Bradley, *J. Phys. : Condens. Matter* **2002,** *14,* 9975.

[71.] A. J. Cadby, P. A. Lane, H. Mellor, S. J. Martin, M. Grell, C. Giebeler, D. D. C. Bradley, M. Wohlgenannt, C. An, Z. V. Vardeny, *Phys. Rev. B* **2000,** *62,* 15604.

[72.] S. Janietz, D. D. C. Bradley, M. Grell, C. Giebeler, M. Inbasekaran, E. P. Woo, *Appl. Phys. Lett.* **1998,** *73,* 2453.

[73.] N. Dieter, *Macromol. Rapid Commun.* **2001,** *22,* 1365.

[74.] E. M. Conwell, *Synth. Met.* **1996,** *83,* 101.

[75.] J. Y. Li, C. W. Ma, J. X. Tang, C. S. Lee, S. T. Lee, *Chem. Mater.* **2005,** *17,* 615.

[76.] C. Y. Chi, C. Im, V. Enkelmann, A. Ziegler, G. Lieser, G. Wegner, *Chem. Eur. J.* **2005,** *11,* 6833.

[77.] A. L. T. Khan, P. Sreearunothai, L. M. Herz, M. J. Banach, A. Kohler, *Phys. Rev. B* **2004,** *69.*

[78.] D. Neher, *Macromol. Rapid Commun.* **2001,** *22,* 1365.

[79.] W. Chunwaschirasiri, B. Tanto, D. L. Huber, M. J. Winokur, *Phys. Rev. Lett.* **2005,** *94,* 107402.

[80.] M. Ariu, M. Sims, M. D. Rahn, J. Hill, A. M. Fox, D. G. Lidzey, M. Oda, J. Cabanillas-Gonzalez, D. D. C. Bradley, *Phys. Rev. B* **2003,** *67,* 195333.

[81.] S. H. Chen, A. C. Su, C. H. Su, S. A. Chen, *Macromolecules* **2005,** *38,* 379.

[82.] M. Knaapila, V. M. Garamus, F. B. Dias, L. Almasy, F. Galbrecht, A. Charas, J. Morgado, H. D. Burrows, U. Scherf, A. P. Monkman, *Macromolecules* **2006,** *39,* 6505.

[83.] M. J. Winokur, J. Slinker, D. L. Huber, *Phys. Rev. B* **2003,** *67,* 184106.

[84.] A. Moliton, R. C. Hiorns, *Polym. Int.* **2004,** *53,* 1397.

[85.] S. Gamerith, C. Gadermaier, U. Scherf, E. J. W. List, *Phys. Status Solidi A* **2004,** *201,* 1132.

[86.] D. Marsitzky, R. Vestberg, P. Blainey, B. T. Tang, C. J. Hawker, K. R. Carter, *J. Am. Chem. Soc.* **2001,** *123,* 6965.

[87.] T. Rabe, M. Hoping, D. Schneider, E. Becker, H. H. Johannes, W. Kowalsky, T. Weimann, J. Wang, P. Hinze, B. S. Nehls, U. Scherf, T. Farrell, T. Riedl, *Adv. Funct. Mater.* **2005,** *15,* 1188.

[88.] M. R. Craig, M. M. de Kok, J. W. Hofstraat, A. P. H. J. Schenning, E. W. Meijer, *J. Mater. Chem.* **2003,** *13,* 2861.

[89.] S. Gamerith, H. G. Nothofer, U. Scherf, E. J. W. List, *Jpn. J. Appl. Phys. , Part 2* **2004,** *43,* L891-L893.

[90.] M. Yan, L. J. Rothberg, F. Papadimitrakopoulos, M. E. Galvin, T. M. Miller, *Phys. Rev. Lett.* **1994,** *73,* 744.

[91.] M. Gaal, E. J. W. List, U. Scherf, *Macromolecules* **2003,** *36,* 4236.

[92.] X. O. Gong, P. K. Iyer, D. Moses, G. C. Bazan, A. J. Heeger, S. S. Xiao, *Adv. Funct. Mater.* **2003,** *13,* 325.

[93.] J. Jacob, J. Y. Zhang, A. C. Grimsdale, K. Mullen, M. Gaal, E. J. W. List, *Macromolecules* **2003,** *36,* 8240.

[94.] F. Montilla, R. Mallavia, *Adv. Funct. Mater.* **2007,** *17,* 71.

[95.] S. Sinha, C. Rothe, R. Guntner, U. Scherf, A. P. Monkman, *Phys. Rev. Lett.* **2003,** *90*.

[96.] A. Köhler, J. S. Wilson, R. H. Friend, M. K. Al-Suti, M. S. Khan, A. Gerhard, H. Bassler, *J. Chem. Phys.* **2002,** *116,* 9457.

[97.] J. M. Lupton, A. Pogantsch, T. Piok, E. J. W. List, S. Patil, U. Scherf, *Phys. Rev. Lett.* **2002,** *89,* 167401.

[98.] M. A. Baldo, D. F. O'Brien, Y. You, A. Shoustikov, S. Sibley, M. E. Thompson, S. R. Forrest, *Nature* **1998,** *395,* 151.

[99.] V. Cleave, G. Yahioglu, P. Le Barny, R. H. Friend, N. Tessler, *Adv. Mater.* **1999,** *11,* 285.

[100.] R. J. Holmes, B. W. D'Andrade, S. R. Forrest, X. Ren, J. Li, M. E. Thompson, *Appl. Phys. Lett.* **2003,** *83,* 3818.

[101.] C. Adachi, M. A. Baldo, M. E. Thompson, S. R. Forrest, *J. Appl. Phys.* **2001,** *90,* 5048.

[102.] M. Ikai, S. Tokito, Y. Sakamoto, T. Suzuki, Y. Taga, *Appl. Phys. Lett.* **2001,** *79,* 156.

[103.] A. Tsuboyama, H. Iwawaki, M. Furugori, T. Mukaide, J. Kamatani, S. Igawa, T. Moriyama, S. Miura, T. Takiguchi, S. Okada, M. Hoshino, K. Ueno, *J. Am. Chem. Soc.* **2003,** *125,* 12971.

[104.] S. Lamansky, R. C. Kwong, M. Nugent, P. I. Djurovich, M. E. Thompson, *Org. Electr.* **2001,** *2,* 53.

[105.] W. J. Finkenzeller, P. Stossel, H. Yersin, *Chem. Phys. Lett.* **2004,** *397,* 289.

[106.] S. A. Bagnich, C. Im, H. Bassler, D. Neher, U. Scherf, *Chem. Phys.* **2004,** *299,* 11.

[107.] M. A. Baldo, M. E. Thompson, S. R. Forrest, *Pure Appl. Chem.* **1999,** *71,* 2095.

[108.] X. Gong, J. C. Ostrowski, G. C. Bazan, D. Moses, A. J. Heeger, M. S. Liu, A. K. Y. Jen, *Adv. Mater.* **2003,** *15,* 45.

[109.] C. L. Lee, K. B. Lee, J. J. Kim, *Appl. Phys. Lett.* **2000,** *77,* 2280.

[110.] M. D. McGehee, T. Bergstedt, C. Zhang, A. P. Saab, M. B. O'Regan, G. C. Bazan, V. I. Srdanov, A. J. Heeger, *Adv. Mater.* **1999,** *11,* 1349.

[111.] Y. L. Tung, S. W. Lee, Y. Chi, Y. T. Tao, C. H. Chien, Y. M. Cheng, P. T. Chou, S. M. Peng, C. S. Liu, *J. Mater. Chem.* **2005,** *15,* 460.

[112.] X. H. Yang, D. Neher, *Appl. Phys. Lett.* **2004,** *84,* 2476.

[113.] X. W. Chen, J. L. Liao, Y. M. Liang, M. O. Ahmed, H. E. Tseng, S. A. Chen, *J. Am. Chem. Soc.* **2003,** *125,* 636.

[114.] A. J. Sandee, C. K. Williams, N. R. Evans, J. E. Davies, C. E. Boothby, A. Kohler, R. H. Friend, A. B. Holmes, *J. Am. Chem. Soc.* **2004,** *126,* 7041.

[115.] C. C. Kwok, S. C. Yu, I. H. T. Sham, C. M. Che, *Chem. Commun.* **2004,** 2758.

[116.] P. T. Furuta, L. Deng, S. Garon, M. E. Thompson, J. M. J. Frechet, *J. Am. Chem. Soc.* **2004,** *126,* 15388.

[117.] D. Wöhrle, A. D. Pomogailo, *Metal Complexes and Metals in Macrocycles*, (Eds.: D. Wöhrle, A. D. Pomogailo) Wiley-VCH, Weinheim **2003**.

[118.] X. H. Yang, D. Neher, in *Organic Light Emitting Devices* Eds.: K. Müllen, U. Scherf), WILEY-VCH, Weinheim **2006**, p. 333.

[119.] L. S. Sapochak, A. Padmaperuma, N. Washton, F. Endrino, G. T. Schmett, J. Marshall, D. Fogarty, P. E. Burrows, S. R. Forrest, *J. Am. Chem. Soc.* **2001,** *123,* 6300.

[120.] P. A. Lane, L. C. Palilis, D. F. O'Brien, C. Giebeler, A. J. Cadby, D. G. Lidzey, A. J. Campbell, W. Blau, D. D. C. Bradley, *Phys. Rev. B* **2001,** *63,* 235206.

[121.] D. F. O'Brien, C. Giebeler, R. B. Fletcher, A. J. Cadby, L. C. Palilis, D. G. Lidzey, P. A. Lane, D. D. C. Bradley, W. Blau, *Synth. Met.* **2001,** *116,* 379.

[122.] X. H. Yang, D. Neher, D. Hertel, T. K. Daubler, *Adv. Mater.* **2004,** *16,* 161.

[123.] S. C. Lo, N. A. H. Male, J. P. J. Markham, S. W. Magennis, P. L. Burn, O. V. Salata, I. D. W. Samuel, *Adv. Mater.* **2002,** *14,* 975.

[124.] F. I. Wu, H. J. Su, C. F. Shu, L. Y. Luo, W. G. Diau, C. H. Cheng, J. P. Duan, G. H. Lee, *J. Mater. Chem.* **2005,** *15,* 1035.

[125.] C. D. Müller, T. Braig, H. G. Nothofer, M. Arnoldi, M. Gross, U. Scherf, O. Nuyken, K. Meerholz, *Chem. Phys. Chem.* **2000,** *1,* 207.

[126.] C. D. Müller, A. Falcou, N. Reckefuss, M. Rojahn, V. Wiederhirn, P. Rudati, H. Frohne, O. Nuyken, H. Becker, K. Meerholz, *Nature* **2003,** *421,* 829.

[127.] X. H. Yang, D. C. Muller, D. Neher, K. Meerholz, *Adv. Mater.* **2006,** *18,* 948.

[128.] C. Adachi, T. Tsutsui, S. Saito, *Appl. Phys. Lett.* **1990,** *56,* 799.

[129.] A. R. Brown, D. D. C. Bradley, J. H. Burroughes, R. H. Friend, N. C. Greenham, P. L. Burn, A. B. Holmes, A. Kraft, *Appl. Phys. Lett.* **1992,** *61,* 2793.

[130.] G. Hughes, M. R. Bryce, *J. Mater. Chem.* **2005,** *15,* 94.

[131.] W. G. Zhu, Y. Q. Mo, M. Yuan, W. Yang, Y. Cao, *Appl. Phys. Lett.* **2002,** *80,* 2045.

[132.] D. Hertel, S. Setayesh, H. G. Nothofer, U. Scherf, K. Mullen, H. Bassler, *Adv. Mater.* **2001,** *13,* 65.

[133.] A. P. Monkman, H. D. Burrows, L. J. Hartwell, L. E. Horsburgh, I. Hamblett, S. Navaratnam, *Phys. Rev. Lett.* **2001,** *86,* 1358.

[134.] A. van Dijken, J. J. A. M. Bastiaansen, N. M. M. Kiggen, B. M. W. Langeveld, C. Rothe, A. Monkman, I. Bach, P. Stossel, K. Brunner, *J. Am. Chem. Soc.* **2004,** *126,* 7718.

[135.] W. Zhao, T. Cao, J. M. White, *Adv. Funct. Mater.* **2004,** *14,* 783.

[136.] A. C. Grimsdale, P. Leclere, R. Lazzaroni, J. D. Mackenzie, C. Murphy, S. Setayesh, C. Silva, R. H. Friend, K. Mullen, *Adv. Funct. Mater.* **2002,** *12,* 729.

[137.] Y. Ohmori, M. Uchida, C. Morishima, A. Fujii, K. Yoshino, *Jpn. J. Appl. Phys. , Part 2* **1993,** *32,* L1663.

[138.] K. H. Weinfurtner, H. Fujikawa, S. Tokito, Y. Taga, *Appl. Phys. Lett.* **2000,** *76,* 2502.

[139.] S. Galambosi, M. Knaapila, A. Soininen, K. Nygard, S. Huotari, F. Galbrecht, U. Scherf, A. Monkman, K. Hämäläinen, *Appl. Phys. Lett.* **2006**, 39, 9261.

[140.] A. P. Kulkarni, X. X. Kong, S. A. Jenekhe, *J. Phys. Chem. B* **2004,** *108,* 8689.

[141.] M. Ranger, M. Leclerc, *Macromolecules* **1999,** *32,* 3306.

[142.] M. Heeney, C. Bailey, M. Giles, M. Shkunov, D. Sparrowe, S. Tierney, W. M. Zhang, I. McCulloch, *Macromolecules* **2004,** *37,* 5250.

[143.] G. B. Bachman, S. Polansky, *J. Org. Chem.* **1951,** *16,* 1690.

[144.] H. G. Nothofer, PhD Thesis, Potsdam, Logos Verlag Berlin, **2001**.

[145.] B. S. Nehls, PhD Thesis, Bergische Universität Wuppertal, **2005**.

[146.] F. Galbrecht, X. H. Yang, B. S. Nehls, D. Neher, T. Farrell, U. Scherf, *Chem. Commun.* **2005,** 2378.

[147.] E. C. Hagberg, D. A. Olson, V. V. Sheares, *Macromolecules* **2004,** *37,* 4748.

[148.] S. I. Hintschich, C. Rothe, S. Sinha, A. P. Monkman, P. S. de Freitas, U. Scherf, *J. Chem. Phys.* **2003,** *119,* 12017.

[149.] F. Jaramillo-Isaza, M. L. Turner, *J. Mater. Chem.* **2006,** *16,* 83.

[150.] J. Li, M. Li, Z. S. Bo, *Chem. Eur. J.* **2005,** *11,* 6930.

[151.] Q. S. Hu, D. Vitharana, G. Y. Liu, V. Jain, M. W. Wagaman, L. Zhang, T. R. Lee, L. Pu, *Macromolecules* **1996,** *29,* 1082.

[152.] M. Noji, M. Nakajima, K. Koga, *Tetrahedron Lett.* **1994,** *35,* 7983.

[153.] H. Benmansour, T. Shioya, Y. Sato, G. C. Bazan, *Adv. Funct. Mater.* **2003,** *13,* 883.

[154.] T. Hattori, K. Sakurai, N. Koike, S. Miyano, H. Goto, F. Ishiya, N. Harada, *J. Am. Chem. Soc.* **1998,** *120,* 9086.

[155.] G. D. Y. Sogah, D. J. Cram, *J. Am. Chem. Soc.* **1979,** *101,* 3035.

[156.] T. Förster, *Discuss. Faraday Soc.* **1959,** 7.

[157.] X. Gong, D. Moses, A. J. Heeger, S. Xiao, *J. Phys. Chem. B* **2004,** *108,* 8601.

[158.] X. H. Yang, F. Jaiser, D. Neher, P. V. Lawson, J. L. Bredas, E. Zojer, R. Guntner, P. S. de Freitas, M. Forster, U. Scherf, *Adv. Funct. Mater.* **2004,** *14,* 1097.

[159.] C. Rothe, F. Galbrecht, U. Scherf, A. Monkman, *Adv. Mater.* **2006,** *18,* 2137.

[160.] J. X. Jiang, C. Y. Jiang, W. Yang, H. G. Zhen, F. Huang, Y. Cao, *Macromolecules* **2005,** *38,* 4072.

[161.] S. W. Thomas, S. Yagi, T. M. Swager, *J. Mater. Chem.* **2005,** *15,* 2829.

[162.] C. M. Che, S. C. Chan, H. F. Xiang, M. C. W. Chan, Y. Liu, Y. Wang, *Chem. Commun.* **2004,** 1484.

[163.] E. N. Jacobsen, in *Catalytic Asymmetric Synthesis* Ed.: I. Ojima), VCH, New York **1993**, p. 159.

[164.] O. Lavastre, I. Illitchev, G. Jegou, P. H. Dixneuf, *J. Am. Chem. Soc.* **2002,** *124,* 5278.

[165.] A. C. W. Leung, J. H. Chong, B. O. Patrick, M. J. MacLachlan, *Macromolecules* **2003,** *36,* 5051.

[166.] P. F. Wang, Z. R. Hong, Z. Y. Xie, S. W. Tong, O. Y. Wong, C. S. Lee, N. B. Wong, L. S. Hung, S. T. Lee, *Chem. Commun.* **2003,** 1664.

[167.] T. Sano, Y. Nishio, Y. Hamada, H. Takahashi, T. Usuki, K. Shibata, *J. Mater. Chem.* **2000,** *10,* 157.

[168.] R. Royer, J. P. Buisson, *Eur. J. Med. Chem.* **1980,** *15,* 275.

[169.] X. H. Yang, F. Jaiser, B. Stiller, D. Neher, F. Galbrecht, U. Scherf, *Adv. Funct. Mater.* **2006,** *16,* 2156.

[170.] S. Lamansky, P. I. Djurovich, F. bdel-Razzaq, S. Garon, D. L. Murphy, M. E. Thompson, *J. Appl. Phys.* **2002,** *92,* 1570.

[171.] X. J. Zhang, C. Y. Jiang, Y. Q. Mo, Y. H. Xu, H. H. Shi, Y. Cao, *Appl. Phys. Lett.* **2006,** *88.*

[172.] F. Galbrecht, T. W. Bünnagel, U. Scherf, T. Farrell, *Macromol. Rapid Commun.* **2006**.

[173.] B. S. Nehls, U. Asawapirom, S. Fuldner, E. Preis, T. Farrell, U. Scherf, *Adv. Funct. Mater.* **2004,** *14,* 352.

[174.] B. W. D'Andrade, J. Brooks, V. Adamovich, M. E. Thompson, S. R. Forrest, *Adv. Mater.* **2002,** *14,* 1032.

[175.] K. Brunner, A. van Dijken, H. Borner, J. J. A. M. Bastiaansen, N. M. M. Kiggen, B. M. W. Langeveld, *J. Am. Chem. Soc.* **2004,** *126,* 6035.

[176.] Y. C. Chen, G. S. Huang, C. C. Hsiao, S. A. Chen, *J. Am. Chem. Soc.* **2006,** *128,* 8549.

[177.] P. I. Shih, C. L. Chiang, A. K. Dixit, C. K. Chen, M. C. Yuan, R. Y. Lee, C. T. Chen, E. W. G. Diau, C. F. Shu, *Org. Lett.* **2006,** *8,* 2799.

[178.] Y. H. Niu, M. S. Liu, J. W. Ka, A. K. Y. Jen, *Appl. Phys. Lett.* **2006,** *88.*

[179.] F. C. Chen, S. C. Chang, G. F. He, S. Pyo, Y. Yang, M. Kurotaki, J. Kido, *J. Polym. Sci. , Part B: Polym. Phys.* **2003,** *41,* 2681.

[180.] R. J. Holmes, S. R. Forrest, Y. J. Tung, R. C. Kwong, J. J. Brown, S. Garon, M. E. Thompson, *Appl. Phys. Lett.* **2003,** *82,* 2422.

[181.] P. I. Shih, C. H. Chien, C. Y. Chuang, C. F. Shu, C. H. Yang, J. H. Chen, Y. Chi, *J. Mater. Chem.* **2007,** *17,* 1692.

[182.] S. Hoshino, H. Suzuki, *Appl. Phys. Lett.* **1996,** *69,* 224.

[183.] M. W. Wolf, K. D. Legg, R. E. Brown, L. A. Singer, J. H. Parks, *J. Am. Chem. Soc.* **1975,** *97,* 4490.

[184.] S. Hoshino, H. Suzuki, *Appl. Phys. Lett.* **1996,** *69,* 224.

[185.] U. Scherf, K. Mullen, *Makromol. Chem. Rapid Commun.* **1991,** *12,* 489.

[186.] U. Scherf, K. Müllen, *Adv. Polym. Sci.* **1995,** 1.

[187.] U. Scherf, *J. Mater. Chem.* **1999,** *9,* 1853.

[188.] C. Winder, N. S. Sariciftci, *J. Mater. Chem.* **2004,** *14,* 1077.

[189.] J. X. Duan, L. H. Zhang, W. R. Dolbier, *Synlett* **1999,** 1245.

[190.] H. M. Colquhoun, M. G. Zolotukhin, L. M. Khalilov, U. M. Dzhemilev, *Macromolecules* **2001,** *34,* 1122.

[191.] S. A. Choulis, V. E. Choong, M. K. Mathai, F. So, *Appl. Phys. Lett.* **2005,** *87,* 113506.

[192.] J. S. Kim, R. H. Friend, I. Grizzi, J. H. Burroughes, *Appl. Phys. Lett.* **2005,** *87,* 02356.

[193.] A. Pogantsch, N. Zaami, C. Slugovc, *Chem. Phys.* **2006,** *322,* 399.

[194.] R. D. Xia, G. Heliotis, D. D. C. Bradley, *Synth. Met.* **2004,** *140,* 117.

[195.] H. F. Xiang, S. C. Chan, K. K. Y. Wu, C. M. Che, P. T. Lai, *Chem. Commun.* **2005,** 1408.

[196.] X. W. Zhang, Z. Chen, C. L. Yang, Z. G. Li, K. Zhang, H. Q. Yao, J. G. Qin, J. W. Chen, Y. Cao, *Chem. Phys. Lett.* **2006,** *422,* 386.

[197.] B. S. Nehls, F. Galbrecht, A. Bilge, U. Scherf, T. Farrell, *Macromol. Symp.* **2006,** *239,* 21.